



HAL
open science

Study of the cholinergic system in the heart and its potential pharmacological targeting

Dominika Neuschlová Dingová

► **To cite this version:**

Dominika Neuschlová Dingová. Study of the cholinergic system in the heart and its potential pharmacological targeting. Neuroscience. Université Sorbonne Paris Cité; Univerzita Komenského (Bratislava), 2015. English. NNT : 2015USPCB021 . tel-01266053

HAL Id: tel-01266053

<https://theses.hal.science/tel-01266053>

Submitted on 2 Feb 2016

HAL is a multi-disciplinary open access archive for the deposit and dissemination of scientific research documents, whether they are published or not. The documents may come from teaching and research institutions in France or abroad, or from public or private research centers.

L'archive ouverte pluridisciplinaire **HAL**, est destinée au dépôt et à la diffusion de documents scientifiques de niveau recherche, publiés ou non, émanant des établissements d'enseignement et de recherche français ou étrangers, des laboratoires publics ou privés.



THÈSE

PRÉSENTÉE A

L'UNIVERSITÉ PARIS DESCARTES

ÉCOLE DOCTORALE : Cerveau, Cognition, Comportement

Par Dominika DINGOVÁ

POUR OBTENIR LE GRADE DE

DOCTEUR

SPÉCIALITÉ : Neurosciences

Etude du système cholinergique dans le cœur et des effets pharmacologiques potentiels

Study of the Cholinergic System in the Heart and its Potential Pharmacological Targeting

Co-directeur de recherche : Eric KREJCI

Co-directeur de recherche : Anna HRABOVSKÁ

Soutenue le : 14.5.2015

Devant la commission d'examen formée de :

Mme Rachel SHERRARD	Professeur Université Pierre et Marie Curie	Examineur
Mr Ján KYSELOVIČ	Professeur Université Comenius	Examineur
Mme Oľga PECHÁŇOVÁ	Docteur Slovak Academy of Science	Examineur
Mr Patrick MASSON	Professeur Institut de Biologie Structurale	Rapporteur
Mme Daniela JEŽOVÁ	Professeur Slovak Academy of Science	Rapporteur
Mr Kamil KUČA	Professeur University of Defence	Rapporteur
Mme Anna HRABOVSKÁ	Assoc. Professeur Université Comenius	Co-directeur de thèse
Mr Eric KREJCI	Directeur de recherche CNRS	Co-directeur de thèse

COMENIUS UNIVERSITY IN BRATISLAVA

FACULTY OF PHARMACY

DPT. OF PHARMACOLOGY AND TOXICOLOGY



PARIS DESCARTES UNIVERSITY

CNRS UMR 8257 MD4

COGNAC G



Dissertation thesis

Study of the Cholinergic System in the Heart and its Potential Pharmacological Targeting

Štúdium cholinergického systému v srdci a možnosti jeho farmakologického ovplyvnenia

Etude du système cholinergique dans le cœur et des effets pharmacologiques potentiel

Field of study (Bratislava): Pharmacology 7.3.2

Field of study (Paris): Neuroscience

Author: PharmDr. Dominika Dingová

Supervisor (Bratislava): Assoc. prof. PharmDr. Anna Hrabovská, PhD

Supervisor (Paris): Eric Krejci, PhD

Bratislava, Paris 2015

Declaration on Word of Honour

I hereby declare that I created my thesis independently using only the quoted literature and under leadership of my supervisors Assoc. prof. PharmDr. Anna Hrabovská, PhD. and Eric Krejci, PhD.

.....

Dissertation thesis was supported by:

- Bourse du Gouvernement Français for the thesis cotutorship between Comenius University in Bratislava and Paris Descartes University in Paris
- Grant of Ministry of Education, Science, Research and Sport of the Slovak republic VEGA 1/1139/12 (project manager – Assoc. prof. PharmDr. Anna Hrabovská, PhD,)
- Grant of Slovak Research and Development Agency, APVV SK-FR-0031-09 and SK-FR-0048-11 (project manager - Assoc. prof. PharmDr. Anna Hrabovská, PhD, Eric Krejci, PhD,) and SK-CZ-0028-09 (project manager – Assoc. prof. PharmDr. Anna Hrabovská, PhD, Prof. MUDr. Jaromir Mysliveček, PhD)
- Grant of Faculty of Pharmacy, Comenius University, Bratislava, FaFUK/44/2012 (project manager – PharmDr. Dominika Dingova) and FaFUK/38/2014 (project manager – PharmDr. Dominika Dingova)
- Grant of Comenius University, UK/294/2013 (project manager – PharmDr. Dominika Dingova)
- Centre of excellence for glycomics, ITMS 26240120031, supported by the Research & Development Operational Programme funded by the ERDF (responsible at the faculty Assoc. prof. PharmDr. Anna Hrabovská, PhD).

Acknowledgement

I would like to express my deepest gratitude to my supervisors Assoc. prof. PharmDr. Anna Hrabovská, PhD. and Eric Krejci, PhD. for their professional leadership, willingness, comments and many inspirational ideas and discussions that occurred during the creation of this work. I would also like to thank Marc Abitbol, PhD who has helped me a lot and for his valuable inputs. Last but not least, I would like to thank all my family, Cesare Colasante, PhD, Guilhem Calas, PhD, PharmDr. Matej Kučera, Jacqueline Leroy, Chloé Reymond, Jennifer Awd, PhD, Marie Vandestienne, PharmD. Aurelie Nervo, PharmDr. Zuzana Kilianova, PhD and everyone else who spent their precious time helping me, brightning up my days, cheering me up, pushing me forward and making my work much more enjoyable.



Comenius University in Bratislava
Faculty of Pharmacy

THESIS ASSIGNMENT

Name and Surname: PharmDr. Dominika Dingová
Study programme: farmakológia (Teacher preparation programme, Ph.D. III. deg., full time form)
Field of Study: 7.3.2. Pharmacology
Type of Thesis: Dissertation thesis
Language of Thesis: English
Secondary language: Slovak

Title: Study of the Cholinergic System in the Heart and its Potential Pharmacological Targeting

Tutor: doc. PharmDr. Anna Hrabovská, PhD.
Department: FaF.KFT - Department of Pharmacology and Toxicology
Head of Department: doc. RNDr. Ingrid Tumová, CSc.

Assigned: 07.07.2011

Approved: 07.07.2011 prof. PharmDr. Ján Kyselovič, CSc.
Guarantor of Main Study Field

.....
Student

.....
Tutor



Univerzita Komenského v Bratislave
Farmaceutická fakulta

ZADANIE ZÁVEREČNEJ PRÁCE

Meno a priezvisko študenta: PharmDr. Dominika Dingová
Študijný program: farmakológia (Učiteľské štúdium, doktorandské III. st., denná forma)
Študijný odbor: 7.3.2. farmakológia
Typ záverečnej práce: dizertačná
Jazyk záverečnej práce: anglický
Sekundárny jazyk: slovenský

Názov: Study of the Cholinergic System in the Heart and its Potential Pharmacological Targeting
Štúdium cholinergického systému v srdci a možnosti jeho farmakologického ovplyvnenia

Školiteľ: doc. PharmDr. Anna Hrabovská, PhD.
Katedra: FaF.KFT - Katedra farmakológie a toxikológie
FaF vedúci katedry: doc. RNDr. Ingrid Tumová, CSc.

Dátum zadania: 07.07.2011

Dátum schválenia: 07.07.2011
prof. PharmDr. Ján Kyselovič, CSc.
garant študijného odboru

.....
študent

.....
školiteľ

ABSTRACT

DINGOVÁ, Dominika: Study of cholinergic system in the heart and potential of its pharmacological effect. (Dissertation Thesis). Comenius University in Bratislava, Faculty of Pharmacy, Department of Pharmacology and Toxicology. Supervisor: Doc. PharmDr. Anna Hrabovská, PhD. and Paris Descartes University, CNRS UMR 8257 MD4, COGNAC G. Supervisor: Eric Krejci, PhD, 2015, number of pages = 138

Introduction: The results of current research suggest that acetylcholine has a protective role during heart failure and atrial or ventricular fibrillation. Cholinesterases (ChE) control the level of acetylcholine and thus play an important role in the cholinergic system of the heart. However, detail information about these enzymes in the heart is still missing. **The aim** of this thesis was to provide a complex study of acetylcholinesterase (AChE) and butyrylcholinesterase (BChE) in the heart, specifically of their activities, molecular forms and precise localization. **Methods:** Mutant mice with lack of ChE or their anchoring proteins, ColQ and PRiMA, were used. AChE and BChE activities in heart compartments were determined by 2-step Ellman's method, developed by us. Molecular forms of ChE were determined in 5-20 % sucrose gradients and localized in the hearts filled with gelatin and in the cryosections by activity staining method and by immunohistochemistry. Nerve and endothelial cells were identified using specific markers. Basic heart morphology was studied in the transversal sections stained with hematoxyline and eosine. **Results and conclusion:** The highest AChE activity was determined in the atria, the lowest activity in the left ventricle and septum. In all compartments, PRiMA AChE and ColQ AChE were observed. Both anchored forms were distributed epicardially on the heart base, co-localized with intracardiac neurons. PRiMA AChE formed a subtle branching in the proximity of intracardiac neurons. The lack of AChE anchored forms led to significantly lower cardiomyocyte diameter. The BChE activity was higher than that of AChE. The highest BChE activity was detected in the left ventricle and septum. Amphiphilic monomers were the predominant form of BChE in the heart. In myocardium, the staining of BChE activity was diffused, while in epicardium it co-localized with a single intracardiac neuron. In this work, we have provided a complex study of ChE in heart. Our results could help in the design of new, more effective pharmacotherapy, which may reduce morbidity and mortality of the patients with various heart diseases.

Keywords: cholinesterase activity, molecular forms of cholinesterases, localization of cholinesterases, Ellman's method, heart.

ABSTRAKT

DINGOVÁ, Dominika: Štúdium cholinergického systému v srdci a možnosti jeho farmakologického ovplyvnenia (Dizertačná práca). Univerzita Komenského v Bratislave. Farmaceutická fakulta, Katedra farmakológie a toxikológie. Školiteľ: Doc. PharmDr. Anna Hrabovská, PhD a Paris Descartes University, CNRS UMR 8257 MD4, COGNAC G. Školiteľ: Eric Krejci., 2015, počet strán = 138

Úvod: Výsledky súčasného výskumu nasvedčujú protektívnemu vplyvu acetylcholínu pri srdcovom zlyhávaní, či pri predsieňovej a komorovej fibrilácii. Cholínesterázy (ChE) regulujú hladinu acetylcholínu a tak zohrávajú dôležitú úlohu v cholinergickom systéme srdca. Avšak, hlbšie informácie o týchto enzýmoch v srdci chýbajú. **Cieľom** tejto práce bolo komplexné štúdium acetylcholínesterázy (AChE) a butyrylcholínesterázy (BChE) v srdci, konkrétne ich aktivít, molekulových foriem a presnej lokalizácie. **Metódy:** V projekte sme používali mutantné myši s chýbaním ChE alebo ich kotviacich proteínov, ColQ a PRiMA. Aktivity AChE a BChE sme v jednotlivých častiach srdca stanovili nami vyvinutou modifikovanou dvoj-krokovou Ellmanovou metódou. Molekulové formy ChE sme študovali v 5-20 % sacharózových gradientoch. ChE sme lokalizovali v srdciach vyplnených želatínou a v kryostatických rezoch, a to pomocou aktivitného farbenia a imunohistochemiou. Nervové a endotelové bunky sme identifikovali na základe špecifických markerov. Základnú morfológiu tkaniva sme študovali v priečnych rezoch srdca nafarbených hematoxylínom a eozínom. **Výsledky a záver:** V predsieňach sme pozorovali najvyššiu a v ľavej komore a septe najnižšiu aktivitu AChE, kotvenú pomocou PRiMA aj ColQ proteínov. PRiMA AChE aj ColQ AChE boli v epikarde distribuované na báze srdca a ko-lokalizované s intrakardiálnymi neurónmi. PRiMA AChE vytvárala jemnú spleť v blízkosti intrakardiálnych neurónov. Chýbanie kotvených foriem AChE viedlo ku signifikantne menším priemerom kardiomyocytov. Aktivita BChE v srdci bola vyššia ako aktivita AChE, s najvyššou aktivitou v ľavej komore a septe. Predominatnou formou BChE v srdci boli amfifilné monoméry. BChE aktivita bola v myokarde lokalizovaná difúzne a v epikarde ko-lokalizovala s jedným intrakardiálnym neurónom. V predloženej práci sme poskytli komplexný obraz o ChE v srdci. Naše výsledky môžu vo významnej miere napomôcť v dizajne novej, efektívnejšej farmakoterapie, ktorá by mohla znížiť morbiditu a mortalitu pacientov s vybranými chorobami srdca.

Kľúčové slová: aktivita cholínesteráz, molekulové formy cholínesteráz, lokalizácia cholínesteráz, Ellmanova metóda, srdce

RÉSUMÉ

DINGOVÁ, Dominika: Etude du système cholinergique dans le cœur et des effets pharmacologiques potentiel (Thèse). Université Comenius à Bratislava, Faculté de Pharmacie, Département de Pharmacologie and Toxicologie. co-directeur: PharmDr. Anna Hrabovská, PhD ; Université Paris Descartes, CNRS UMR 8257 MD4, co-directeur de thèse: Eric Krejci, PhD, 2015, nombre de pages = 138

Introduction: Des résultats récents indiquent que l'acétylcholine joue un rôle protecteur contre les insuffisances cardiaques et les fibrillations atriales ou ventriculaires. Les cholinestérases (ChE) contrôlent le niveau d'acétylcholine et jouent donc un rôle important pour le système cholinergique du cœur. Cependant, ces enzymes dans le cœur sont peu connues. **L'objectif** de cette thèse est d'étudier l'acétylcholinestérase (AChE) et la butyrylcholinestérase (BChE) dans le cœur, de quantifier ces enzymes et leurs formes moléculaires et localiser au niveau cellulaire. **Méthodes :** Nous avons utilisé des souris sans AChE ou BChE et sans ColQ et PRiMA leur protéines d'ancrage. Les activités de l'AChE et de la BChE ont été déterminées par la méthode d'Ellman, que nous avons adaptée pour la faible quantité de ChE dans un extrait brut. Les formes moléculaires des ChE ont été séparées en gradient de saccharose 5-20% et localisées dans des cœurs gonflés par la gélatine et sur coupe à froid. La morphologie globale du cœur a été étudiée en coupes transversales colorées avec l'hématoxyline et l'éosine. **Résultats et conclusions :** La plus forte activité en AChE a été mesurée dans les oreillettes, la plus faible activité dans le ventricule gauche et le septum. Dans tous les compartiments, PRiMA AChE et ColQ AChE ont été observés. Chacune des formes ancrées est distribuée sur l'épicarde à la base du cœur, et sont co-localisées avec des neurones intracardiaques. PRiMA AChE forme des branches fines à proximité des neurones intracardiaques. L'absence d'ancrage de l'AChE aboutit à une diminution significative du diamètre des cardiomyocytes. L'activité de la BChE est plus élevée que celle de l'AChE. La plus haute activité en BChE a été détectée dans le ventricule gauche et le septum. Le monomère amphiphilic constitue la forme prédominante dans le cœur. Dans le myocarde, le marquage de l'activité BChE est diffus, alors que dans l'épicarde il colocalise avec un seul neurone intracardiaque. Dans ce travail, nous avons réalisé une étude complète des ChE dans le cœur. Nos résultats peuvent aider à définir de nouvelles thérapies pharmacologiques plus efficaces.

Mots Clés : activité cholinestérasique, formes moléculaire des cholinestérases, localisation des cholinestérases, méthode d'Ellman, coeur

PREFACE

The heart is one of the most frequently studied tissues. While at first sight its function seems simple, in deeper view it is a complicated and still relatively undiscovered organ. Moreover, cardiovascular diseases are one of the most often causes of death in human in middle age. Thus, new information about heart, its function, mechanism of regulation or innervations is desired.

Heart is innervated by sympathetic and parasympathetic nerves. So far, the most attention was pointed at sympathetic regulation of heart and also drugs, used for symptomatic or causal treatment of heart diseases, affect predominantly sympathetic system. In the process of parasympathetic regulation, acetylcholine, neurotransmitter of cholinergic system, plays an important role.

Latest research showed that acetylcholine has a protective effect on the heart in the diseases like heart failure, which is the third most often cause of death in Slovak Republic reported by World Health Organization. Thus, study of cholinergic system in the heart deserves more attention and new approaches to pharmacotherapy of heart diseases are desired. Based on the recently emerging information about cholinergic system in heart, one of the targets of new, effective pharmacotherapy can be cholinesterases, enzymes, which regulate the level of acetylcholine in heart. However, available data about these enzymes in heart is poor. In the presented project, we have focused on the deep study of cholinesterases in heart. We have acquired complex information about these enzymes, their activity, molecular forms and localization in heart. We believe that our results may contribute to the development of new, effective pharmacotherapy of various cardiovascular diseases.

CONTENTS

INTRODUCTION	16
1 LITERATURE REVIEW	18
1.1 STRUCTURE OF THE HEART	19
1.1.1 HEART GROSS ANATOMY	19
1.1.1.1 Layers of the Heart Wall	19
1.1.1.2 Chambers of the Heart	20
1.1.2 HEART HISTOLOGY	23
1.1.2.1 The Muscle Cells	23
1.1.2.2 The Connective Tissue Cells	26
1.1.2.3 The Endothelial Cells	26
1.1.2.4 The Nervous Tissue Cells	27
1.1.2.5 Heart Histological Methods	27
1.2 INNERVATIONS OF THE HEART	30
1.2.1 EXTRACARDIAC NERVOUS SYSTEM	30
1.2.2 INTRACARDIAC NERVOUS SYSTEM	31
1.3 HEART CHOLINERGIC SYSTEM	34
1.3.1 EFFECTS OF NEURONAL ACETYLCHOLINE IN THE HEART	36
1.3.2 EFFECTS OF NON-NEURONAL ACETYLCHOLINE IN THE HEART	36
1.3.3 CHOLINESTERASES	37
1.3.3.1 Substrate Specificity and Distribution of Cholinesterases	37
1.3.3.2 Structure of Cholinesterases	37
1.3.3.3 Kinetics of Cholinesterases	40
1.3.3.4 Function of Cholinesterases	41
1.3.3.5 Inhibition of Cholinesterases	41
1.3.3.6 Molecular Forms of Cholinesterases	43
1.3.3.7 Cholinesterase Mutant Mice	47
1.3.3.8 Cholinesterases in Heart	49
1.3.3.9 Methods for Studying of Cholinesterases	52
2 AIMS OF PROJECT	56
3 METHODS	58
3.1 MATERIALS AND ANIMALS	59
3.1.1 CHEMICALS	59
3.1.2 PURIFIED ENZYMES	59
3.1.3 ANTIBODIES	59
3.1.3.1 Primary antibodies	59
3.1.3.2 Secondary antibodies	60
3.1.4 ANIMALS	60
3.2 PREPARATION OF THE TISSUE SAMPLES	61
3.2.1 TISSUE PREPARATION	61
3.2.1.1 Heart Tissue Preparation	61
3.2.1.2 Other Tissues Preparation	62
3.2.2 EXTRACT PREPARATION	62
3.3 BIOCHEMICAL ANALYSIS	63
3.3.1 ELLMAN'S METHOD	63
3.3.1.1 Ellman's Reagent	63
3.3.1.2 Stability Assays	63
3.3.1.3 Standard Ellman's Assay (EA)	64
3.3.1.4 Modified Two-Step Ellman's Assay (2s-EA)	64

3.3.1.5	Alteration of BChE Activity in Presence of DTNB	65
3.3.2	ISOTHERMAL TITRATION CALORIMETRY	66
3.3.3	SUCROSE GRADIENTS	66
3.3.3.1	Sample Preparation and Separation Procedure.....	66
3.3.3.2	Evaluation of the Results.....	67
3.3.4	ELISA METHOD.....	68
3.4	MICROSCOPIC ANALYSIS	69
3.4.1	HEMATOXYLIN AND EOSIN STAINING.....	69
3.4.2	TSUJI'S ACTIVITY STAINING METHOD.....	69
3.4.2.1	Cryosections	69
3.4.2.2	Whole-mounted heart	70
3.4.3	IMMUNOHISTOCHEMISTRY	70
4	RESULTS.....	71
4.1	ACTIVITY OF CHOLINESTERASES IN HEART	72
4.1.1	OPTIMIZATION OF ELLMAN'S METHOD	72
4.1.1.1	Stability of Ellman's reaction.....	72
4.1.1.2	Modification of Ellman's assay.....	76
4.1.1.3	Interaction of BChE and DTNB	78
4.1.1.4	Enzyme-linked immunosorbent assay.....	80
4.1.2	ACTIVITY OF CHOLINESTERASES IN HEART.....	81
4.2	MOLECULAR FORMS OF CHOLINESTERASES IN THE HEART	83
4.2.1	ACETYLCHOLINESTERASE IN THE HEART	83
4.2.1.1	Acetylcholinesterase in the Atria.....	85
4.2.1.2	Acetylcholinesterase in the Ventricles and the Septum	86
4.2.1.3	Acetylcholinesterase in the Apex and on the Base of the Heart.....	87
4.2.2	BUTYRYLCHOLINESTERASE IN THE HEART	88
4.2.2.1	Butyrylcholinesterase in the Heart Compartments.....	90
4.3	LOCALIZATION OF CHOLINESTERASES IN THE HEART.....	91
4.3.1	BASIC MORPHOLOGY OF THE HEART	91
4.3.2	CHOLINESTERASES ON THE BASE OF THE HEART	92
4.3.3	CHOLINESTERASES IN THE VENTRICLES	93
4.3.4	CHOLINESTERASES IN THE ATRIA	96
5	DISCUSSION	98
	CONCLUSION AND PRACTICAL IMPLEMENTATION OF RESULTS.....	111

ABBREVIATIONS

2s-EA	double-step Ellman's assay
A ₄	one ChE tetramer anchored by ColQ
A ₈	two ChE tetramers anchored by ColQ
A ₁₂	three ChE tetramers anchored by ColQ
ACh	acetylcholine
AChE	acetylcholinesterase
AChE del E 5+6 ^{-/-}	mice lacking anchored forms of AChE
Asp	aspartate
Ala	alanine
ATC	acetylthiocholine chloride
BChE	butyrylcholinesterase
BChE ^{-/-}	butyrylcholinesterase knockout mouse
BTC	butyrylthiocholine iodide
BW	1,5-bis(4-allyldimethylammoniumphenyl)pentan-3-one dibromide
Cys	cysteine
ChE	cholinesterases
ChT	high-affinity choline transporter
ColQ	collagen Q
ColQ ^{-/-}	mice lacking ChE anchored by ColQ
ColQ AChE	AChE anchored by ColQ
DAPI	4',6-diamidino-2-phenylindole
DTNB	Ellman's reagent
EA	standard Ellman's assay
G ₁ ^a	amphiphilic monomers
G ₁ ^{na}	non-amphiphilic monomers
G ₂ ^a	amphiphilic dimers
G ₄ ^a	amphiphilic tetramers
G ₄ ^{na}	nonamphiphilic tetramers
Glu	glutamic acid
Gly	glycine
GPI AChE	AChE dimers anchored by glycoposphatidylinositol
His	histidine

Ile	isoleucine
Iso-OMPA	tetraisopropyl pyrophosphoramidate
Leu	leucine
PECAM1	endothelial marker, platelet/endothelial cell adhesion molecule
Phe	phenylalanine
PRAD	proline-rich attachment domain
PRiMA	proline-rich membrane anchor
PRiMA ^{-/-}	mice lacking ChE anchored by PRiMA
PRiMA AChE	AChE anchored by the PRiMA protein
Pro	proline
Ser	serine
TCh	thiocholine
Trp	tryptophan
TUJ1	neuronal class III β -tubulin
Tyr	tyrosine
Val	valine
WAT	tryptophan amphiphilic tetramerization domain
WT	“wild type” mice

INTRODUCTION

Cholinesterases (ChE) control the level of acetylcholine (ACh) in tissues. The existence of these exceptional enzymes was proposed in 1914 by Sir Henry Dale and confirmed for the first time in heart muscle by Otto Loewi. Since then, hundred years have passed and study of this topic is still attractive. However, in spite of enormous amount of acquired information, there are still a lot of unanswered questions in this field. This is especially true in case of heart, where study of entire cholinergic system has been neglected over last few decades. Recently, however, the protective effect of ACh in the heart was discovered and consequently, study of the cholinergic system in heart became interesting again.

Inhibition of ChE leads to an increase of the level of ACh in the heart, which causes a slow-down of the conducting system. Complete inhibition of ChE leads to cardiac arrest. Recent studies showed that affecting ChE could be promising in patients with heart failure, arrhythmia, ischemia/reperfusion injury and hypertension. However, deeper information about ChE in heart is still missing.

In the presented thesis, we have therefore focused on the complex study of ChE, acetylcholinesterase (AChE) and butyrylcholinesterase (BChE), in mouse heart, in term of their activities, molecular forms and localization. We have determined activities of ChE in heart compartments by a double-step Ellman's assay designed by us. The details of this modification have been thoroughly described within this thesis. We have also determined and quantified molecular forms of ChE in all heart compartments using sucrose gradients. Moreover, we have localized these forms within the heart by activity staining and immunohistochemistry, described their origin using neuronal and endothelial markers and examined an impact of lack of these enzymes on heart morphology. In order to achieve these goals, we have used mouse mutant strains lacking ChE or their anchoring proteins.

1 LITERATURE REVIEW

1.1 STRUCTURE OF THE HEART

The heart continuously pumps blood throughout the body and thus ensures the distribution of dissolved gases, circulated hormones, neurotransmitters and other molecules to the tissues (Boron, 2003). Each day, the human heart makes approximately 100 000 contractions. In healthy adults, it weighs 250 - 350 grams, however it was shown that due to hypertrophy, it can enlarge its weight more than two times (Loe and Edwards, 2004). Mouse heart weighs only 150 - 180 milligrams (Doevendans et al., 1998) and beats approximately ten times faster than human heart (Ho et al., 2011). The main physiological characteristics describing the heart of both mentioned species are automaticity, excitability, contractility and conductivity (Trojan S, 2003).

1.1.1 HEART GROSS ANATOMY

1.1.1.1 Layers of the Heart Wall

The heart is located in mediastinum and is covered by pericardium. Pericardium is a thin, fibrous, double-walled sac filled with pericardial fluid (Šteiner I., 2010). It protects the heart from shock, injury, friction, excessive dilatation, infections and also provides a smooth lubricated sliding surface (Opie, 2004; O’Rahilly, 2008; Šteiner I, 2010).

The cardiac wall consists of three layers: epicardium, myocardium and endocardium (Figure 1). The outer layer, epicardium, is morphologically characterized as visceral layer of pericardium (Katz AM, 2010). Between epicardium and myocardium, there is a film of epicardial fat, which covers 80 % of the heart’s surface (Rabkin, 2007; Šteiner I., 2010). Higher amount of epicardial fat is usually present around the right than the left ventricle (Loe and Edwards, 2004), but its total amount depends on individual (Iacobellis and Willens, 2009). An increased thickness of epicardial fat was confirmed in obese patients (Rabkin, 2007; Sacks and Fain, 2007). It was shown, that nerves, coronary veins and other veins are located in epicardial fat (Šteiner I., 2010).

The myocardium is the middle layer of the heart and it forms three dimensional network of cardiomyocytes in a matrix of fibrous tissue (Ho and Nihoyannopoulos, 2006). It is the thickest part of the heart wall; however, it is well-known that levels of myocardial

mass are different within the organ. The thinnest part is the left atrium and the thickest part is the left ventricle (Šteiner I., 2010).

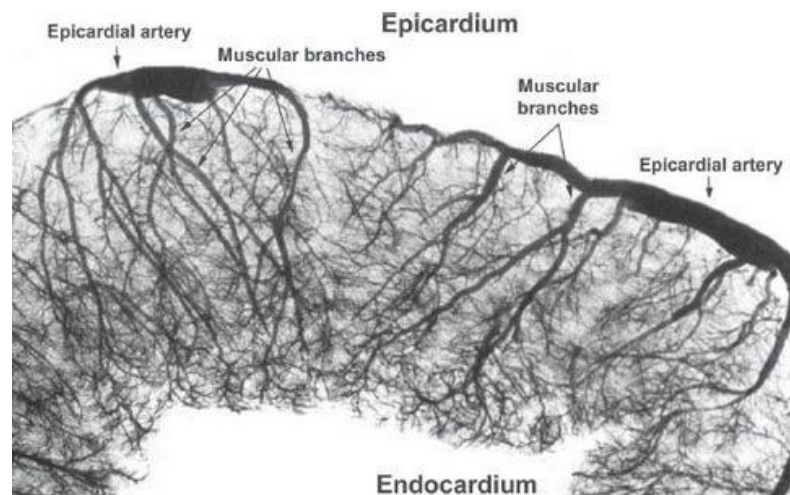


Figure 1: X-ray microphotograph of transversal section of the left ventricle after injection with radiopaque dye (Katz AM, 2010)

The inner layer, endocardium, is in contact with blood. This large surface area is firmly attached to myocardium and lines the cavities and valves. The endocardium itself is layered into endothelium, smooth muscle cells and connective tissue and subendocardial layer (Katz AM, 2010, Šteiner I., 2010). Endocardium, which is primarily made up of the endothelial cells, is considered to be the modulator of cardiac performance, rhythmicity and growth. It is also suggested that cardiac endothelium controls the development of the heart in the embryo as well as in the adult, e.g., during hypertrophy (Brutsaert et al., 1998). The endocardial endothelium may also act as “blood-heart barrier” and thus control the ionic composition of the extracellular fluid (Brutsaert et al., 1998; Dejana and Del Maschio, 1995; Milgrom-Hoffman et al., 2011).

1.1.1.2 Chambers of the Heart

The heart contains an apex and a base. The apex is the rounded lowest superficial part of the heart. The base is the broader end where cardiac plexus is located. Majority of the great vessels (e.g., pulmonary trunk, aorta and superior vena cava) emerge upward from the base of the heart (Katz AM, 2010). Heart consists of four chambers, two superior atria and two inferior ventricles (Figure 2).

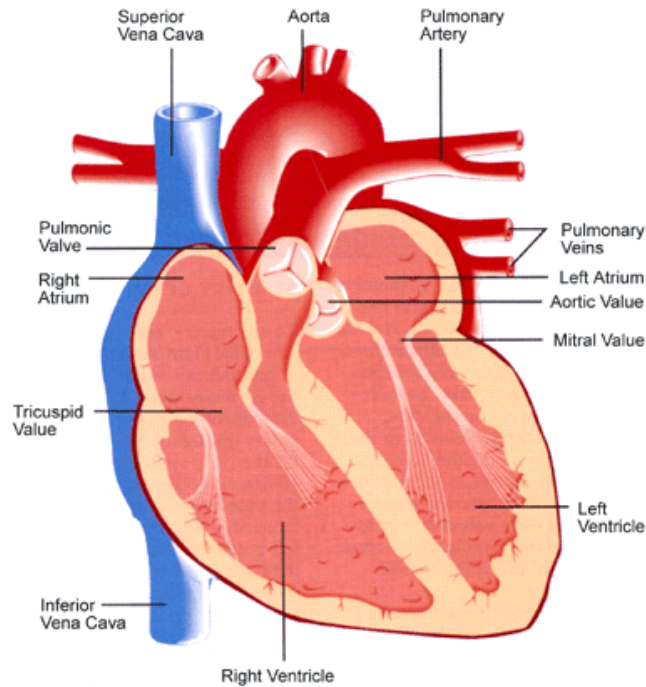


Figure 2: Heart anatomy (Chunq MK and Rich MW, 1990)

The right atrium is irregularly shaped, thin-walled muscular chamber, which is located in the upper right side of the heart, superior to the right ventricle. The right atrium is composed of a smooth concavity and a rough muscular part, formed by pectinate muscles, called auricle or right atrial appendage. These two regions are separated by an internal ridge known as *crista terminalis* and a vertical groove - *sulcus terminalis*. Coronary sinus, superior vena cava, inferior vena cava and also pacemakers of the heart – sinoatrial and atrioventricular nodes, are located in the right atrium (Katz AM, 2010; Šteiner I., 2010). While the sinoatrial node can be found next to the superior vena cava, atrioventricular node is located in the posteroinferior region of the interatrial septum, near the coronary sinus (Anderson RM, 1993). Recently, the new three-dimensional model for simulation of behavior of both nodes was introduced. This can be very useful for prediction of node behavior in specific pathologies (Li et al., 2014).

The walls of the left atrium are slightly thinner than that of the right atrium. It is situated behind the right atrium and forms a greater part of the base. The openings of the pulmonary veins are located here. The left atrium also consists of a smooth concavity and a muscular left auricle. Recently, the left atrium was studied more precisely; because its changes are associated to many cardiovascular disorders (Appleton and Kovács, 2009; Kurt et al., 2009; Mehrzad et al., 2014). For example, the size of the left atrium was used

as a biomarker and powerful predictor of mitral regurgitation, atrial fibrillation, congestive heart failure or stroke (Mehrzaad et al., 2014). The atria are separated by thin wall of tissue called the interatrial septum. This septum prevents blood from passing between the atria (Hara et al., 2005).

The left ventricle is located at the bottom left portion of the heart, below the left atrium. Its shape approximates to a cone and in cross-section, its concavity presents a circular outline (Ho, 2009). Myofibers of the left ventricle are longitudinally, obliquely and also circularly orientated. Fiber direction is aligned mostly in the base-apex course in the endocardial and epicardial area and rotating to circumferential direction in the midwall (Helm et al., 2006). This arrangement contributes to the complex movement of the left ventricle including torsion, rotation and thickening (Haddad et al., 2008). Organization of the cardiac fibers plays a key role in clinically and physiologically relevant functions, affecting contraction and relaxation, electrical conduction, electrical defibrillation and coronary perfusion (Burton et al., 2006; Vetter et al., 2005). In general, the left ventricle is the thickest part of the heart, three or four times thicker than the right ventricle. The wall of the left ventricle is the thinnest at the apex and it gradually becomes thicker towards the base (Ho, 2009). It was shown that left ventricular free wall width changes with advancing age (Kitzman and Edwards, 1990). It is also known, that cardiac output of the left ventricle is five times higher than the cardiac output of the right ventricle (Katz AM, 2010; Trojan S, 2003).

For many years, research of the left ventricle overshadowed the study of the right ventricle (Williams and Frenneaux, 2008). In the first half of the 20th century, the hypotheses that human circulation can adequately work without the right ventricle function was presented. However, later, the importance of the right ventricle was clearly recognized and its defect was connected especially with myocardial infarction, heart failure, pulmonary hypertension or congenital heart disease (for review see Farb et al., 1992). Thus, its structure and function were studied more precisely (Farb et al., 1992; Haddad et al., 2008). The right ventricle is the most anterior cardiac chamber. In contrast to the circular shape of the left ventricle, the right ventricle is triangular in longitudinal view and is crescent, when viewed in cross-section (Haddad et al., 2008; Katz AM, 2010). Fibers are arranged circumferentially, obliquely and longitudinally, similar to the left ventricle organization (Farb et al., 1992; Ho and Nihoyannopoulos, 2006).

The left and the right sides of the heart are separated by the septum. The septum is curved, convexing into the right ventricle. It consists of muscles, except for a small portion of thin fibrous structure beneath aortic valve (Ho, 2009). The septum divides the heart into two functionally separate and anatomically distinct units (Opie, 2004; Trojan S, 2003).

1.1.2 HEART HISTOLOGY

The heart is a highly organized heterogeneous structure with great diversity in cell type and their distribution. All these cell types contribute to structural, electrical, biochemical, and mechanical properties of the tissue. The largest volume of heart is occupied by cardiomyocytes (working cardiomyocytes and pacemaker cells), while non-myocytes (vascular smooth muscle, endothelial cells, nervous cells, connective tissue cells etc.) predominate in terms of cell numbers (Burton et al., 2006; Katz and Katz, 1989; Kohl, 2004). Both, cardiomyocytes and also non-myocytes are stretch-sensitive and contribute to the functional interaction of cardiac mechanics, electrophysiology and structure (Kohl et al., 1999).

1.1.2.1 The Muscle Cells

There are two types of cardiac muscle cells: cardiomyocytes, which have the ability to contract easily and modified cardiomyocytes, the pacemaker cells of the conducting system (Kapoor et al., 2013). The contractile cells react to impulses of action potential from the pacemaker cells. As a response to these impulses, they immediately contract and thus pump blood through the body (Katz AM, 2010; Šteiner I., 2010).

1.1.2.1.1 The Working Cardiomyocytes

The atria and ventricles are made up of millions of individual rod-shaped contractile cardiomyocytes (Ho and Nihoyannopoulos, 2006). The ventricular myocytes are columnar shaped cells and fill approximately 50 % of the heart weight. While human left ventricle is built of 2 - 4 billion of cardiomyocytes (Nakano et al., 2012), in mouse, the number of the left ventricle cardiomyocytes range between 2 - 3.3 million (Eisele et al., 2007). Approximately 50 % of the cell volume in an individual contracting cardiomyocyte is constituted by myofibrils (composed by myosin and actin filaments) (Forbes, 2001; Nakano et al., 2012), 25 % is formed by mitochondria (Lemieux and Hoppel, 2009;

Mettauer et al., 2006) and the rest consists of longitudinal nucleus, sarcoplasmic reticulum, sarcolemma, cytosol and other structures (Nakano et al., 2012).

The cardiomyocytes form a branched network called syncytium. Actually, the heart consists of two syncytia – one in the atria and second in the ventricles. Transmission of contractile force from one cardiomyocyte to another is arranged by irregularly-spaced dark bands between myocytes called intercalated disks (Gutstein, 2003; Katz AM, 2010). Each cell in heart is electrically coupled to the next one and thus, the heart can behave as a single motor unit. This enables rapid conduction of electrical impulses throughout the heart (Gutstein, 2003; Perriard et al., 2003).

Myocytes in atria are smaller with ellipsoidal shape (Nakano et al., 2012). They contain granules with precursor of atrium natriuretic peptide. It influences excretion of sodium, potassium and water by kidneys and in this way decreases volume of body fluids and blood pressure. This means that the heart is not only a pump, but also an endocrine organ (Katz AM, 2010; Šteiner I., 2010).

1.1.2.1.2 The Pacemaker Cells

The pacemaker cells are specialized cardiomyocytes that generate and conduct electrical impulses (Figure 3). They build just 1 % of all the cells in heart. Pacemaker cells are generally much smaller than the contractile cells, have just few myofilaments running in all directions and are not organized into myofibrils (Boyett et al., 2000; Katz AM, 2010). Group of pacemaker cells, which are located beneath the epicardial surface in the right atrium at the junction of the *crista terminalis* and veins, form the sinoatrial node. Because the firing rate of the sinoatrial node is more rapid than in other structures, it works as cardiac pacemaker. Its fibers are directly in touch with atrium fibers; hence, the action potential, which arises in sinoatrial node is immediately spread to atrioventricular node (Boyett et al., 2000; Katz AM, 2010). Atrioventricular node is located subendocardially between the atria and the ventricles in vicinity of tricuspid valve. It conducts an electrical impulse from the atria to the ventricles. This region is typical for a little slowdown of impulses. Subsequently, impulses are spread through the atrioventricular His bundle, which is divided into left and right bundle branch. Terminal part of conducting system is ensured by Purkinje fibers, a subendocardial network of rapidly conducting cells that synchronizes ventricular activation. Purkinje cells are larger with few myofibrils and huge

level of glycogen. They can be observed as pale cells by microscopy (Forbes, 2001; Katz AM, 2010; Šteiner I., 2010).

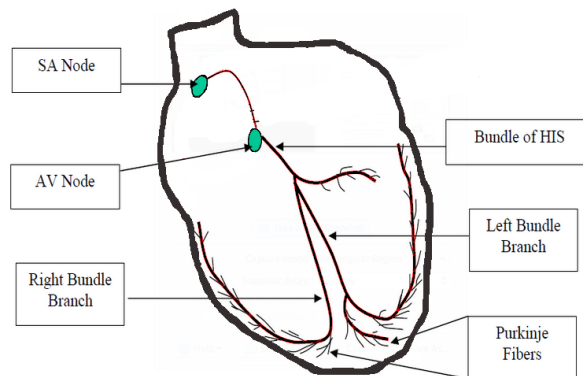


Figure 3: Cardiac conduction system. SN node – sinoatrial node, AV Node – atrioventricular node

It was shown that atrophy and loss of specialized conduction tissue in the atria and the ventricles appear in older age. It might decrease the ability of the aged heart to adapt to the stresses imposed by cardiovascular diseases (Kitzman and Edwards, 1990). Recent experiments revealed the possibility of working cardiomyocytes converting to pacemaker cells by re-expression of the embryonic transcription factor T-box 18 (Kapoor et al., 2013). This could be a viable therapy for patients with malfunction of the pacemaker. However, additional experiments are needed to verify safety and efficacy in a large-model animal (Hu et al., 2014).

1.1.2.1.3 The Vascular Smooth Muscle Cells

Cardiac tissue is highly vascularized (Nam et al., 2013). Recently published results showed that large diameter coronary veins develop close to the epicardium, whereas coronary arteries arise in the deeper myocardial layer (Red-Horse et al., 2010). The majority of the wall in blood vessels e.g., aorta, coronary arteries, inflow and outflow vasculature, is composed of vascular smooth muscle cells. They provide structural integrity of veins and regulate the caliber of the blood vessels in the body by contraction or relaxation in response to vasoactive stimuli (Metz et al., 2012). Abnormal patterning or distribution of the coronary vasculature is often associated with congenital heart disease (Kayalar et al., 2009).

1.1.2.2 The Connective Tissue Cells

Connective tissue surrounds individual cardiac myocytes, groups of cells and also encloses the entire muscle (Rossi et al., 1998). It contributes to heart tensile strength and stiffness (Katz AM, 2010). It was shown, that the numbers of myocytes and the number of connective cells in human heart increase at a similar rate in early development until several weeks after birth. Consequently, number of cardiomyocytes remains almost constant and number of connective cells is increasing with heart weight (Kohl, 2003). Sinoatrial node contains a lot of connective tissue, mainly collagen and fibroblasts. The extent of connective tissue is species-dependent and varies from 50 % in rabbit, guinea-pig and rat to 75 – 90 % in cat (Boyett et al., 2000).

More than 60 % of the cells in heart are cardiac fibroblasts. The new therapeutic approach, focused on conversion of fibroblasts into cardiomyocytes for repairing injured hearts, is intensely explored. Although reprogramming of fibroblasts into cardiomyocytes has been successful, a major limitation to using this approach to treat heart disease in human is the teratogenicity and the oncogenic potential (Xin et al., 2013).

1.1.2.3 The Endothelial Cells

The endothelial cells are firmly attached squamous cells, which line the entire vascular system, from heart to the smallest capillary. They create an adaptable life-support system, because blood supply depends on function of endothelial cells. If a part of the vessel wall is damaged, neighboring endothelial cells proliferate and migrate in, to cover the exposed surface (Alberts B, et al., 1989; Katz AM, 2010). Endothelial cells in heart play an extraordinary role in regulating and maintaining cardiac function. Recent studies showed that cardiac endothelial-cardiomyocyte interaction is necessary for normal cardiac development, growth and angiogenesis. Cardiac endothelial cells also express and release a variety of substances, such as nitric oxide, endothelin, angiotensin II or prostaglandin I₂, which directly affect cardiac metabolism, growth, contractile performance and rhythmicity of adult heart (Brutsaert, 2003). Endothelial cells are distinguished from myocardium by the expression of endothelial markers. Many of them are present at early stages of development (e.g., platelet/endothelial cell adhesion molecule (PECAM1), cadherin 5, factor VIII-related antigen) (Drake and Fleming, 2000; Garlanda and Dejana, 1997). However, it was shown that PECAM1 (Baldwin et al., 1994) and endothelial-leukocyte

adhesion molecule-1 (Hwang et al., 1997) are expressed also in the adult subjects (Paranya et al., 2001).

1.1.2.4 The Nervous Tissue Cells

Nerve cells receive, conduct and transmit signals in form of electrical impulses to other nerve cell, muscle or gland (Alberts Bruce et al., 1989; Sperelakis, 1998). Intracardiac nerves are covered by epineurium that is mostly composed of collagen fibrils. The thickness of epineurium is related to nerve diameter. In the thin nerves, the epineurium is sparse, almost absent and thus, the thin intracardiac nerves in human are separated from connective tissue only by a sheath, consisting of 1 - 12 layers (number is related to the nerve diameter) of perineurial cells. Endoneurium, a surrounding of the individual nerve fiber, is variable, with no dependence on nerve diameter (Pauziene et al., 2000; Pauziene and Pauza, 2003).

Myelinated and also unmyelinated axons are present in heart. Thin cardiac nerves possess fewer unmyelinated axons (Pauziene et al., 2000). Both myelinated and unmyelinated axons display typical ultrastructure, i.e., large nucleus, endoplasmic reticulum, cytoplasm rich in ribosomes, large numbers of neurofilaments, microfilaments, microtubules and other cytoskeletal proteins, which cross-link and form a tight meshwork (Alberts Bruce et al., 1989; Sperelakis, 1998).

Interesting suggestions appeared in the literature that structural alterations in the sensory and autonomic nerves may be a indicator of tissue inflammation and/or dysfunction of tissue homeostasis (Koistinaho et al., 1989; Wadhvani et al., 1989; Weerasuriya and Hockman, 1992).

1.1.2.5 Heart Histological Methods

The heart consists of different cell types described above. All these cell types contribute to structural, biochemical, mechanical and electrical properties of the functional heart (Xin et al., 2013). Any change in the cell content or distribution may have significant effects on cardiac function (Burton et al., 2006). Thus, the methods for identification of cardiac histo-anatomical features are important in research and in clinical applications. Usually, combination of dyes is used to visualize entire basic morphology of the tissue. For specific visualization of desired proteins, immunohistochemistry is often preferred.

1.1.2.5.1 Dyes Used in Histology

Hematoxylin and eosin staining is widely used to recognize various tissue types and morphologic changes in tissues (Fischer et al., 2008; Gibson et al., 2014). The staining is used in diagnosis of different pathologies, e.g., cancer (Fischer et al., 2008) or amyloidosis (Doganavsargil et al., 2015). Hematoxylin stains nuclei by deep blue-purple color. Eosin is a synthetic pink dye, which binds to positively charged proteins in the cytoplasm and connective tissue. As a result, cytoplasm and extracellular matrix staining varies in shades of pink; erythrocytes are bright red/pink and collagen exhibits pink color (Ankle and Joshi, 2011; Cardiff et al., 2014; Fischer et al., 2008). The advantages of this method are simplicity, short duration of procedure, compatibility with many fixatives and steadiness of the staining, remaining for many years without losing its intensity. Limitation of this method is incompatibility with immunofluorescence (Fischer et al., 2008).

Hematoxyline and eosin staining can be modified for many other specific applications. When mucin or cartilages are specifically examined, staining is usually coupled with alcian blue, which stains these structures in blue. Eosin can be substituted by acid Orange G, which stains cytoplasm yellow or orange and specifically stains the granules of acidophilic cells.

Masson trichrome staining is used for visualization of collagen fibers. Most protocols produce red muscle fibers, blue collagen and bone, light red/pink cytoplasm and dark black nuclei (Garvey, 1984). The staining is inexpensive and successfully used in diagnosis of fibrosis (Zhu et al., 2015) and tumors (Chang and Kessler, 2008; Wu et al., 2014). However, the method is more time consuming than hematoxylin and eosin staining (Garvey, 1984).

1.1.2.5.2 Immunohistochemistry

Immunohistochemistry is widely used in research and also in clinical practice. It combines histological, immunological and biochemical techniques to localize specific cellular components by interaction of target antigens with specific antibodies (Renshaw, 2005). Polyclonal antibodies recognize several epitopes, while monoclonal antibodies show specificity for a single epitope and are more specific to the target antigen (Odell and Cook, 2013).

Several different approaches can be used to detect antigens in tissue. Direct approach uses a labeled primary antibody. This method is simple and fast, however, usually its sensitivity is low due to limited signal amplification. The amplification can be achieved if the primary antibodies are conjugated to biotin molecules, which can recruit complexes of avidin or streptavidin (Cook, 2006; Hockfield et al., 1993; Renshaw, 2005). Indirect techniques use an unlabeled primary antibody, which is bound to the tissue antigen and secondary antibody directed against the precise region of the heavy and/or light chains of the primary antibody. The indirect technique allows the signal amplification and is usually the more preferred approach (Cook, 2006; Hockfield et al., 1993).

Immunohistochemistry enables visualization of only specific proteins and thus different cell types in heart can be distinguished (Odell and Cook, 2013). Endothelial cells can be detected by targeting endothelial markers e.g., PECAM1 (Nam et al., 2013) or endothelial nitric oxide synthase, which catalyzes synthesis of nitric oxide (Gentile et al., 2013). Vascular smooth muscle cells can be identified through targeting 22-kDa long protein of smooth muscle cell, commonly abbreviated SM22 α , which is extensively expressed in heart (Li et al., 1996; Nam et al., 2013). Reliable marker for nerve cells is β -tubuline (Nam et al., 2013). Other markers of neuronal phenotype are microtubule-associated protein 2 (Izant and McIntosh, 1980) and neuron-specific nuclear protein commonly referred to as NeuN (Wolf et al., 1996). The immunohistochemistry can be used in combination with non-antibody fluorescent methods, for example 4',6-diamidino-2-phenylindole (DAPI) to label DNA.

Nevertheless, the immunohistochemistry is a very specific technique with numbers of advantages; it has a few limitations that need to be considered in the experiments. As with most fluorescence techniques, significant problems are bleaching, autofluorescence of some tissues (including heart) and non-selectivity of antibodies. Moreover, dilution of antibodies has to be properly examined to reach high signal-to-background ratio (Odell and Cook, 2013).

1.2 INNERVATIONS OF THE HEART

Cardiac tissue is extensively innervated by autonomic sympathetic and parasympathetic nerves (Figure 4) (Kanazawa et al., 2010; Nam et al., 2013). These nerves enable communication between central nervous system and heart (Kukanova and Mravec, 2006). In ideal case, there is a balance in sympathetic and parasympathetic regulation of heart. Excessive up-regulation of one of these systems can have fatal consequences (Kanazawa et al., 2010).

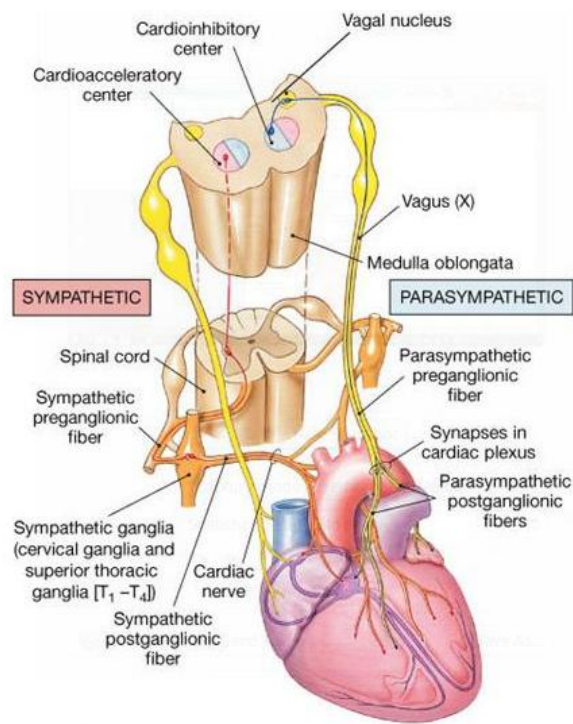


Figure 4: Innervation of heart by sympathetic and parasympathetic nerves (Olshansky et al., 2008)

1.2.1 EXTRACARDIAC NERVOUS SYSTEM

Sympathetic pre-ganglionic nerves originate in the lateral grey columns of the spinal cord. The predominant neurotransmitter of these neurons is ACh. Post-ganglionic sympathetic neurons originate in cervical and stellate sympathetic ganglia (Kawashima, 2005; San Mauro MP et al., 2009) and the neurotransmitter of most sympathetic post-ganglionic neurons is noradrenaline. Activation of sympathetic system increases chronotropy, dromotrophy, inotropy, lusitropy and batmotropy of heart (Triposkiadis et al., 2009).

The parasympathetic nervous system performs its control on heart through the *nervus vagus*. It originates from brainstem as cranial nerve X. The parasympathetic ganglia are located very proximally or actually within the target organ (Katz AM, 2010; San Mauro MP et al., 2009). While the neurotransmission in ganglia is modulated by ACh *via* nicotinic receptors, in the post-ganglionic parasympathetic nerves ACh affects cardiac muscarinic receptors (Olshansky et al., 2008). Activation of parasympathetic system leads to reduction of cardiac performance, especially to decreased chronotropy, batmotrophy and inotropy (Kanazawa et al., 2010; Triposkiadis et al., 2009).

The afferent nerves of both systems in heart share the same pathway with gastrointestinal, genitourinal, baroreceptors, chemoreceptors and transmit signals to the spinal cord (Kiernan and Rajakumar, 2013; Kukanova and Mravec, 2006). The cardiac sensory nervous system is responsible for nociception, providing information about blood pressure and for initiating a protective cardiovascular response during myocardial ischemia. The sensory signals are conducted through cardiac afferents, primarily thinly myelinated A-fibers and unmyelinated C-fibers that project to the upper thoracic dorsal horn via dorsal root ganglia (Kiernan and Rajakumar, 2013; Kimura et al., 2012).

1.2.2 INTRACARDIAC NERVOUS SYSTEM

Intracardiac nervous system integrates information from a variety of sources, including sympathetic and parasympathetic postganglionic neurons, sensory neurons, local interneurons and local paracrine signals, such as mast cell signals (Armour, 2004; Hardwick et al., 2009). Mentioned neurons are concentrated in the multiple ganglia and synthesize many different neurotransmitters. Communication between neurons in the ganglia and between individual ganglia operates as complex nervous network in the heart (Kukanova and Mravec, 2006).

Extrinsic parasympathetic and sympathetic cardiac nerves enter the tissue on the base of the heart under the aortic arch (heart hilum), where they form the net of sympathetic and parasympathetic branches called cardiac plexus (Pauza et al., 1997a). This phenomena was observed in human (Pauza et al., 2000), mouse (Rysevaite et al., 2011a), sheep (Saburkina et al., 2010), rat, guinea pig (Pauza et al., 1997b), dog (Pauza et al., 1999) and rabbit (Saburkina et al., 2014). Cardiac plexus contains the highest density of

epicardial ganglia (up to 50 % of all ganglia) (Pauza et al., 2000), which are closely associated with epicardial fat (Hasan, 2013).

The area of cardiac plexus is anatomically divided into two parts (San Mauro MP et al., 2009) – arterial and venous parts. From the arterial part, the nerves continue predominantly into the ventricles. From venous part, the nerves extend to the ventricles and also to the atria (Pauza et al., 2000). These epicardial extensions of nerves in cardiac plexus form ganglionated subplexuses, which proceed separately into regions of innervation (Pauza et al., 2000). Armour et al. (Armour et al., 1997) suggested ten subplexuses in human heart. However, later, it was described, that some of them are actually fused (Pauza et al., 2000). Pauza et al. (Pauza et al., 2000) defined seven ganglionated subplexuses in human heart: left and right coronary subplexuses, ventral right and left atrial subplexuses, left dorsal subplexus, middle dorsal subplexus and dorsal right atrial subplexus. The right atrium is innervated by two subplexuses, the left atrium by three, the right ventricle by one and the left ventricle by three subplexuses (Pauza et al., 2000). This opinion is accepted to date. The number of subplexuses and their routes of innervation vary just slightly between different species, e.g., dog (Pauza et al., 2002), pig (Batulevicius et al., 2008), guinea pig (Batulevicius et al., 2005) and mouse (Rysevaite et al., 2011a). Topography of mentioned subplexuses is preserved within species, however the precise structural organization substantially varies between them (Pauza et al., 2000; Rysevaite et al., 2011a). In human, the density of nerves changes from infancy to senility (Chow et al., 2001; Pauza et al., 2000; San Mauro MP et al., 2009). But age-related changes in neuronal number were not proven in guinea pig (Batulevicius et al., 2005).

Innervation is richer on the base of heart compared to the apex and in the atria compared to the ventricles. The distribution of sympathetic and parasympathetic nerves within heart is not uniform (Kukanova and Mravec, 2006). Studies showed that more parasympathetic nerves than sympathetic are located in atria (mainly in area of sinoatrial and atrioventricular nodes), while more sympathetic nerves are located in the ventricles (Kawashima, 2005). Parasympathetic endings are also observed in the ventricles, but form only less than one half of sympathetic division. Sympathetic innervation in the ventricles is more concentrated toward the base of the heart (Kawashima, 2005).

The accumulated evidence in recent decades indicates that intracardiac nervous system significantly regulates heart activity (cardiac chronotropy, inotropy, dromotropy,

bathmotropy and coronary blood flow) (Randall et al., 2003; Tsuboi et al., 2000). Recent observations suggest, that this system seems to be involved not only in heart physiology but also in some cardiac pathologies, e.g., ischemia (Hopkins et al., 2000), atrial arrhythmias (Armour et al., 2005), ventricular arrhythmias (Armour, 2008).

1.3 HEART CHOLINERGIC SYSTEM

ACh is involved in cell-to-cell signaling in almost all life-forms on earth (Kawashima and Fujii, 2008). It plays an important role in the organism as a key neurotransmitter of cholinergic synapse (Figure 5) in the central and the peripheral nervous system (Alberts Bruce et al., 1989).

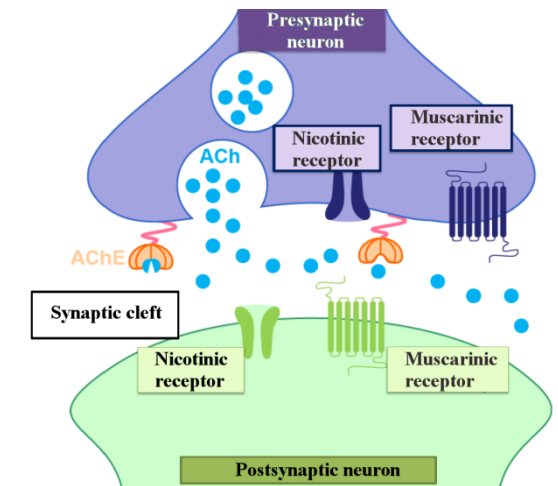


Figure 5: Cholinergic synapse (Hrabovska A)

Moreover, numerous non-neuronal cells, including cardiomyocytes, have the ability to produce, transport and release ACh (Kakinuma et al., 2009; Lara et al., 2010; Rana et al., 2010). It was suggested that ACh concentrations are significantly higher in young cardiomyocytes than in old cells, while regardless of the age, ACh concentration is significantly lower in the ventricles than in atria (Rana et al., 2010).

In both, nerve endings and cardiomyocytes, ACh is synthesized from acetyl-Co A and choline by cholinacetyltransferase (Eckenstein and Baughman, 1984). It was shown that activity of this enzyme is 50 % lower in ventricles than in atria (Slavíková and Tucek, 1982) and it is down-regulated in old cardiomyocytes compared to adults (Rana et al., 2010). In periphery, carnitine acetyltransferase may also participate in ACh synthesis (Tucek, 1982). Acetyl-Co A is a product of a pyruvate metabolism and can be found in the majority of cells (Taylor and Brown, 1999). A decrease in activity of pyruvate and ketoglutarate dehydrogenase complex results in a decreased amount of Acetyl-Co A, which consequently leads to reduction of cholinergic function (Jankowska-Kulawy et al., 2010). The second substance necessary for ACh synthesis is choline. In the presynaptic nerve

endings, choline is reuptaken from the synaptic cleft after ACh hydrolysis (Alberts Bruce et al., 1989). Other source of choline are phospholipids, which serve as a storage pool of choline for ACh syntheses (Blusztajn et al., 1987). Moreover, choline enters into the organism within the food and it is necessary for the formation of membrane phospholipides.

Extracellular choline is transferred into the cell by a sodium-dependent high-affinity choline transporter (ChT). In the nerve, this structure is localized at the presynaptic membrane (Michel et al., 2006). Recent studies indicate that ChT is also present intracellularly in vesicles and that it has a capability to migrate between the vesicles and the membrane (Ferguson and Blakely, 2004; Ribeiro et al., 2003). ChT is up-regulated in old atrial myocytes, but down-regulated in old ventricular myocytes (Rana et al., 2010). It was shown that expression of the ChT increases by cholinergic stimulation. Specific inhibition of ChT dramatically decreases cholinergic function (for review see Ribeiro et al., 2006) and genetic deletion leads to death within an hour after birth (Ferguson et al., 2004).

Synthesized ACh is uptaken into presynaptic vesicles by vesicular ACh transporter. This protein is localized on the vesicular membrane and it mediates the exchange of ACh for two protons. In cardiomyocytes, expression of vesicular ACh transporter is up-regulated in old ventricular myocytes, but down-regulated in the old atrial myocytes (Rana et al., 2010). Changes in the activity of transporter are linked to the change of ACh release or at least to the altered storage of ACh (for review see Prado et al., 2002). Recent publications deal with the question, whether this vesicular transporter is an appropriate target for pharmacotherapy of various pathologies, since it defines the volume of ACh that enters the vesicles (Van Liefferinge et al., 2013) and decreased expression leads to decreased cholinergic function and autonomic imbalance (Lara et al., 2010; Roy et al., 2012). In the cholinergic synapse, release of ACh from vesicles, requires the presence of extracellular calcium ions. Subsequently, vesicles move towards membrane and ACh is released into the synaptic cleft by exocytosis, where it stimulates the receptors (Choate et al., 1993).

1.3.1 EFFECTS OF NEURONAL ACETYLCHOLINE IN THE HEART

In the heart, secreted ACh from *nervus vagus* acts *via* the metabotropic muscarinic receptors (Van der Zee et al., 2011). In the heart of various mammalian species, M2 subtype is predominantly present (Brodde and Michel, 1999). Activation of M2 muscarinic receptors has negative chronotropic, inotropic and batmotropic effects. The autoexcitation rate of sinoatrial node and excitability of atrioventricular node also decreases (Cifelli et al., 2008; Olshansky et al., 2008). The positive effect of vagal stimulation was shown in the heart failure, atrial and ventricular fibrillation (Hamann et al., 2013; Olshansky et al., 2008). It reduces cardiac remodeling, inhibits fatal arrhythmia and thus also mortality in rodent (Ando et al., 2005; Li et al., 2004) and canine (Zhang et al., 2009) models of heart failure. In addition, the latest research shows that *nervus vagus* stimulation significantly improves the function of the left ventricle, which may result in creation of a new, more effective pharmacotherapy in future (Hamann et al., 2013).

M2 receptors were long-time considered to be the only receptor type responsible for ACh effect in heart. However, there is an emerging evidence that M1 and M3 receptors also possess physiological and pharmacological relevance and their precise function and localization is being further examined (for review see Wang et al., 2007).

1.3.2 EFFECTS OF NON-NEURONAL ACETYLCHOLINE IN THE HEART

Kakinuma et al. suggested that myocytes are able to synthesize and release ACh. This process appears to be continuous and is controlled by produced ACh. Thus, released ACh stimulates cardiomyocytes to synthesize new ACh (Kakinuma et al., 2009). The role of ACh produced by cardiomyocytes has not yet been fully clarified. Some authors believe that it secures the intercellular communication between cardiomyocytes and fibrocytes, neurocytes or endothelial cells in vessels (Rana et al., 2010). Other publications indicate that ACh synthesized by cardiomyocytes intensifies the protective effects of parasympathetic system, resulting in partial neutralization of hypertrophic adrenergic system (Rocha-Resende et al., 2012) and can protect heart against ischemia (Kakinuma et al., 2013). Roy et al. (Roy et al., 2012) showed that in the absence of the non-neuronal ACh, recovery of heart rate in stress conditions or after exercise is impaired. Thus they

suggest that ACh produced by cardiomyocytes maintains the heart homeostasis and plays a role in regulation of heart activity (Roy et al., 2012).

1.3.3 CHOLINESTERASES

ChE (EC 3.1.1), AChE (EC 3.1.1.7) and BChE (EC 3.1.1.8), are serine hydrolases, which catalyze hydrolysis of ACh and other choline-esters (Hrabovská et al., 2006b). AChE and BChE differ in their substrate specificity, distribution, structure, kinetics, function in organism, sensitivity to inhibitors and also in their molecular forms (Giacobini, 2003a; Massoulié, 2002).

1.3.3.1 Substrate Specificity and Distribution of Cholinesterases

AChE hydrolyses preferentially small substrates, such as ACh (Figure 6). The highest activities of AChE can be localized in skeletal muscle (at neuromuscular junction) (Bernard et al., 2011), brain (Dobbertin et al., 2009a; Li et al., 2000) or erythrocyte membrane (Igisu et al., 1994).

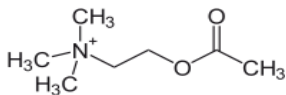


Figure 6: Acetylcholine

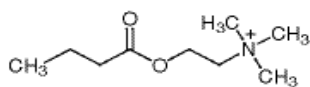


Figure 7: Butyrylcholine

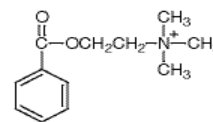


Figure 8: Benzoylcholine

BChE is also called plasma ChE or pseudocholinesterase and is able to accommodate bulkier substrates such as butyrylcholine (Figure 7) or benzoylcholine (Figure 8). It hydrolyzes small molecules such ACh, too (Giacobini, 2003a). BChE has been found in all mouse and human tissues studied to date. In all organs, except of brain and muscle, activity of BChE is much higher than AChE activity (Li et al., 2000). The highest activities of BChE were observed in liver, serum, intestine, heart and skin (Li et al., 2000; Schallreuter et al., 2006).

1.3.3.2 Structure of Cholinesterases

ChE are glycoproteins containing one, two or four catalytic subunits. The catalytic subunits of ChE possess interchain disulfide bonds, which stabilize protein structure. The

primary structure of the mature catalytic subunit is formed by more than 500 amino acids, followed by C-terminal and N-terminal peptides (Blong et al., 1997; Giacobini, 2003a; Lockridge et al., 1987a; Massoulié et al., 1993).

AChE and BChE are the product of two different genes (Arpagaus et al., 1990; Getman et al., 1992; Pezzementi and Chatonnet, 2010). Their amino acid sequence homology is 53-65 % identical and their active site structures are similar (Lockridge et al., 1987b). One of the most important differences is the amount of possible N-glycosylation sites. In general, AChE is less glycosylated than BChE. AChE from *Torpedo californica* has four N-glycosylated sites, human AChE possesses three, while human BChE has ten, of which only nine are glycosylated in a native enzyme. Glycosylation affects biosynthesis, stability, immunogenicity and pharmacokinetic parameters, but does not have any influence on catalytic characteristics (Giacobini, 2003a; Lockridge et al., 1987b; Nachon et al., 2002; Nicolet et al., 2003; Velan et al., 1993). Moreover, studies with recombinant human AChE showed that level of glycosylation affects circulatory time of enzymes (Chitlaru et al., 2001).

Active site is situated at the bottom of a 20 Å deep gorge in the protein covered mostly by hydrophobic residues (Axelsen et al., 1994). The active site of BChE is much larger than the active site of AChE (Figure 9). Active site of AChE is lined with fourteen aromatic residues. These are substituted by smaller aliphatic residues in case of BChE. The most notable consequence of this inequality is in the catalytic properties (substrate specificity) observed in these two enzymes (Dvir et al., 2010; Giacobini, 2003a; Nicolet et al., 2003).

A peripheral anionic site is situated at the rim of the gorge, in a narrow hydrophobic pocket (Bourne et al., 2006). In AChE, this site contains three principal amino acids, Trp279, Tyr70 and Asp72 (Barak et al., 1994). In BChE, it contains Asp70 and Tyr332 linked by a hydrogen bond. A positively charged substrate forms a cation- π complex with aromatic skeleton of Tyr332, while at the same time it reacts with a negatively charged Asp70. This process triggers the conformational change of the monomer (Nicolet et al., 2003). Flexible sides of the Ω -loop get closer and the substrate slides towards Trp82 (Trp84 in *Torpedo californica* AChE) at a cation- π site (Sussman et al., 1991). This site was originally named as anion site. Nowadays, it is already known that there are no negatively charge residues, which would be responsible for binding quaternary nitrogen

atom of the substrate (Colletier et al., 2006; Dvir et al., 2010; Giacobini, 2003a; Nese Cokugras A, 2003; Nicolet et al., 2003).

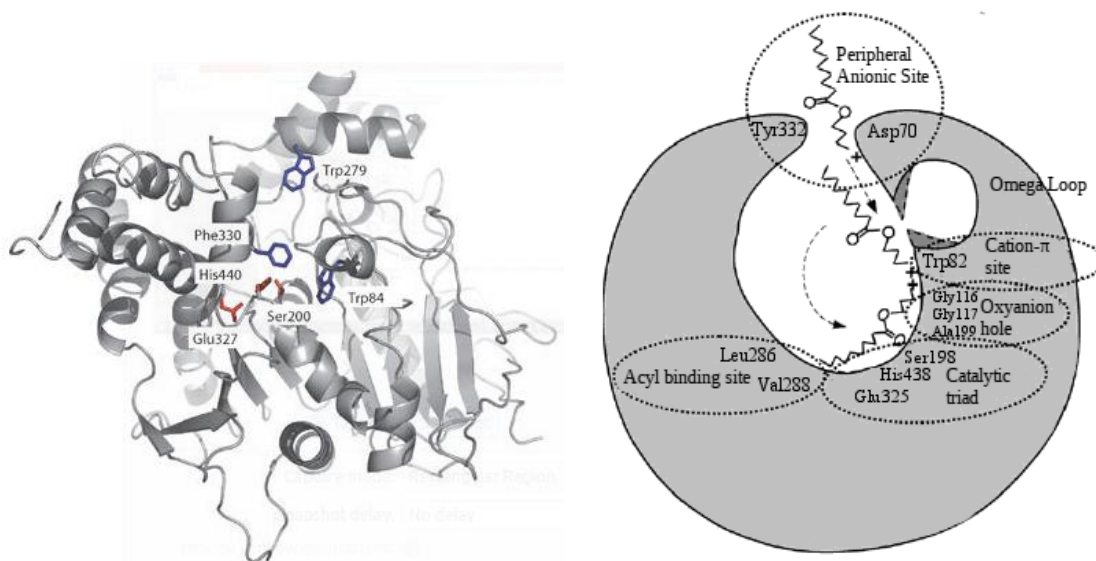


Figure 9: Schematic structure of the active site of AChE (left) (Colletier et al., 2006) and BChE (left) (Nese Cokugras A, 2003)

An oxyanion hole is located in the proximity of the cation- π site. It is composed of three N-H dipoles from the chain of residues Gly116, Gly117 and Ala199 in BChE and Gly118, Gly119 and Ala201 in *Torpedo californica* AChE. It assures rotation of the substrate. In parallel, the acyl part of the substrate links to the acyl-binding pocket containing Leu286 and Val288. These two aliphatic residues, which replace the Phe288 and Phe290 from structure of *Torpedo californica* AChE, facilitate the catalysis of hydrolysis of bigger substrates, such as butyrylcholine. Substrate stabilized between the oxyanion hole and acyl-binding pocket is ready to be hydrolyzed by the catalytic triad (Dvir et al., 2010; Giacobini, 2003a; Nese Cokugras A, 2003; Nicolet et al., 2003).

The catalytic triad differs from serine proteases especially because of Glu, which is incorporated instead of usual Asp. Catalytic triad of BChE consists of Ser198, His438 and Glu325 and *Torpedo californica* AChE Ser200, His440 and Glu327 (Dvir et al., 2010; Giacobini, 2003a; Nese Cokugras A, 2003; Nicolet et al., 2003).

Product of the hydrolysis exits the active site through the peripheral anionic site. ChE are able to hydrolyze the substrate in a very rapid manner. However, since the active site is so deeply buried, it raised a question about another exit route for product. Some authors proposed that thiocholine (TCh), product of substrate (acetylthiocholine (ATC) or

butyrylthiocholine (BTC)) hydrolysis) exits active-site gorge through back-doors or side-doors (Alisaraie and Fels, 2006; Wiesner et al., 2010; Xu et al., 2010).

An interesting fact about BChE substrate - butyrylcholine has been discovered. Crystallography studies showed that butyrylcholine is continually bound at the BChE active site and is edged out by other substrate molecule during hydrolysis. The whole complex is thus more stable and energetically more efficient (Nicolet et al., 2003).

1.3.3.3 Kinetics of Cholinesterases

AChE and BChE also differ in their kinetic properties. AChE is capable of very rapid ACh hydrolysis, which is nearly at the rate of diffusion. It exhibits one of the highest second-order rate constant (Ordentlich et al., 1998). The enzyme from the electric eel electroplax turns over up to 10 000 ACh molecules per second (Rosenberry, 1975; Stojan, 2008). In the neuromuscular junction, AChE is able to hydrolyze about 4000 molecules of ACh per active site per second (Evers et al., 2011).

ChE do not follow the Michaelis-Menten kinetics and display a hysteretic behavior with certain neutral and positively charged substrates, e.g., N-methylindoxyl acetate (Masson et al., 2002a), benzoylcholine (Hrabovská et al., 2006a). A characteristic slow, few minutes lasting induction phase was observed with those substrates in the approach to steady state. This abnormality can be explained by slow transition from an inactive enzyme form to the functional enzyme form and their interactions with substrate. A more complex hysteresis, where damped oscillations covered long induction phase, was observed with substrates that exist in different, slowly interconvertible, and conformational or micellar forms, of which only the minor form is capable of reacting with enzyme (Hrabovská et al., 2006a; Masson, 2012; Masson et al., 2005, 2004). These time-dependent abnormalities in kinetic behavior are observed for both AChE and BChE from different sources (Badiou et al., 2008; Masson, 2012; Masson et al., 2005). Temperature, pH, organic solvents, osmotic pressure or hydrostatic pressure can probably also affect this phenomenon. The physiological or toxicological significance of hysteresis is not understood so far (Masson, 2012; Masson and Lockridge, 2010).

Moreover, AChE shows substrate inhibition (Hofer and Fringeli, 1981; Rosenberry, 1975) and BChE shows substrate activation by excess of substrate (Cauet et al., 1987) at neutral pH (7-8). At low pH, activation of both enzymes can be detected and at high pH, inhibition of both enzymes can be observed. (Kalow, 1964; Masson et al., 2003, 2002b).

1.3.3.4 Function of Cholinesterases

AChE is responsible for rapid hydrolysis of neurotransmitter ACh. Thus, it protects muscarinic and nicotinic cholinergic receptors from overstimulation (Tripathi and Srivastava, 2010). Prolonged action of ACh is toxic and leads to respiratory paralysis, convulses and death (Flynn and Wecker, 1986; Wecker et al., 1986). AChE seems to play also several non-classical roles, independent of its catalytic function (Tripathi and Srivastava, 2010). It was found to modulate haematopoietic differentiation (Deutsch et al., 2002), play a role in neurite growth (Sharma et al., 2001), synaptogenesis (Silman and Sussman, 2005) and embryogenesis (Hanneman and Westerfield, 1989). Moreover, it is believed to accelerate formation of beta-amyloid plaques in the brain (Bartolini et al., 2003),

Physiological role of BChE is unknown so far. However, the high amount of this enzyme in almost all tissues suggests that BChE has a function (Masson and Lockridge, 2010). Understanding the role of BChE in the body is complicated by the fact that BChE has no endogenous physiological substrate. However, it is able to substitute cholinergic function of AChE in ACh hydrolysis (Chatonnet et al., 2003; Hartmann et al., 2007). BChE has an important role in metabolism of some drugs, such as some muscle relaxants (Baraka et al., 2005), local anesthetics (Pérez-Guillermo et al., 1987), cocaine (Mattes et al., 1996), acetylsalicylic acid (Masson et al., 1998) or bambuterol (Pistolozzi et al., 2015). It is an endogenous scavenger of toxic organophosphorus and carbamate compounds, which are used as insecticides, pesticides or misused as chemical warfare agents and inhibit both ChE (for review see Lenz et al., 2007). Recent data suggest that BChE may play a role in lipid metabolism (Iwasaki et al., 2007). Its activity is positively associated with triglyceride levels, LDL cholesterol and total cholesterol concentrations in serum. BChE activity correlates positively with body mass index in subjects fed with high fat diet (Calderon-Margalit et al., 2006; B. Li et al., 2008b; Rustemeijer et al., 2001; Vallianou et al., 2014) and is negatively associated with malnutrition (Santarpia et al., 2013).

1.3.3.5 Inhibition of Cholinesterases

There are two main types of ChE inhibitors – reversible and irreversible. Complete irreversible inhibition of ChE activity causes seizures, convulses, muscle paralysis and acute death by respiratory failure (Nese Cokugras A, 2003). Irreversible inhibitors such as

organophosphates can be misused as chemical warfare agents against civilian or military populations. Less toxic irreversible inhibitors are used as insecticides or pesticides. All these compounds affect ChE by phosphorylation of its active site Ser (Mason et al., 1993; for review see Sharma et al., 2014). Thus, ChE are not able to hydrolyze ACh and it leads to its accumulation in the synaptic cleft (Levin and Rodnitzky, 1976). Therapy of this type of toxicity includes immediate administration of cholinolytic agents (e.g., atropine), oxime reactivators (Jun et al., 2008; Petroianu et al., 2007) and anticonvulsants (Bajgar et al., 2007). Pure BChE is a potential prophylactic agent against organophosphate poisoning (Kayser and Warzecha, 2012; Raveh et al., 1993). It binds organophosphorus compounds preferentially, irreversibly and in stoichiometric ratio 1:1. It is usually well tolerated and thermally stable. Level of BChE can also be used as a diagnostic marker of organophosphorus exposure (for review see Nese Cokugras A, 2003).

Reversible inhibitors of ChE are used in clinical practice. Alzheimer disease and Lewy body disease are chronic, progressive neurodegenerative diseases, characterized by central cholinergic deficit with substantially reduced level of ACh. Therefore, it is desirable to partially inhibit ChE and thus increase the level of ACh in brain (for review see Giacobini, 2003b). There are three ChE inhibitors approved and clinically used in the treatment of dementia in Europe and USA: rivastigmine, galantamine and donepezil (Hrabovska and Krejci, 2014; Matsunaga et al., 2014). ChE inhibitors are also used in treatment of glaucoma. It reduces intraocular pressure by increasing aqueous outflow (for review see McLellan and Miller, 2011). Reasonable use of ChE inhibitors was shown in myasthenia gravis, which is an autoimmune disease characterized by muscle weakness. Precise etiology of this disorder is unknown, but presence of the antibodies directed against the nicotinic receptor is well known. ChE inhibitors are used for diagnosis and also symptomatic therapy of myasthenia gravis. Administration of ChE inhibitors helps to increase amount of available ACh at the neuromuscular junction. Nevertheless, these drugs do not influence progression of disease (for review see Jayam Truth et al., 2012). ChE inhibitors show positive effect in some cardiovascular diseases e.g., heart failure, atrial and ventricular tachycardia. Currently, effect of ChE inhibitor, pyridostigmine bromide, during the heart failure is tested in the phase 2 of clinical trials (clinicaltrials.gov NCT01415921).

1.3.3.6 Molecular Forms of Cholinesterases

ChE exhibit an extremely wide molecular diversity, which originates at the genetic, post-transcriptional and post-translational levels (Massoulié et al., 2008). The BChE gene in human is located on the chromosome 3, at 3q26 (Arpagaus et al., 1990). In mouse, BChE gene is located in the middle of chromosome 3 (B. Li et al., 2008a). It consists of 4 exons, 3 introns and its length is at least 73 kb. Exon 1 contains untranslated sequences. Exon 2 has the most important function. It contains 83 % of the protein coding sequence. Smaller part of the catalytic subunit is coded by exon 3 and exon 4. It is responsible for C-terminus coding (Arpagaus et al., 1990; Massoulié et al., 1993). BChE gene exists in large numbers of allelic variants. These variants affect activity of enzyme, its stability and production (Primo-Parmo et al., 1996).

AChE is also a product of a single gene (Figure 10) in vertebrates. This gene is located on the long arm of chromosome 7, at 7q22 in human (Getman et al., 1992) and on chromosome 5 in mouse (Rachinsky et al., 1992, 1990). Gene consists of 6 exons. Exon 1 is non-coding. Exons 2, 3 and 4 code 535 amino acid long catalytic domain. C-terminus is coded by alternative exons 5 and 6 (Massoulié, 2002; Sikorav et al., 1988).

Depending on various coding sequences in acceptor sites in the 3' region of the primary AChE gene transcript for alternative splicing, different types of catalytic subunits (70-80 kDa) can be produced (Massoulié et al., 1993).

S transcript (“soluble”) produces soluble non-amphiphilic AChE monomers. These forms are secreted by venom glands of Elapidae snakes and can be found also in muscles and liver of these snakes. Their presence does not affect the toxicity of the poison (Cousin et al., 1998).

R transcript (“readthrough”) produces soluble, non-amphiphilic monomeric AChE subunits, which contain catalytic subunit and 26 amino acid long C-terminus, encoded by the non-splicing of the last exon. This molecular form of AChE can be found in human and rodent embryonic and tumor cells (Karpel et al., 1996; Massoulié et al., 1993). Some authors suggested their possible function in embryogenesis and stress regulation (Karpel et al., 1996, 1994). Increased level of this form was linked to apoptosis, neuronal development, inflammation diseases and Alzheimer disease (Massoulié, 2002; Perrier et al., 2005).

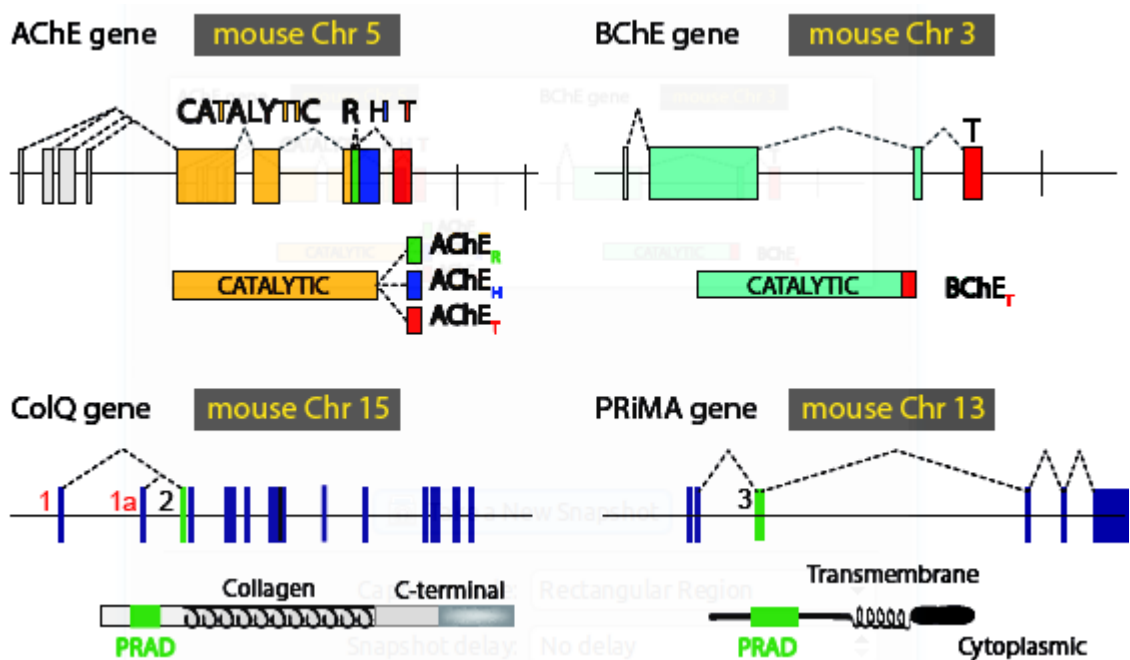


Figure 10: AChE, BChE, ColQ and PRiMA genes (Krejci E)

H transcript (“hydrophobic”) produces amphiphilic dimers anchored on the cell membrane by glycosphosphatidylinositol (GPI). C-terminus is a result of alternative splicing on the exon 5. AChE anchored by GPI (GPI AChE) can be predominantly found on the erythrocyte membrane; however, its presence was also described in skeletal muscle and colon (Massoulié, 2002; Montenegro et al., 2006; Moral-Naranjo et al., 2010). GPI AChE exist in *Torpedo* tissues, mammals, invertebrates and moreover, it is a predominant form in *Drosophila* (Incardona and Rosenberry, 1996; Massoulié et al., 2008). The structure of GPI anchor depends on the biochemical properties of the cell (Massoulié, 2002; Montenegro et al., 2006; Moral-Naranjo et al., 2010).

T transcript (“tailed”) is present in mammals in the largest amounts. It generates catalytic subunits, which are characterized by 40 amino acid long C-terminal T peptides, encoded by exon 6. Disulfide bonds are formed between catalytic subunits or between catalytic subunit and anchoring protein. In this manner, various homo-oligomeric (monomers, dimers, tetramers) and heteromeric (anchored tetramers) forms are produced (Figure 11). Generated molecular forms are responsible for ACh hydrolysis in synapses. It is a single transcript yielded by BChE (for review see Massoulié, 2002; Massoulié et al., 1993).

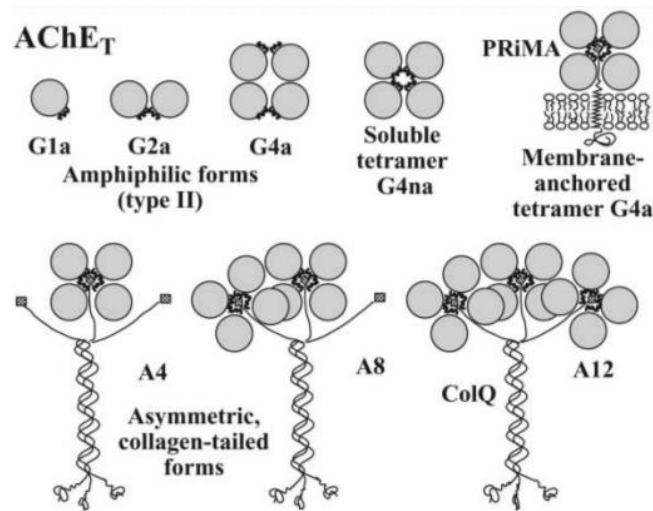


Figure 11: Molecular forms of AChE (Massoulié, 2002)

Hetero-oligomers are produced by an interaction between catalytic subunits and anchoring proteins. The presence of C-terminal T-peptide is necessary. It contains the Trp amphiphilic tetramerization domain (WAT) and Cys, needed for the dimerization (Simon et al., 1998). On the other hand, the anchoring proteins contain proline-rich attachment domain (PRAD domain) (Bon et al., 1997), that is a set of sequential Pro at the N-terminal. Interaction of PRAD with tetramer of ChE (containing four WAT domains) produces hetero-oligomeric forms of ChE. Interactions between the domains are hydrophobic and polar (Dvir et al., 2004). Formation of disulphide bonds contributes to the stabilization. Anchored ChE are more stable and more resistant to degradation than individual catalytic subunits (Bon et al., 1997; Massoulié et al., 2005). It was shown, that hetero-oligomeric forms are functional forms of ChE in central nervous system and at the neuromuscular junction. In the central nervous system, ChE are anchored by small, transmembrane, proline-rich membrane anchor (PRiMA) (Perrier et al., 2002). At the neuromuscular junction (along the nerve terminus) ChE are predominantly anchored to the basal lamina by collagen Q anchor (ColQ) (Bernard et al., 2011; Feng et al., 1999).

1.3.3.6.1 Collagen Q

ColQ forms are more abundant for AChE than for BChE. They are characterized by the presence of a specific collagen-like tail (Massoulié, 2002). This structure is important for anchorage to the basal lamina. ColQ consists of a signal peptide, an N-terminal domain, C-terminal region and collagen domain (Figure 10). The N-terminal domain contains a PRAD that is required for the organization of AChE and BChE tetramer. Collagen domain contains two clusters, which constitute heparin-binding sites. These domains are

responsible for heparin interaction and they differ in their affinity for heparin (Deprez et al., 2003). C-terminal domain enables binding of ColQ on the basal lamina by interaction with muscle-specific kinase (Cartaud et al., 2004). Asymmetric form is formed of the triple helical structure of three collagenic subunits Q. Each of the Q subunits may be associated to one catalytic tetramer. Thus, molecules can contain one, two or three catalytic tetramers (A₄, A₈ and A₁₂) (Massoulié, 2002; Massoulié et al., 1993). It is known, that two transcripts can be present in organism - ColQ1 and ColQ1a. Fast muscles contain ColQ1a transcript and A₁₂ form is predominant here. Slow soleus muscle contains ColQ1 and ColQ1a transcripts and in these muscles mainly A₄ and A₈ forms are present (Krejci et al., 1999). In rat, expression of ColQ gene was proven in brain, heart, lung and testis (Krejci et al., 1997). Presence of high-salt buffers is needed for efficient solubilization of ColQ ChE. ColQ ChE are characterized by their sensitivity to collagenase (Massoulié, 2002; Massoulié et al., 1993).

1.3.3.6.2 Proline rich membrane anchor

PRiMA is a transmembrane protein with 70 kb long gene. The gene consists of 5 exons separated by 4 introns (Perrier et al., 2002). PRiMA consists of signal peptide, N-terminal extracellular domain, transmembrane domain and C-terminal domain. Extracellular domain of PRiMA contains a PRAD domain, which organizes AChE_T and BChE_T in tetramer (Perrier et al., 2002). Two different transcripts of PRiMA (PRiMA I and II) exist in the body. Variant II is probably present only in cerebellum (Perrier et al., 2003). Assembly of catalytic domains with PRiMA protein is being executed in endoplasmic reticulum. Subsequently, protein is transported through Golgi apparatus on the cell surface, where protein is anchored. In case of absence of PRiMA, AChE is retained in endoplasmic reticulum, while the retention signal is the exposed WAT domain. This suggests a role of PRiMA in stabilization, transport and localization of ChE (Dobbertin et al., 2009). PRiMA is predominant form of ChE in the central nervous system (present in axons, dendrites, soma) of mammals (Henderson et al., 2010). ChE anchored by PRiMA were found in brain, kidney, heart (Perrier et al., 2002) and in muscle, where they are diffusely distributed along the muscle in extrajunctional regions (Bernard et al., 2011). PRiMA is important in the targeting ChE to the cell surface, stabilizing ChE and targeting the enzyme to the membrane of axonal varicosities in striatum. It is also the key element for the maturation of AChE *in vivo* in the brain (Dobbertin et al., 2009a; Perrier et al., 2002).

1.3.3.6.3 Hybrid Cholinesterase

Presence of hybrid ChE in chicken was described in literature. This mixed form is typical by presence of both, AChE and BChE subunits, assembled with PRiMA or ColQ anchors (Tsim et al., 1988a, 1988b). To date, the knowledge about this topic is quite limited. It is known that ColQ or PRiMA anchors are necessary for generation of hybrid enzyme. In the absence of anchor, formation of mixed enzyme is not possible (Chen et al., 2011).

Presence of mixed enzyme, anchored by ColQ, was confirmed in muscle of one-day chick (Tsim et al., 1988a). It was reported that composition of subunits is age-related with increasing content of AChE. In the muscle of adult chicken, BChE is completely replaced by AChE (Tsim et al., 1988b). In the chicken brain, hybrid enzyme is anchored by PRiMA protein and amount of hybrid enzyme increases till adulthood. Some authors hypothesize, that hybrid enzyme can play a role in the development of cholinergic system (Chen et al., 2010). Interestingly, presence of hybrid enzyme was confirmed also in astrocytomatous cyst and gliomas. It seems to be present only in some types of tumors, while it was not observed in brain, meningiomas or neurinomas (García-Ayllón et al., 2001).

1.3.3.7 Cholinesterase Mutant Mice

Mutant mice with deletion of ChE or their molecular forms were developed during the past 15 years (Figure 12). They were prepared by homologous recombination in embryonic stem cells to delete specific exons of AChE, BChE, ColQ and PRiMA.

ColQ^{-/-} mice were prepared by the deletion of exon 2 encoding the PRAD domain. Consequently, AChE and BChE cannot be organized into the tetramers with ColQ and thus these mice are characterized by absence of AChE and BChE anchored by ColQ protein. Mice are smaller and typical tremor and muscle weakness can be observed. Only 10 - 20 % of the mice live till adulthood. Absence of ColQ AChE in cardiac muscle was observed in these mice (Feng et al., 1999).

PRiMA^{-/-} mice were prepared by the deletion of exon 3 encoding the PRAD domain in the PRiMA gene. PRiMA^{-/-} mice are characterized by the absence of AChE and BChE anchored by PRiMA protein. When PRiMA is absent, ChE are retained in the endoplasmic reticulum. Mice are indistinguishable from WT mice in physical appearance, (Dobbertin et al., 2009), temperature and ventilation (Boudinot et al., 2009). Detailed behavior analysis uncovered motoric deficit (Farar et al., 2013).

AChE del E 5+6^{-/-} mice are produced by the deletion of the exon 5 and exon 6. Exon 5 is responsible for formation of GPI AChE and exon 6 for the production of PRiMA AChE and ColQ AChE. Thus, mice do not contain any anchored form of AChE. They are characteristic by presence of soluble monomers of AChE. Their phenotype is very similar to ColQ^{-/-} mice. Muscle weakness, tremor and smaller weight are also present (Camp et al., 2005).

BChE^{-/-} mice were prepared by the gene-targeted deletion of splice junction between introns 1 and 2, and the signal peptide including the translation site. The first 102 amino acids of the mature BChE protein were also deleted (Li et al., 2006). BChE^{-/-} mice are typical for their complete absence of BChE in organism and serve as a model for human BChE deficiency (Li et al., 2008a,b). There is no evident change in the phenotype. Heart rate, blood pressure and respiration are similar to WT littermates (B. Li et al., 2008a). However, these mice are prone to obesity when fed with high fat diet (B. Li et al., 2008b).

All described mouse mutant strains are very useful in the study of ChE in the mice. When selective ChE inhibitors are used, other than studied systems or tissues may be affected, and thus results can be easily misinterpreted. Moreover, there are no available specific inhibitors for ColQ and PRiMA ChE. Thus, only this type of mutant mice can be used to discover precise localization of ChE and their molecular forms in the mice. Described mutant mice were, for example, successfully used in the localization of molecular forms in the neuromuscular junction (Bernard et al., 2011; Petrov et al., 2014) and in the brain (Dobbertin et al., 2009).

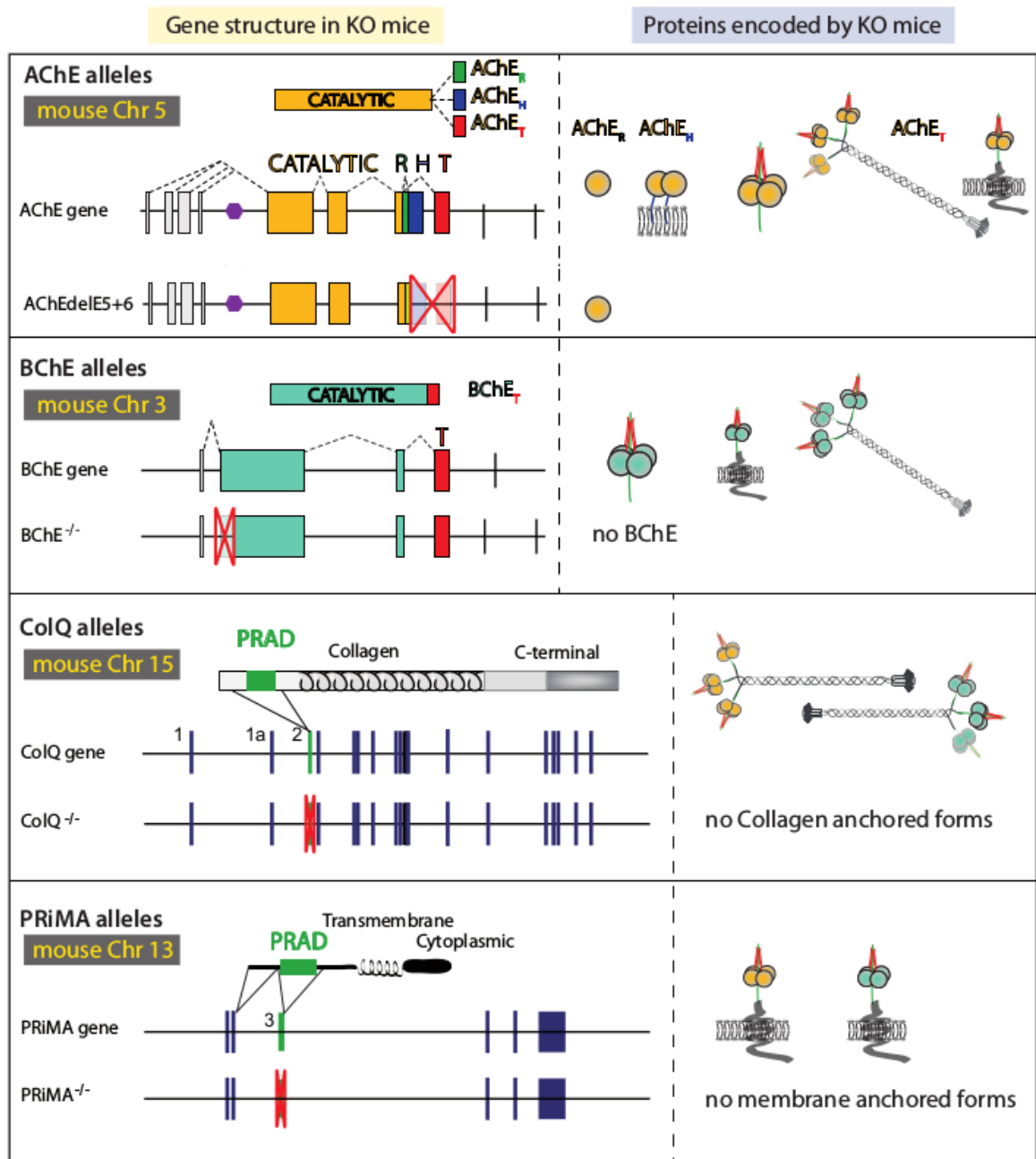


Figure 12: Structure of AChE, BChE, ColQ and PRiMA genes. Deleted sequences in mutant mice (KO) are displayed. Picture also depicts protein encoded by mutant mice.

1.3.3.8 Cholinesterases in Heart

Inhibition of ChE remarkably affects cardiac functions (Masuda, 2004). It causes an increase of ACh level in the myocardium, which results in cardioinhibitory effect. Decreased frequency, force of contraction, rate of sinoatrial node autoexcitation, excitability of atrioventricular node and beat by beat fluctuation are reduced (Malone and Lindsay, 2007; Masuda, 2004, Cifelli et al., 2008; Olshansky et al., 2008). Detailed

information about ChE, in term of their activity, molecular forms and also localization in heart are needed. Recent studies showed, that affecting ChE activities could be promising in heart failure, arrhythmia, ischaemia/reperfusion injury and hypertension (for review see He et al., 2014; Lataro et al., 2013).

1.3.3.8.1 Activity and Localization of Cholinesterases in Heart

AChE and BChE are both present in mammalian heart. In mouse heart, activity of BChE is much higher than AChE activity (Li et al., 2000). AChE was localized in epicardial intrinsic cardiac nervous system in whole mount mouse heart (Rysevaite et al., 2011a).

In dog, higher BChE activity was reported in the ventricles than in the atria. On the contrary, AChE activity was higher in the atria than in the ventricles. AChE activity was present mainly in conduction system, with the highest activity located in sinoatrial node. (Sinha et al., 1976). Recent studies showed localization of AChE in cardiac plexus of canine heart (Pauza et al., 2002)

In rat, experiments also demonstrate non-uniform distribution of AChE. The majority of its activity was found in the right atrium whereas the lowest level was detected in the ventricles (Nyquist-Battie and Trans-Saltzman, 1989). BChE contribution of total ChE activity in rat is higher than that of AChE (Nyquist-Battie et al., 1987; Stanley et al., 1978). Localization studies based on activity of ChE showed no precise localization in cryosections (Karnovsky, 1964), but confirmed the presence of AChE in cardiac plexus of whole mounted rat heart (Batulevicius et al., 2003). Electron microscopy revealed the presence of BChE in sarcoplasmic reticulum of adult rat cardiomyocytes (Karnovsky, 1964) and AChE in conducting system of embryonic and newborn rat hearts (Nakamura et al., 1994).

In human, available information are quite controversial. Sinha et al. (Sinha et al., 1976) described the highest AChE activity in the right atrium, lower activity in the left atrium and the lowest in the ventricles. They suggested that 90 % of ChE activity in human heart belongs to AChE and only 10 % belongs to BChE activity (Sinha et al., 1976). However, they used Triton detergent for homogenization (Sinha et al., 1976). According to the current knowledge, this detergent strongly inhibits BChE activity (Li et al., 2000). Jbilo et al (Jbilo et al., 1994) showed that human heart contains less AChE mRNA than BChE mRNA. Chow et al. (Chow et al., 2001) presented that BChE activity predominates over

AChE in the heart of infants. They localized AChE in the sinus and atrioventricular nodes but not in the His bundle or Purkinje fibers in infant. Further on, they observed a progressive increase of AChE-positive nerves in nodes and in branching bundles until adulthood and then a decline in elders (Chow et al., 2001). AChE was localized also in cardiac plexus of human heart (Pauza et al., 2000).

ChE activity and quantitative ChE levels are age-related (Sinha et al., 1979, 1976). In chick heart, AChE was found during the first 14 days of development, but then seemed to be replaced by BChE (Taylor, 1976). In rat, the activity of AChE in atria increased more rapidly after birth than AChE in the ventricles (Nyquist-Battie, 1990). In atrioventricular node, in the first 4 postnatal days, heart contained BChE and after 12 days AChE was predominant (Taylor, 1977). In human, the density of AChE in the conducting system increases from the infancy to adulthood and then gradually declines in the elders to a level similar to that in infancy. BChE activity seems to be the highest in the infancy and its activity decreases with advancing age (Chow et al., 2001).

1.3.3.8.2 Molecular forms of Cholinesterases in Heart

Molecular forms of ChE in adult rat heart were extensively studied. Based on the published data, monomers and dimers of AChE are present in all heart compartments, including the left atrium and the ventricles (41-45 % of total activity in these compartments) in the interventricular septum (37 % of total activity in the septum) and the intraatrial septum and the right atrium (28-33 % of total activity in these compartments). Tetrameric AChE forms represent 60-64 % of total activity in the right atrium, in the interatrial septum and 54 % in the interventricular septum. The lowest values (48 %) were detected in the ventricles and the left atrium (Nyquist-Battie and Trans-Saltzman, 1989). The asymmetric AChE form was present in all studied parts of the heart in 8-10 % of total AChE activity (Nyquist-Battie et al., 1987). It was shown, that the ratio of these molecular forms changes from the fetal to the neonatal period. The activity of asymmetric AChE forms remains relatively stable, however, the activity of other forms increases (Nyquist-Battie, 1990). Molecular forms of AChE were studied also in main components of conducting system. There were very similar quantities of molecular forms in sinoatrial and atrioventricular nodes. Monomers and dimers of AChE represent 25-30 %, tetrameric forms 67 %, and A₁₂ about 8 % of total AChE activity in heart. Despite of the similar distribution of AChE molecular forms in nodes, lower activity was detected in atrioventricular node (Nyquist-Battie and Trans-Saltzman, 1989).

It was shown, that PRiMA and ColQ transcripts are expressed in the mouse heart (Feng et al., 1999; Krejci et al., 1997; Perrier et al., 2002). Sedimentation studies in mice revealed that AChE monomers and dimers form a major fraction (about 51 %) of the enzyme forms in heart. PRiMA AChE forms about 15 %. Asymmetric form A₁₂ forms about 15 % and A₈ about 11 % of total AChE in the heart. There is also a small amount of non-amphiphilic tetramer, which probably comes from plasma. In case of BChE, there is approximately 84 % of monomers and dimers and only small percentage of total BChE form non-amphiphilic tetramers and tetramers anchored by PRiMA (Gómez et al., 1999). However, information about precise distribution of ChE molecular forms in particular components of mouse heart are still missing.

1.3.3.9 Methods for Studying of Cholinesterases

1.3.3.9.1 Biochemical analysis

When determining ChE activities, many factors have to be taken into account e.g. enzyme source, substrates, pH value, buffers, temperature or available apparatus. pH-detection methods are considered to be old-fashioned and in many cases, their sensitivity is not sufficient. Currently, the most often used methods are spectrophotometric methods. Results are precise, reproducible and there is low consumption of chemicals and biological material. Radiometric methods are more sensitive, highly reproducible, but technical equipment and sufficient safety is not available in every lab (for review see Holas et al., 2012).

One of the most commonly used colorimetric methods for determination of ChE activities is Ellman's method (Ellman et al., 1961). The principle of this method lies in a two-step reaction (Figure 13). ChE hydrolyze the substrate (ATC or BTC) and TCh is produced. The TCh interacts with Ellman's reagent (DTNB, 5,5'-dithiobis-(2-nitrobenzoic acid)) (Ellman, 1959). The product is a yellow anion (5-thio-2-nitrobenzoic acid), which has an absorbance maximum at wavelength of 412 nm. The reaction is stoichiometric, which allows for a detailed analysis of hydrolytic behavior of ChE (Ellman et al., 1961). Even though the Ellman's method is nowadays clearly the most popular method for determination of ChE activity, it does have its limitations and many modifications can be found in the literature. For example, the sensitivity of the DTNB solution to light can be affected by proper storage of the reagent in darkness (Walmsley et al., 1987). The stability of the DTNB solution is also limited. Therefore many laboratories deal with this by storing

the stock solution of the reagent at temperature of 4 °C, or alternatively at -20 °C. When working with blood samples there is also an issue with the absorbance maximum of the reaction product itself ($\lambda = 412$ nm), which overlaps with the hemoglobin Soret band in mammals ($\lambda = 415$ nm) (George and Abernethy, 1983). In order to avoid this interference, the experiments should be performed either with plasma or with serum (preventing haemolysis), or the blood samples must be diluted appropriately. Most of the optimizations of this method are related to the efforts to reduce these interferences with hemoglobin by changing the wavelength of the measurement (e.g., $\lambda = 436, 450$ nm) (George and Abernethy, 1983; MacQueen et al., 1971; Reiner et al., 2000). The following complication of Ellman's method also concerns to measuring activity in biological samples. DTNB has a specific capability to interact with molecules that contain free sulfhydryl groups, such as glutathione, albumin or hemoglobin. Some of the authors propose a 10-20 minute pre-incubation of the biological sample with the reagent, during which the interaction with free thiol groups occurs (Reiner et al., 2000). ChE activity determination can be problematic in the presence of oxims, since the non-specific yellow anion of 5-thio-2-nitrobenzoic acid can be produced. This can lead to a wrong interpretation of the results (Sinko et al., 2007).

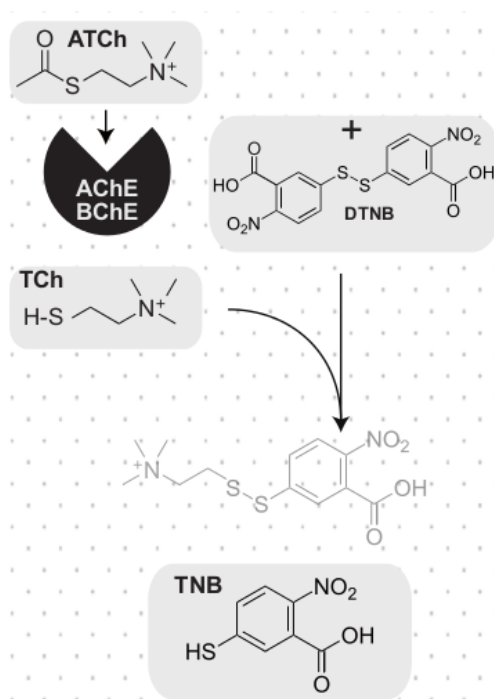


Figure 13: Principle of Ellman's reaction adapted from (Dingova et al., 2014)

Even though there is a rather large spectrum of colorimetric methods, most of the scientists use Ellman's experiment for determination of ChE activity. The main reasons are

simplicity of the methodology, the fact that it can be done very quickly, its low overall price that is linked to low consumption of chemicals and biological material, since the reaction can be done very easily even in microplates. Nowadays, the Ellman's method is also used in practice, during the evaluation of health condition in patients that frequently come into contact with organophosphate or carbamate inhibitors.

Ellman's method can also be used as a final step in determination of ChE activity based on the Enzyme-Linked Immunosorbent Assay (ELISA). ChE are rather complex antigens, thus numerous attempts to create antibodies against ChE failed. The first successful results came in form of polyclonal antibodies against AChE (Ogert et al., 1990; Wasserman et al., 1993). Only in most recent years, new selective and specific monoclonal antibodies against BChE were introduced (Hrabovska et al., 2010). ELISA proposed by us is based on catching ChE from the sample using antibody that is anchored at the immunological plate and subsequent determination of activity using Ellman's assay (Mrvova et al., 2013). This method not only allows the determination of ChE activity, but also quantification of ChE protein that is present in the analyzed sample (Mrvova et al., 2013).

The other methods with unique sensitivity, high reproducibility and accuracy are radiometric methods. Winteringham and Disney suggested determination of AChE activity based on production of acetic acid containing [C^{14}] (Winteringham and Disney, 1962). Principle of Johnson and Russell method lies in hydrolysis of [3H]-ACh and released acetate [3H] is detected. This method is extremely sensitive and it is suitable when large numbers of samples are needed to be analyzed in short time (Johnson and Russell, 1975).

1.3.3.9.2 Histochemical analysis

Koelle and Friedenwald introduced unique TCh histochemical method (Koelle and Friedenwald, 1949). This method enables acquiring of important information about localization of ChE in tissues. The method involves incubation of cryostatic sections in a medium (pH 8.0) that contains ATC iodide as a substrate, copper sulphate and glycine. The released TCh reacts with the copper salt and insoluble product is created – copper TCh (Koelle and Friedenwald, 1949). The sections can be treated with a yellow solution of ammonium sulfide in order to achieve the transformation of the white copper TCh precipitate into a brown amorphous residue of copper sulfide. To ease the precipitation and to avoid the undesired diffusion, the authors suggested saturation of slides by copper TCh prior to placing them into the staining medium. To lower the diffusion, Koelle suggested to

decrease the pH of the incubation solution to 6.4 and introduce phosphate buffer (Koelle, 1950). Later, he substituted the phosphate buffer with a maleate buffer, due to its larger buffering capacity and introduced BTC as a substrate for BChE (Koelle, 1951). Additional modifications of Koelle's method involved choosing the most appropriate pH for solutions, optimizing the concentration of sodium sulfate, replacing copper with lead or gold, going through various methods for tissue fixation, testing various incubation times etc. (for review see Naik NT, 1963).

Perhaps the most accepted innovation of the histochemical method was introduced by Karnovsky and Roots (Karnovsky and Roots, 1964). The method also utilizes TCh iodide esters as substrates, which provide TCh after hydrolysis. The TCh causes the reduction of ferricyanide to ferrocyanide, which then reacts with copper ions. It produces copper ferrocyanide (Hatchett brown), which precisely delimits areas of enzymatic activity. Copper ions are in the medium complexly bound to a citrate, in order to avoid the creation of copper ferricyanide. The produced precipitate is granular and easily visible. The authors experimented with different concentrations of chemicals and found out that 10-fold higher concentration of ferrocyanide and 3-fold lower concentration of copper ions causes massive diffusion of precipitates and nuclear staining. If pH lower than 6.0 is needed, concentration of citrate should be increased for stability of the staining solution (Karnovsky and Roots, 1964). A number of modifications of this histochemical method was presented over time. They dealt specifically with concentrations of chemicals, variation of substrates, pH of reaction mixture etc. (Tsuji and Larabi, 1983). Accepted modification by Tsuji (Tsuji et al., 2002) suggested replacement of 65 mM maleate buffer by 10 mM citrate buffer. This increased stability of the staining solution. Other modifications included only slight changes in the concentrations of ferrocyanide (from 0.5 mM to 0.47 mM) and copper ions (from 3 mM to 2.8 mM) (Tsuji et al., 2002).

Nowadays, immunohistochemistry begin to be a popular method in studying ChE localization. As mentioned in chapter ELISA (1.3.3.9.1 Biochemical Analysis), only recently, new selective and specific antibodies against ChE were introduced and thus, immunohistochemistry is increasingly used also in context of ChE localization. Detailed principle of the method is described in chapter 1.1.2.5.2 Immunohistochemistry.

2 AIMS OF PROJECT

The main objective of the project was a detail characterization of ChE in mouse heart, in term of their activities, molecular forms and precise localization.

The first aim of the project was to determine activity of AChE and BChE in individual compartments of mouse heart. We used Ellman's method. Even though the Ellman's method is nowadays clearly the most popular method for determination of ChE activity, it has some limitations, which cause problems especially when performed in biological samples. Thus, we focused on optimization of the Ellman's assay and consequently used this modified assay to determine activities of ChE in heart compartments.

The second aim of the project was to characterize the molecular forms of ChE present in different heart compartments. Biochemical method of sucrose gradients were used to determine abundance of each molecular form of ChE and their relative ratio in different heart compartment. Mouse mutant strains with specific deletion of ChE or their anchoring proteins were used to address the aim while results were compared to WT.

The third aim of the project was to localize individual molecular forms of ChE in mouse heart. Morphology of hearts was studied by hematoxylin and eosin staining. Localization of ChE was observed using activity staining in cryosections and in whole-mounted preparations, evaluated by light microscopy. Subsequently, we used specific monoclonal and polyclonal antibodies to visualize ChE, neuronal cells and endothelial cells in sections by fluorescent microscopy to address the origin of detected ChE. Similarly to the biochemical analysis, multiple mutant mice were used and compared to WT.

3 METHODS

3.1 MATERIALS AND ANIMALS

3.1.1 CHEMICALS

Chemicals used in the project were obtained from Slovak or French distribution companies. Precise specifications of particular products are referred in the text.

3.1.2 PURIFIED ENZYMES

Purified recombinant mouse AChE monomeric enzyme (rmAChE, 1 mg/ml) was used in the project in the concentration range 0.02 - 2 µg/ml. Enzyme dilutions were made in 0.1 M phosphate buffer pH 7.5. mAChE was a gift from Prof. Palmer Taylor (University of California, San Diego, La Jolla, CA, USA).

Purified recombinant human BChE monomeric enzyme (rhBChE, 10 mg/ml) (Nachon et al., 2002) was used in the project in the concentration range 0.02 - 2 µg/ml. Enzyme was diluted in 0.1 M phosphate buffer pH 7.5. rhBChE was a gift from Prof. Oksana Lockridge, PhD from Eppley Institute, University of Nebraska Medical Centre in Omaha, NE, USA.

BChE tetramer purified from human plasma (hBChE, 20 mg/ml) was used in the experiments of isothermal titration calorimetry. Enzyme was diluted in 0.1 M phosphate buffer pH 7.5. hBChE was a gift from D. Lenz (U.S. Army Medical Research Institute of Chemical Defense, Aberdeen Proving Ground, MD, USA).

3.1.3 ANTIBODIES

3.1.3.1 Primary antibodies

Rabbit polyclonal antibody against mouse AChE (George et al., 2003) diluted to 1:500 in 1 % goat serum/0.01 M phosphate buffer saline (PBS, Sigma Aldrich, P4417) was used in immunohistochemical experiments. The antibody was a gift from Prof. Palmer Taylor (University of California, San Diego, La Jolla, CA, USA).

Mouse monoclonal antibody against mouse BChE (4H1) (Hrabovska et al., 2010; Mrvova et al., 2013) diluted to 1:100 in 0.1 M PBS was used in ELISA method. Biotinylated 4H1 diluted to 1:200 in 1 % goat serum/0.01 M PBS was used in

immunohistochemical experiments. Monoclonal antibody was generated commercially by hybridoma fusion (P.A.R.I.S Production d'Anticorps & Services, Compiègne, France). One batch of antibody was also biotinylated by the company.

Mouse monoclonal antibody against mouse neuronal class III β -tubulin (TUJ1) labeled with Alexa Flour® 488 diluted to 1:500 in 1 % goat serum/0.01 M PBS was used in immunohistochemical experiments (Covance, A488-435L).

Rat monoclonal antibody against mouse platelet/endothelial cell adhesion molecule CD31 (PECAM1) diluted to 1:500 in 1 % goat serum/0.01 M PBS was used in immunohistochemical experiments (Thermo Fisher Scientific, MA140074).

3.1.3.2 Secondary antibodies

Unconjugated AffiniPure goat, anti-mouse immunoglobulin G (IgG) (Jackson Immuno Research, 115-005-003) or AffiniPure rabbit anti-mouse IgG (P.A.R.I.S, BI6297) were used in ELISA assay. Antibody diluted to 1 μ g/0.1ml was immediately applied into the wells of 96-well Nunc-Immuno-Immuno F96 Maxi-Sorp plates (Nunc GmbH & Co) and incubated for two days at 4 °C.

Goat DyLight 594 anti-rabbit IgG diluted to 1:500 in 1 % goat serum/0.01 M PBS was used in immunohistochemical experiments (Vector Laboratories DI-1594).

Goat DyLight 350 anti-rat IgG diluted to 1:500 in 1 % goat serum/0.01 M PBS was used in immunohistochemical experiments (Thermo Fisher Scientific, SA510017).

Alexa Fluor® 488-conjugated Streptavidine diluted to 1:500 in 1 % goat serum/0.01 M PBS was used in immunohistochemical experiments (Jackson ImmunoResearch, 016-540-084).

3.1.4 ANIMALS

All experiments were performed following French and Slovak guidelines for laboratory animal handling. The protocols were approved by the Ethical Committee of Université Paris Descartes in accordance with the European Community Council Directive of February 1, 2013 (82010/63/EEC registration number CEEA34.EK/AGC/LB.111.12). Three to six month old male and female WT mice and mouse mutant strains with specific deletion of ChE genes or their particular molecular forms (BChE^{-/-}, AChE del E 5+6^{-/-}, ColQ^{-/-}, PRiMA^{-/-}) were used in the experiments.

3.2 PREPARATION OF THE TISSUE SAMPLES

3.2.1 TISSUE PREPARATION

3.2.1.1 Heart Tissue Preparation

Mice were decapitated, beating hearts were dissected, cannulated through aorta and Langendorff-perfused for at least 20 minutes with Krebs-Henseleit solution oxygenated with 95 % O₂ and 5 % CO₂ at 37 °C. Freshly prepared Krebs-Henseleit solution contained 116 mM NaCl (Euromedex 885201/13S338), 4.7 mM KCl (Euromedex L11120683/12S57), 1.2 mM MgSO₄ · 7H₂O (Sigma Aldrich 043K00384), 1.1 mM CaCl₂ (Euromedex 120152451), 0.1 mM EDTA (Euromedex 120312/M330), 25 mM NaHCO₃ (Euromedex 373202355/135466), 1.2 mM KH₂PO₄ (Euromedex 1203NBVC1/13S45), 2 mM sodium pyruvate (Bio Basic Canada DU18786), 11 mM glucose (Euromedex 050810) and 1.1 mM mannitol (Bio Basic Canada 90316S335). Solution was constantly stirred and oxygenated with 95 % O₂ and 5 % CO₂.

After perfusion, hearts used for biochemical analysis were immediately dissected into the right atrium, the left atrium, the right ventricle, the left ventricle, and the septum or after atria removal, into the base, and the apex of the heart, flash frozen in liquid nitrogen and stored at -80 °C until used.

Hearts used for microscopic analysis were immediately after perfusion immersed into 3 M KCl to stop its function in diastole. Subsequently, hearts used for cryosections were placed into 20 % sucrose for 2 hours at 4 °C, followed by 2-hour immersion in 40 % sucrose at 4 °C. Hearts were then placed into molds, embedded OCT (Tissue-Tek®, Sakura®) and slowly frozen in isopentane (Sigma-Aldrich, 101306844) and dry ice at -30 °C. Tissues were stored at -80 °C or immediately cut in cryostat to 12 µm thick transversal or longitudinal sections. Sections were then mounted on SuperFrost slides (Fisher, 1820.1106). Slides were stored at -80 °C until used. Hearts used for whole-mounted hearts analysis (Figure 14) were immersed into 3 M KCl and 20 % liquid warm gelatin was injected into all four heart chambers to inflate its volume. Subsequently, hearts were placed into the ice-cold PBS, allowing gelatin to polymerize and thus keeping the hearts inflated.

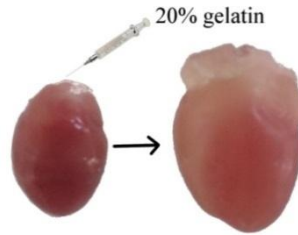


Figure 14: Injection of 20 % gelatin into chambers of the heart enables an inflation of the heart volume

Excessive gelatin was mechanically removed from the surface of hearts. Gelatin-filled hearts were then rinsed in PBS and fixed for 30 minutes at 4 °C with 4 % paraformaldehyde (PFA, Sigma Aldrich P6148) at 4 °C. For better penetration of the staining solution, hearts were incubated with hyaluronidase/0.1M PBS (0.5 mg/100 ml, Sigma Aldrich, H2126) overnight at 4 °C. Hearts were washed briefly in PBS the next day and used for further analysis.

3.2.1.2 Other Tissues Preparation

Mice were anesthetized with chloral hydrate (Sigma Aldrich, 15307), perfused transcardially with ice-cold PBS and euthanized. Brain, diaphragm and liver were dissected and flash frozen in liquid nitrogen. Plasma samples were prepared from human, mouse, rat, and dog venous blood, collected into ethylenediaminetetraacetic acid (EDTA)- or heparin- treated collection tubes (S-Monovette® EDTA K2 Gel, Sarstedt, 04.1931, or Microvette® 200 LH, Sarstedt, 20.1292) and centrifuged at 14,000g for 10 min at 4 °C. Supernatant containing plasma was flash frozen in liquid nitrogen and stored at –80 °C until use (Dingova et al., 2014).

3.2.2 EXTRACT PREPARATION

Tissues were transferred into pre-chilled 2-ml microfuge tubes containing two 5 mm stainless steel beads (Qiagen) and 5 volumes of ice-cold buffer (10 mM HEPES buffer pH 7.5 (Euromedex 933911/13S413), 10 mM EDTA, 0.8 M NaCl, and 1 % Chaps (Euromedex 22021)) and agitated for 2.5 min at frequency 25 Hz in a Mixer Mill MM 300 (Retsch). Homogenates were then centrifuged at 14,000g for 10 minutes at 4 °C and supernatants representing the extracts, were removed into pre-chilled microcentrifuge tubes and used immediately in experiments (Dingova et al., 2014). Total amount of proteins in the sample was determined using commercially available kit Pierce™ BCA Protein Assay Kit (Thermo Scientific, 23227).

3.3 BIOCHEMICAL ANALYSIS

3.3.1 ELLMAN'S METHOD

We have modified an Ellman's method (ELLMAN et al., 1961). This modification enabling detection of low ChE activities in biological samples was published in a paper Dingova et al. "Optimal detection of cholinesterase activity in biological samples: Modifications to the standard Ellman's assay" (Dingova et al., 2014).

3.3.1.1 Ellman's Reagent

Multiple batches of Ellman's reagent (DTNB) obtained from three different companies were assayed (Sigma–Aldrich, D218200, 073K3762, 013K3752, 066K0022, S39637V, 04397LJ; Merck/Calbiochem, 322123, D00090392; Pierce, 22582, OD184651). Stock solutions of 20 mM DTNB were prepared in 0.1 M sodium phosphate or in mixed 0.09 M HEPES /0.05 M sodium phosphate buffer at pH 7.0, 7.5, 8.0, or 8.5. DTNB is not soluble in HEPES buffer. Therefore, solubility was increased by adding experimentally determined 0.05 M sodium phosphate buffer with matching pH. For simplicity, we refer to this solution as HEPES buffer in this thesis. All solutions were prepared freshly before use.

3.3.1.2 Stability Assays

Stability assays were performed in triplicates in 96-well plates at room temperature protected from light. Sodium phosphate buffer (sodium phosphate dibasic: Euromedex, 02783493 and disodium phosphate dibasic Euromedex, 310311, pH 7.0–8.5, with final concentration 0.1 M) and HEPES buffer (Euromedex, 933911/13S41 and Sigma–Aldrich, SLBB0907V, pH 7.0–8.5, with final concentration 5 Mm) were used in the assays.

Stability of 0.5 mM DTNB was tested with or without the presence of 1 mM BTC (Sigma–Aldrich, B3253, 055K2625) over a period of 3 days by measuring the increase in absorbance at 412 nm.

TCh was produced by hydrolysis of 1 mM ATC (Sigma–Aldrich, 01480) catalyzed by 60 µl of human plasma or 0.3 µg of rmAChE (in a 30-µl volume) in a total reaction volume of 1 ml. After 1 hour of incubation at room temperature, the reaction was stopped by the addition of the AChE inhibitor, 1 µM 1,5-bis(4-allyldimethylammoniumphenyl)pentan-3-one dibromide (BW) (Sigma–Aldrich, A9013).

BChE in the human plasma was inhibited by 20 μ M tetraisopropyl pyrophosphoramidate (iso-OMPA) (Sigma–Aldrich, T1505). Stability of the intermediate product, TCh, was tested in 0.1 M phosphate buffer (pH 7.5 or 8.0) and 5 mM HEPES buffer (pH 7.5) by the addition of 20 mM DTNB to a final concentration of 0.5 mM at time points 1, 2, 3, and 4 hours after the addition of inhibitors. Increase in absorbance was measured at 412 nm. The experiment was repeated four times with human plasma and three times with rmAChE.

Stability of the yellow product, TNB, was assayed by following change of absorbance at 412 nm after 1, 2, 3, and 4 hours at 25 °C. The experiment was repeated four times.

3.3.1.3 Standard Ellman’s Assay (EA)

Enzyme was preincubated with 0.5 mM DTNB for 15 minutes. rhBChE activity was assayed in duplicates or triplicates in 0.1 M sodium phosphate buffer (pH 7.5) or 5 mM HEPES buffer (pH 7.5) in the presence of 1 mM BTC (Figure 15A). Increase in the intensity of the yellow color was recorded at 412 nm in a BioTek Synergy™ H4 Hybrid Multi-Mode Microplate Reader at 15-second intervals for up to 20 minutes. Activity of rmAChE was followed at the same conditions using 1 mM ATC as substrate. When AChE activity was measured in mouse brain extracts, BChE activity was inhibited by 20 μ M iso-OMPA after 20 to 30 minutes of pre-incubation. In a parallel sample, BChE activity was measured using BTC to verify the inhibition. As an alternative, a specific reversible inhibitor of BChE may be used, especially in samples with higher BChE activity.

3.3.1.4 Modified Two-Step Ellman’s Assay (2s–EA)

BChE-catalyzed hydrolysis of 1 mM BTC was performed in 0.1 M sodium phosphate buffer or 5 mM HEPES buffer. The reaction was conducted in duplicates or triplicates at seven different time points, and each time point was performed in an independent well of a 96-well plate (i.e., 14 independent wells). An additional well contained no substrate and served as a control. DTNB (0.5 mM) was added to the wells subsequently in 2-minute intervals, and absorbance was measured immediately at 412 nm (Figure 15B). Alternatively, the ChE inhibitor neostigmine (3 mM, Sigma Aldrich, N2001) was added together with the DTNB solution to stop the reaction. AChE activity was determined with 1 mM ATC as substrate after 30 minutes of preincubation with 20 μ M BChE inhibitor iso-OMPA.

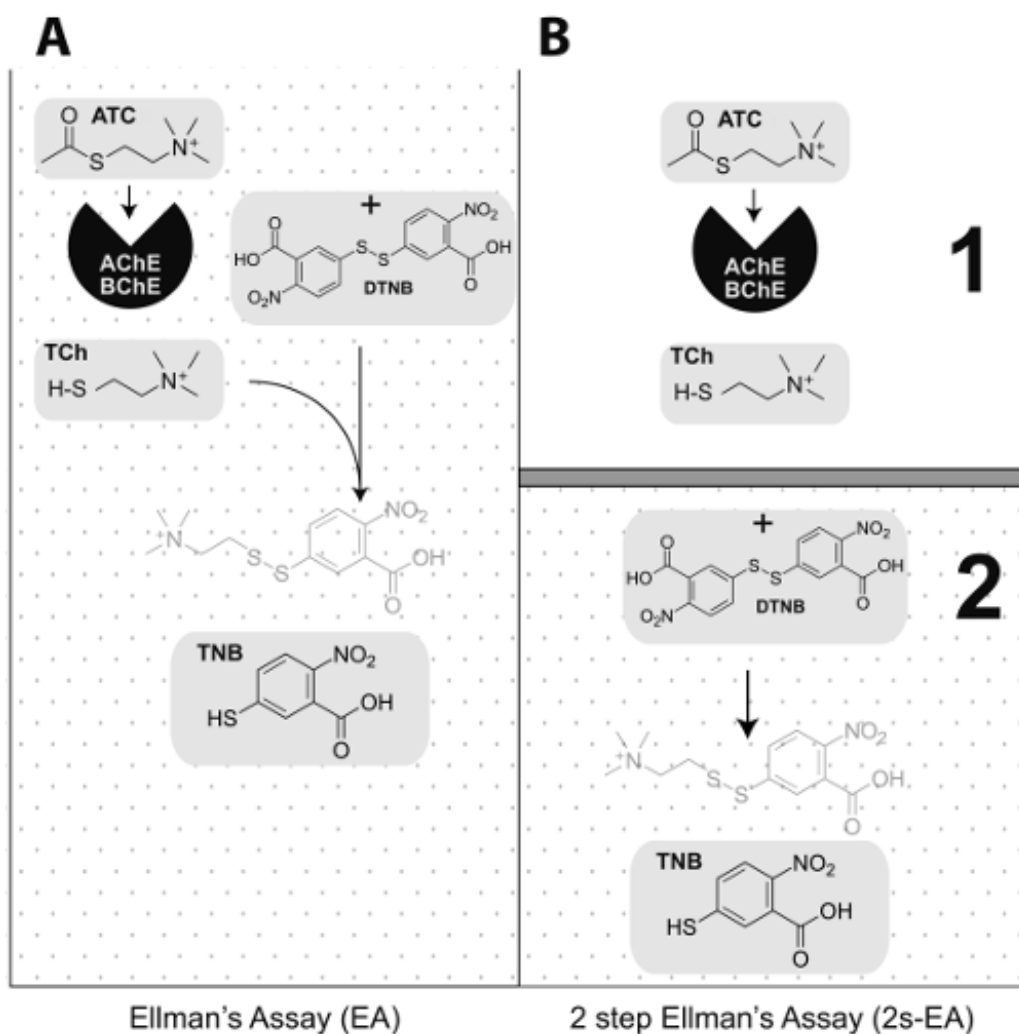


Figure 15: A: Principle of standard Ellman's assay, B: Principle of modified Ellman's assay

3.3.1.5 Alteration of BChE Activity in Presence of DTNB

An effect of DTNB on the activity of rhBChE was examined by two approaches. First, rhBChE activity was measured by EA in 0.2 M phosphate buffer (pH 7.5) using DTNB in the concentration range from 0.2 to 40 mM. An increase in the absorbance at 412 nm was recorded every 6 seconds for up to 10 minutes. rhBChE activity obtained for different DTNB concentrations was evaluated as a percentage of rhBChE activity obtained with 0.2 mM DTNB. Experiments were performed in triplicates and repeated 10 times. Second, rhBChE activity was measured 2s-EA and by EA using six different DTNB concentrations (0.5–30 mM). For each DTNB concentration, 2s-EA and EA were performed in the same 96-well plate. rhBChE activities obtained by EA were evaluated as percentage of 2s-EA of the same DTNB concentration. All experiments were performed in triplicates and repeated three times.

3.3.2 ISOTHERMAL TITRATION CALORIMETRY

Isothermal titration calorimetry is quantitative technique used in the studies of biomolecular interactions. It enables to determine thermodynamic parameters of the interactions in the solution by direct measuring of the heat generated or absorbed during a biomolecular binding.

DTNB was prepared in 0.1 M phosphate buffer (pH 7.5). Isothermal titration calorimetry measurements were carried out using an iTC200 calorimeter (GE Healthcare). A 27- μ M solution of hBChE in 0.1 M phosphate buffer (pH 7.5), in volume 200 μ l was added to the sample cell, and a 20 mM solution of DTNB was loaded into the injection syringe. For each experiment, a 60-second delay at the experiment was followed by 19 injections of 2 μ l of the titrant solution spaced 120 seconds apart. The sample cell was stirred at 1000 rpm throughout and maintained at a temperature of 25 °C. Control titration was performed by injecting DTNB into buffer. The area under each peak of the resultant heat profile was integrated, normalized for DTNB concentrations, and plotted against the molar ratio of DTNB to enzyme using Origin (version 7) supplied with the instrument. Data were analyzed according to a “one set of sites” binding model at low values of c (Turnbull and Daranas, 2003) (the ratio of hBChE concentration and the dissociation constant K_D) with the stoichiometry parameter, n , fixed to 1.0 (Dingova et al., 2014).

3.3.3 SUCROSE GRADIENTS

Principle of the method is based on different distribution of sediments containing different molecular forms of ChE in sucrose gradient during ultracentrifugation. It is routinely used in the study of molecular forms of ChE in biological samples, e.g., brain (Perrier et al., 2002) and neuromuscular junction (Bernard et al., 2011).

3.3.3.1 Sample Preparation and Separation Procedure

Each sample contained 200 μ l of tissue extract, 200 μ l of extraction solution and sedimentation standards: 10 μ l of β -galactosidase (Sigma Aldrich, SLBC2016V) and 2 μ l of alkaline phosphatase (Sigma Aldrich, 039K4000). Prepared mixture (400 μ l) was applied on a top of 5-20 % sucrose gradient containing 10 mM HEPES buffer pH 7.5; 0.8 M NaCl; 10 mM EDTA and 0.2 % BRIJ (Sigma Aldrich 388866) or 1 % CHAPS.

Gradients were inserted into pre-chilled rotor SW41 and centrifuged during 17 hours at 38 000 rpm and 7 °C in Beckman Coulter Optima LE-80K.

Fractions were collected using peristaltic pump (GILSON, MINIPULS 3) and fraction collector (GILSON, FC 2013B) into approximately 48 wells containing 250 µl per well (Greiner bio-one, 655101). Content of each well was then distributed by a multichannel pipette into another plates for further analysis; AChE and BChE activities (80 µl each), activities of sedimentation standards β-galactosidase and alkaline phosphatase (40 µl each). AChE and BChE activities were determined by 2s-EA at 415 nm using BIO-RAD model 680. Activity of β-galactosidase was determined using 3.15 % 2-Nitrophenyl β-D-galactopyranoside (Sigma Aldrich 1430992V) in 0.1 M NaCl, 0.1 M HEPES buffer pH 7.5 and 0.01 M MgCl₂. Activity of alkaline phosphatase was detected in the presence of 1.35 % p-nitrophenyl phosphate (Sigma Aldrich BCBK7060V) in 0.01 M MgCl₂ and 0.1 M TRIS buffer pH 8.0). Activities of sedimentation standards were determined at 415 nm using BIO-RAD model 680.

3.3.3.2 Evaluation of the Results

Based on the peaks of sedimentation standards, sequences of fractions were converted into Svedberg units - S. Molecular forms were assigned to the position of peaks produced in BRIJ detergent following paper Bernard et al., 2011. Peak positions with corresponding molecular forms of ChE are listed in the Table 1 and Table 2. When CHAPS detergent was used, a shift of amphiphilic forms was observed.

Table 1: Position of peaks of AChE molecular forms in BRIJ detergent

Peak position (S)	Molecular forms of AChE
16.1	A ₁₂ – 3 tetramers AChE anchored by ColQ
12.5	A ₈ – 2 tetramers AChE anchored by ColQ
10.5	G ₄ ^{na} – non-amphiphilic AChE tetramers
9.2	G ₄ ^a - amphiphilic AChE tetramers (PRiMA anchored AChE)
4.5	G ₂ ^a / G ₁ ^{na} - amphiphilic dimers or non-amphiphilic monomers
2.4	G ₁ ^a - amphiphilic monomers

Table 2: Position of peaks of BChE molecular forms in BRIJ detergent

Peak position (S)	Molecular forms of BChE
12.5	G₄^{na} - non-amphiphilic BChE tetramers
12.5	G₄^a - amphiphilic AChE tetramers (PRiMA anchored BChE)
4.5	G₁^a - amphiphilic monomers

Program FITYK 0.9.8 (<http://fityk.nieto.pl/>) was used to evaluate the percentage of each molecular form of ChE in individual parts of heart.

3.3.4 ELISA METHOD

Assay was performed as described previously (Hrabovska et al., 2010; Mrvova et al., 2013). Each well of a 96-well Nunc–Immuno F96 Maxi-Sorp plate (Nunc) was coated (48 hours incubation at 4 °C) with 1 µg of affinity pure anti-mouse IgG in a final volume of 100 µl adjusted with 0.05 M phosphate buffer (pH 7.4) and 0.15 M NaCl. Plates were then blocked with 0.1 % bovine serum albumin for a minimum of 48 hours at 4 °C and incubated overnight at 4 °C with primary antibody 4H1 against mouse BChE, followed by 6 hour incubation with mouse diaphragm extract at room temperature. After each incubation, the plates were washed with 0.01 M phosphate buffer (pH 7.4) and 0.05 % Tween in Wellwash 4 Mk 2 (Thermo) or ELx50™ Microplate Strip Washer (BioTek). Signal was revealed as BChE activity and measured using EA at pH 7.5. Experiments were performed in triplicates, repeated three times (Dingova et al., 2014).

3.4 MICROSCOPIC ANALYSIS

3.4.1 HEMATOXYLIN AND EOSIN STAINING

Slides containing transversal sections of heart (prepared as described in 3.2.1.1 Heart Tissue Preparation) were defrosted before staining. Sections were then fixed in 4 % PFA for 15 minutes at room temperature and washed in distilled water. Nuclei were stained with hematoxylin (DIAPATH Microstain division) for 8 minutes. Slides were washed in running tap water for few minutes, rinsed with distilled water and dipped 10 times briefly in 95 % ethanol. Counterstaining was performed with eosin Y (Merck, K14934655) (30 seconds) and rinsed thoroughly in distilled water. Slides were dehydrated in graded alcohol (50 – 100 %, 2 baths for each grade) for 5 minutes, cleared with xylene substitute Ottix (DIAPATH Microstain division) for 10 minutes and mounted with Eukitt® (Sigma-Aldrich, 03989). All steps were performed at room temperature. Staining was observed by light microscopy (Olympus BX61). Cardiomyocyte diameters were measured using program Corel. We obtained 135 ± 45 values from each heart. Statistical analysis was performed by T-test.

3.4.2 TSUJI'S ACTIVITY STAINING METHOD

3.4.2.1 Cryosections

Slides with transversal and longitudinal sections (prepared as described in 3.2.1.1 Heart Tissue Preparation) were defrosted before staining and fixed with 4 % PFA for 15 minutes at room temperature. Slides were then pre-incubated for 30 minutes with inhibitors of ChE. Subsequently, sections were stained for AChE or BChE activity by modified Karnovsky and Roots staining procedure (Tsuji et al., 2002). Shortly, slides were incubated at room temperature for 6 hours in staining solution containing 15 mM citrate buffer pH 5.3, 2.8 mM CuSO_4 , 0.47 mM K_3FeCN_6 , 1.7 mM substrate and ChE inhibitor. AChE activity was revealed with substrate ATC in the presence of BChE inhibitor iso-OMPA ($2 \cdot 10^{-5}$ M). BChE activity was visualized with substrate BTC. Negative control contained AChE inhibitor BW ($1 \cdot 10^{-6}$ M) and BChE inhibitor iso-OMPA ($2 \cdot 10^{-5}$ M). Slides were washed in 0.01 M citrate buffer, pH 5.3 at room temperature, gradually dehydrated in ethanol (50 – 100 %), immersed in xylene substitutes for 10 minutes at room temperature

and mounted with Eukitt® medium. Activity was visualized by light microscopy (Olympus BX61) and pictures were processed in Adobe Photoshop or GIMP.

3.4.2.2 Whole-mounted heart

Activity staining of gelatin-filled heart (prepared as described in 3.2.1.1 Heart Tissue Preparation) followed the same procedure as described in the chapter 3.4.2.1 Cryosections, with exception for the omitted initial fixation and the incubation being shortened to 3 hours at room temperature. Subsequently, hearts were properly washed and post-fixed in 4 % PFA. Hearts were then placed into a Petri dish filled with distilled water and observed using light microscopy (Olympus BX61). As these preparations were 3D objects, multiple pictures with consecutive planar focuses were used for the final pictures, which were composed using extended depth of field in ImageJ program and processed in Adobe Photoshop or GIMP.

3.4.3 IMMUNOHISTOCHEMISTRY

Slides containing transversal and longitudinal sections of the heart (prepared as described in 3.2.1.1 Heart Tissue Preparation) were defrosted before staining and fixed with 4 % PFA for 15 minutes at room temperature. Sections were traced with Dako pen (Dako, S2002). Slides were covered with 50 mM glycine for 10 minutes and subsequently washed with PBS. Dehydration of slides was performed by graded ethanol 50-100 % (each grade for 5 minutes). For better penetration of antibodies, Dent's solution (DMSO:CH₃OH in a ratio 1:4) was applied for 15 minutes. To enhance fluorescence contrast, 30 % H₂O₂:Dent's solution in a ratio 1:4 was applied for 1 hour. Samples were rehydrated in ethanol (100-50 %) and washed 3 times for 5 minutes in PBS. Non-specific sites were blocked with 5 % goat serum diluted in PBS for 30 minutes and subsequently washed 3 times for 5 minutes with PBS. After 2-hour incubation with primary antibodies (described in the chapter 3.1.3 ANTIBODIES), the slides were washed 5 times for 5 minutes. Secondary antibodies (described in the chapter 3.1.3 ANTIBODIES) were applied for 30 minutes and the slides were thoroughly washed with PBS for 1 hour (solution was changed every 10 minutes). Slides were then mounted with Fluoroshield (Sigma-Aldrich, F6182) or with Fluoroshield with DAPI (Sigma-Aldrich, F6057). All steps were performed at room temperature, protected from light. Results were observed with fluorescence microscopy (Nikon Eclipse Ni-U) and pictures were processed in Adobe Photoshop or GIMP.

4 RESULTS

4.1 ACTIVITY OF CHOLINESTERASES IN HEART

Activities of ChE in the individual compartments of mouse heart have not been studied until now. In this thesis, we determined activity of AChE and BChE in the right atrium, the left atrium, the right ventricle, the left ventricle, the septum, the apex and the base of the heart. The activities were measured by 2s-EA that we optimized to study native ChE in biological samples.

4.1.1 OPTIMIZATION OF ELLMAN'S METHOD

Ellman's method is the most commonly used method to measure ChE activity. However, it has some limitations. The most important limiting factors of the Ellman's method are sensitivity of DTNB to light, instability of the DTNB solution over time, high background in biological samples due to the interactions with abundant free sulfhydryl groups, and low detection sensitivity that does not allow detecting low ChE activities. Here, we present optimization of Ellman's method to study ChE in biological sample even at low activity levels. Results introduced in this chapter were described in paper Dingova et al. "Optimal detection of cholinesterase activity in biological samples: Modifications to the standard Ellman's assay" (Dingova et al., 2014).

4.1.1.1 Stability of Ellman's reaction

Measurement of low AChE or BChE activity in tissue homogenates with the Ellman's method often requires prolonged incubation times. A large fraction of the yellow color that slowly develops during the prolonged incubation times is an artifact unrelated to ChE activity. We had observed that replacement of phosphate buffer by HEPES buffer significantly reduced background color. To further define the favorable conditions, we analyzed the stability of the Ellman's mixture (BTC, DTNB), intermediate product (TCh), and final product (TNB) in phosphate and HEPES buffers in the pH range from 7.0 to 8.5. As shown in Figure 16, the velocity of the hydrolytic reaction decreased with the reduction of the pH within our selected range, but the product formation is independent on the pH and the choice of buffer (phosphate vs. HEPES).

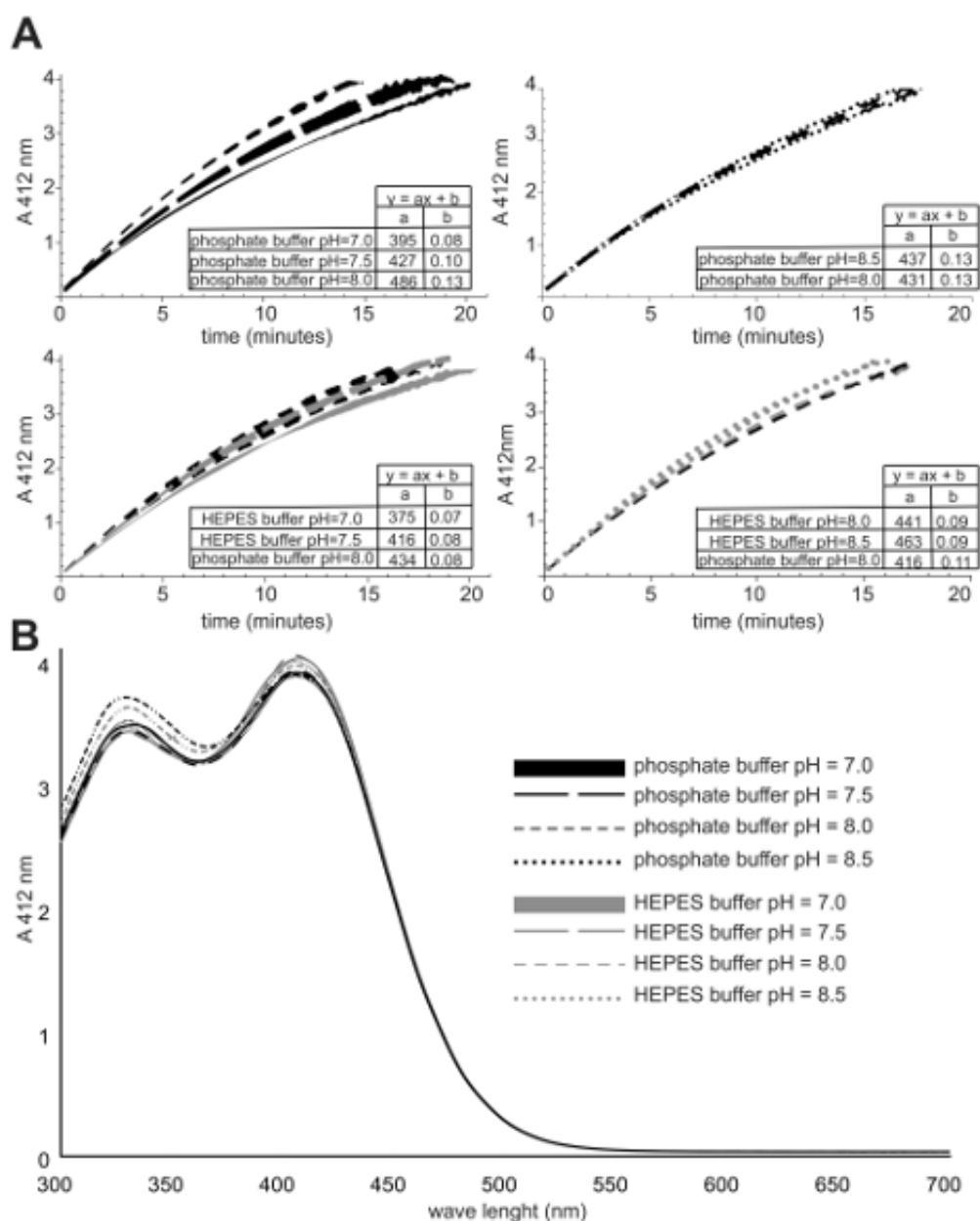


Figure 16: Effect of phosphate and HEPES buffers on product formation: Phosphate buffer pH 8.0 was suggested as the buffer of choice in the original paper (Ellman et al., 1961). We compared velocity of TNB formation in presence of mentioned phosphate buffer pH 8.0 and other studied buffers (A). Velocity of BTC hydrolysis by rhBChE is similar in all buffers, though the reaction rate increased slightly with increasing pH. The velocity of the product formation was almost identical in phosphate buffer pH 8.0, HEPES buffer pH 7.5 and HEPES buffer pH 8.0 formed at the same wave length (B) in all studied buffers. Course and velocity of product formation is almost identical with phosphate buffer pH 8.0 in case of HEPES buffer pH 7.5 and 8.0.

4.1.1.1.1 Stability of thiocholine

After 4 hours of incubation in 0.1 M sodium phosphate buffer (pH 7.5) (Figure 17A), the concentration of TCh, measured as color intensity after the addition of DTNB, was 7.4 % lower compared with the 1-hour time point. This instability of TCh was even higher (10 % lower color intensity) in 0.1 M sodium phosphate buffer (pH 8.0), in agreement with the pKa value of the TCh (7.7–7.8) (Barakat et al., 2009). In contrast, incubation in 5 mM HEPES buffer (pH 7.5) for 4 hours caused less than 1.5 % change in the apparent TCh concentration, suggesting better stability of TCh in HEPES buffer than in phosphate buffer. Thus, TCh, the first intermediate of the reaction, appears to be a very stable compound in HEPES buffer.

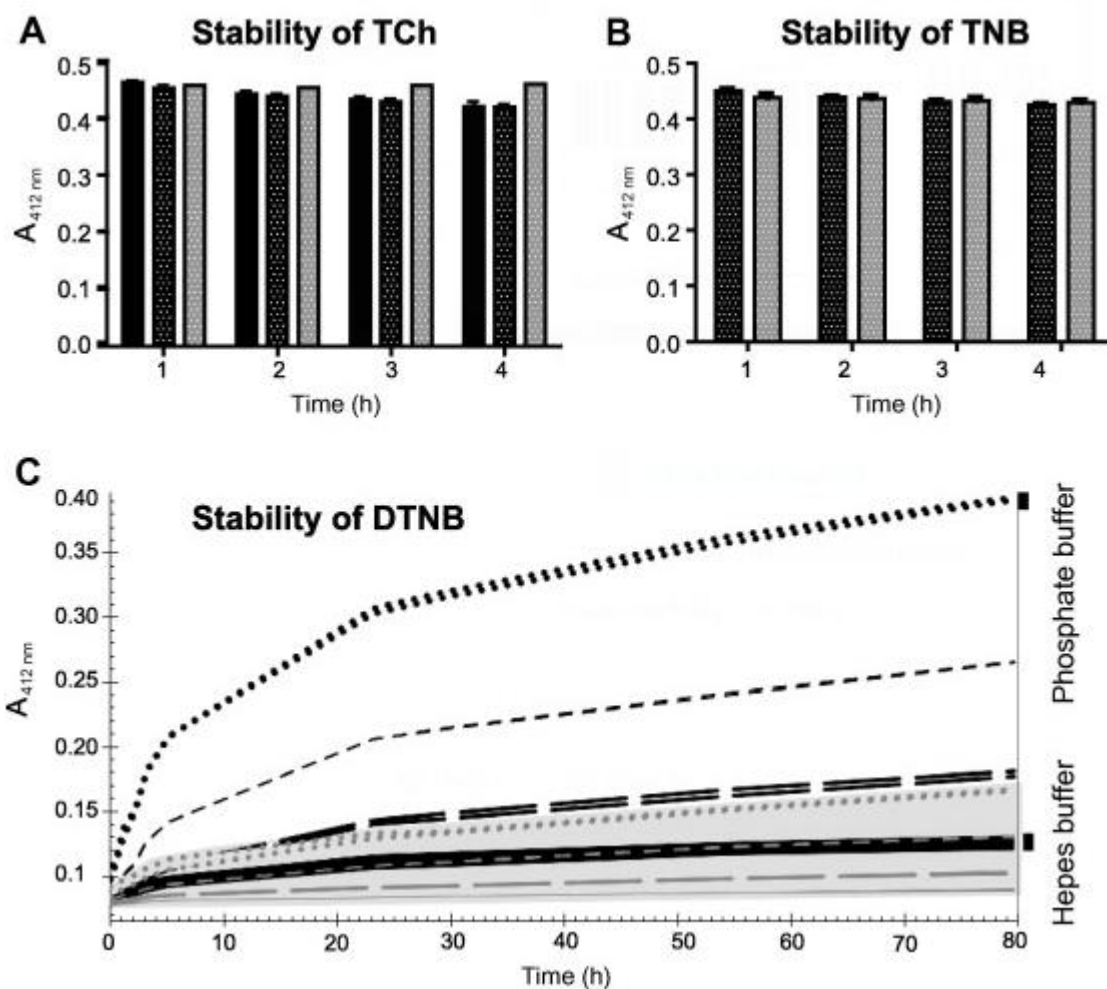

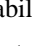
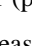



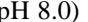

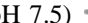




Figure 17: Stability of components of Ellman's reaction: TCh (A), TNB (B), and DTNB (C) in phosphate and HEPES buffers. A trend of decreasing stability of TCh in the presence of phosphate buffer (pH 7.5 , pH 8.0 ) was observed. This effect was not demonstrated in HEPES buffer (7.5 ) . TNB stability was unchanged in HEPES buffer (pH 7.5). However, we observed slight instability in phosphate buffer (pH 7.5). DTNB is more stable in HEPES buffer than in phosphate buffer. Stability decreased with increasing pH

values. Phosphate buffer: (pH 7.0) , (pH 7.5) , (pH 8.0)  and (pH 8.5) ; HEPES buffer: (pH 7.0) , (pH 7.5) , (pH 8.0)  and (pH 8.5) . Figures depict mean values of triplicates with standard deviations. Stabilities of TCh and TNB were tested four times, and stability of DTNB was examined seven times.

4.1.1.1.2 Stability of DTNB

DTNB dissolves in phosphate buffer but not in HEPES buffer. We evaluated conditions to increase DTNB solubility in HEPES buffer. Solubility may be achieved in methanol, ethanol, or dimethyl sulfoxide (DMSO). However, their inhibitory effect on ChE activities (Fekonja et al., 2007; Hamers et al., 2000; Pohanka et al., 2011) makes organic solvents unsuitable for activity assays. We solubilized DTNB in HEPES buffer (0.09 M) by adding 0.05 M sodium phosphate buffer to make a stock 20 mM DTNB solution (as described in the chapter 3.3.1.1 Ellman's reagent). The final concentrations in the reaction or stability incubation mixtures were then 1.25 mM phosphate and 5 mM HEPES buffer.

The stability of DTNB depended strictly on the pH in both buffers; the higher the pH, the lower the stability of DTNB (Figure 17C). The highest increase in the absorbance was observed within the first 5 hours. Absorbance continued to increase during the 80-hour testing period but at a lower rate.

In general, DTNB is more stable in HEPES buffer than in phosphate buffer. Absorbance of DTNB in HEPES buffer (pH 7.0 or 7.5) was close to baseline. DTNB stability in HEPES buffer (pH 8.0) was comparable to that in phosphate buffer (pH 7.0). DTNB in HEPES buffer (pH 8.5) was more stable than that in phosphate buffer (pH 7.5).

The presence of BTC did not change the observed dependence on pH but increased the absolute values of measured absorbance approximately 3.5-fold higher in the presence of 0.5 mM BTC and 7-fold higher in the presence of 1 mM BTC.

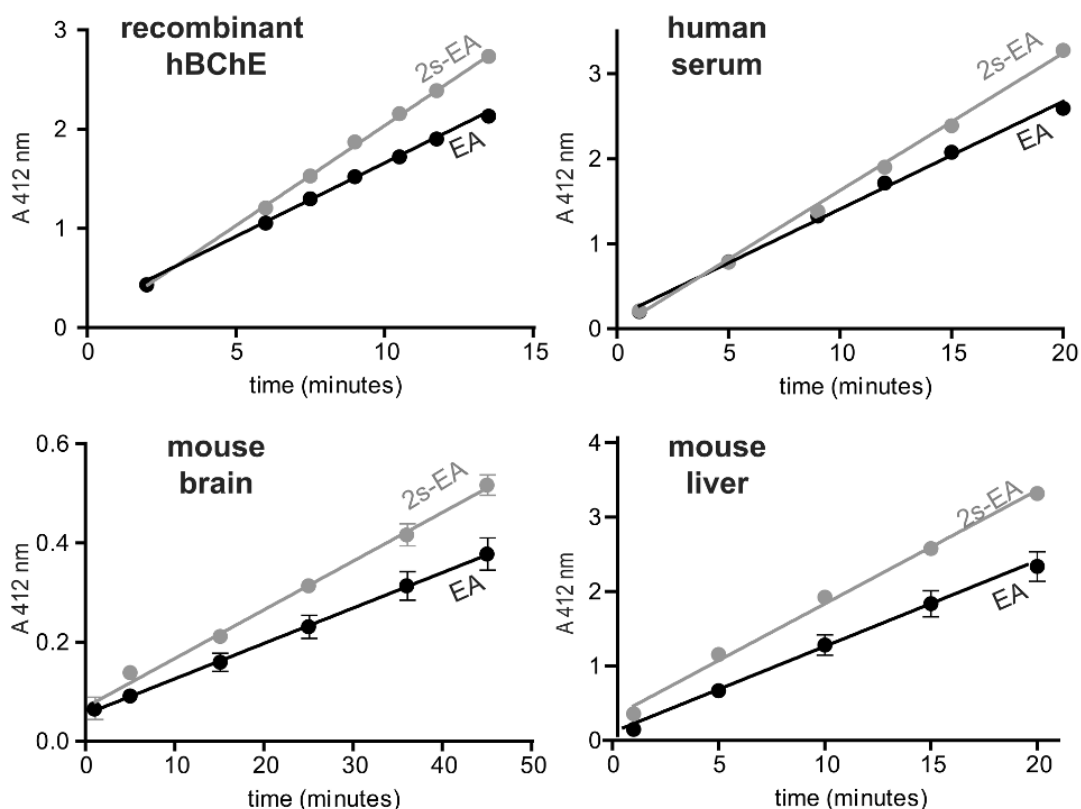
4.1.1.1.3 Stability of TNB

The final product of Ellman's reaction, TNB, was stable over 4 hours at room temperature. We saw only a slight decrease in color (5.4 %) when incubated in phosphate buffer (pH 7.5) and no change in HEPES buffer (pH 7.5) (<1.8 %) (Figure 17B). It is important to note that the final product is highly sensitive to light (Walmsley et al., 1987), and it is essential to maintain the reaction mixture in the dark during the whole experiment. In the absence of light protection, the decrease of TNB colors exceeded 10 % by hour.

4.1.1.2 Modification of Ellman's assay

The higher stability of TCh compared with DTNB suggested that the assay could be improved by separating the two reactions into two steps. In our modified 2s-EA, the first step is substrate hydrolysis by ChE (with no DTNB present in the mixture). In the second step, DTNB is added at different times, followed by measurement of absorbance at 412 nm (Figure 15B). An alternative second step is to stop the reaction by the addition of a ChE inhibitor and to delay the quantification of product by the addition of DTNB later.

Interestingly, we observed that in 2s-EA for rhBChE (regardless of the substrate ATC or BTC) the slope of the increase of absorbance was steeper than that in EA (reaction incubated in the presence of DTNB from time 0). The increase in the slope value represented 20 to 25 % for rhBChE, human plasma, mouse plasma, mouse brain extract, and mouse liver extract (Figure 18). This two-step approach, thus, eliminates a factor of instability of DTNB over the time of incubation and possible DTNB interaction with ChE.



	$\Delta A/\text{minute}$			$\Delta A/\text{minute}$	
	EA	2s-EA		EA	2s-EA
recombinant hBChE	0.148	0.202	human serum	0.126	0.161
mouse brain	0.007	0.010	mouse liver	0.115	0.152

Figure 18: Comparison of BChE activity measured by EA (●) and 2s-EA (●). In EA, DTNB is present from time 0. In 2s-EA, DTNB is absent during BTC hydrolysis but is added at different times of the reaction or after the reaction is stopped (see Figure 15B). Thus, DTNB is not present in the reaction mixture during the product formation. We observed a steeper increase in absorbance at 412 nm in 2s-EA than in EA with rhBChE, human plasma, mouse brain extract, and mouse liver extract. Figure panels show mean values of duplicates with standard deviations. Experiments were repeated at least three times, and with rhBChE 20 times, using DTNB from various sources.

Surprisingly, BTC hydrolysis in rat or dog plasma was unaffected by the presence of DTNB (Figure 19). Moreover, we did not observe such phenomena for AChE. The slopes of absorbance increase with time for ATC hydrolysis with no DTNB in the reaction mixture was comparable to that in the presence of DTNB (Figure 19).

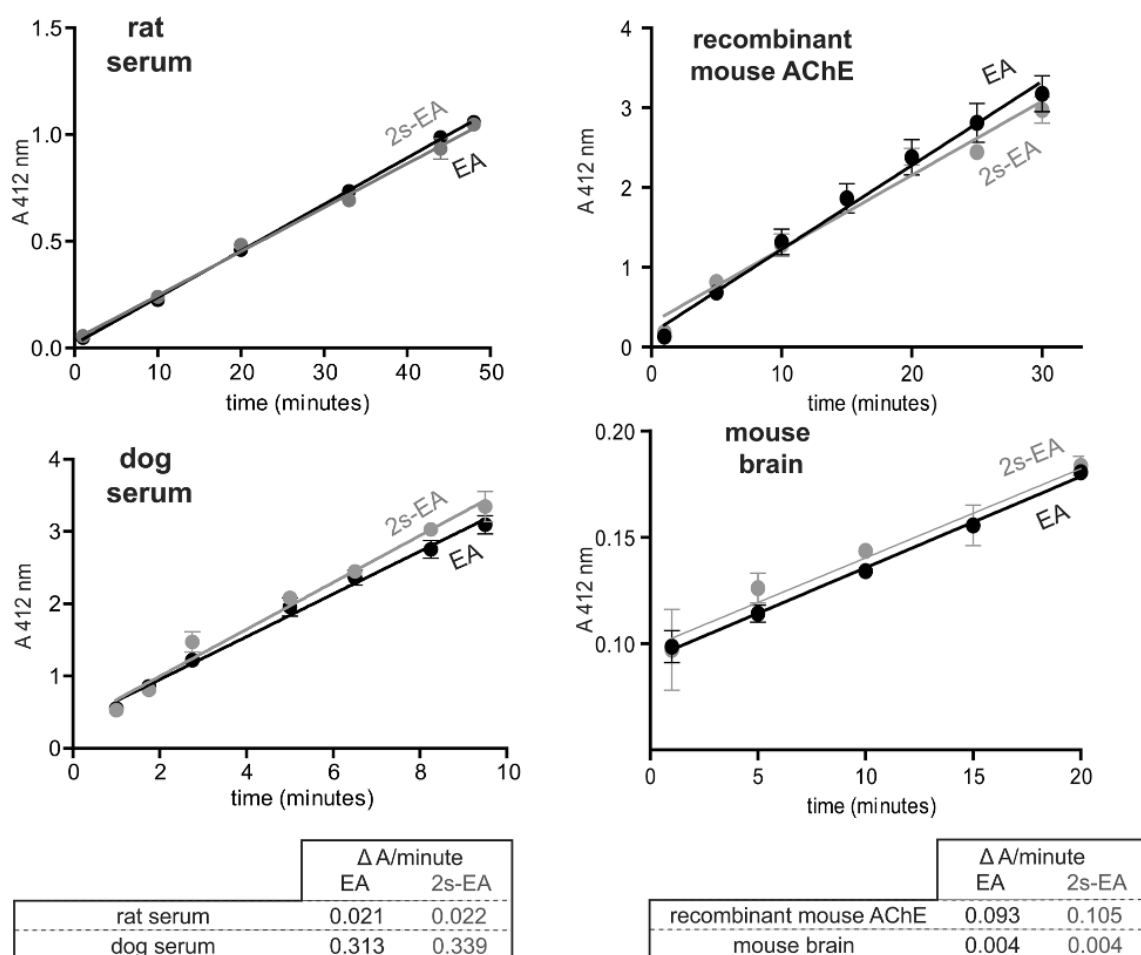


Figure 19: Rat and dog BChE activity is not affected by DTNB. In contrast to mouse and human, no difference between standard EA (●) and 2s-EA (●) was observed in rat plasma and dog plasma. Figure panels depict mean values of duplicates with standard deviations. Experiments were repeated twice.

AChE activity measured by standard EA (●) and 2s-EA (●). We observed no difference between results obtained by the two types of assays for rmAChE or extract from mouse brain. Figure panels show mean values of duplicates with standard deviations. Experiments were repeated twice.

4.1.1.3 Interaction of BChE and DTNB

Results from the modified 2s-EA (Figure 18) suggest interference of DTNB with BChE-catalyzed hydrolysis of BTC. Therefore, we examined the effect of DTNB on activity of purified rhBChE monomer using EA and 2s-EA. First, we evaluated the variation of optical density when the EA is performed with different concentrations of DTNB. As shown in Figure 20A, we observed a reduction of the slope with increasing DTNB concentrations. To compare more directly the effect on DTNB, we measured the variation of optical density using 2s-EA versus the EA at different concentrations of DTNB. As shown in Figure 20B, the 2s-EA was independent of the concentration of DTNB; the slope (gray line) is identical at all studied DTNB concentrations. In contrast, when the EA is performed with different concentrations of DTNB, the slope is reduced according to the concentration of DTNB in the reaction. Measurements from both procedures lead to an apparent reduction of 50 % rhBChE activity at 10 mM DTNB (Figure 20).

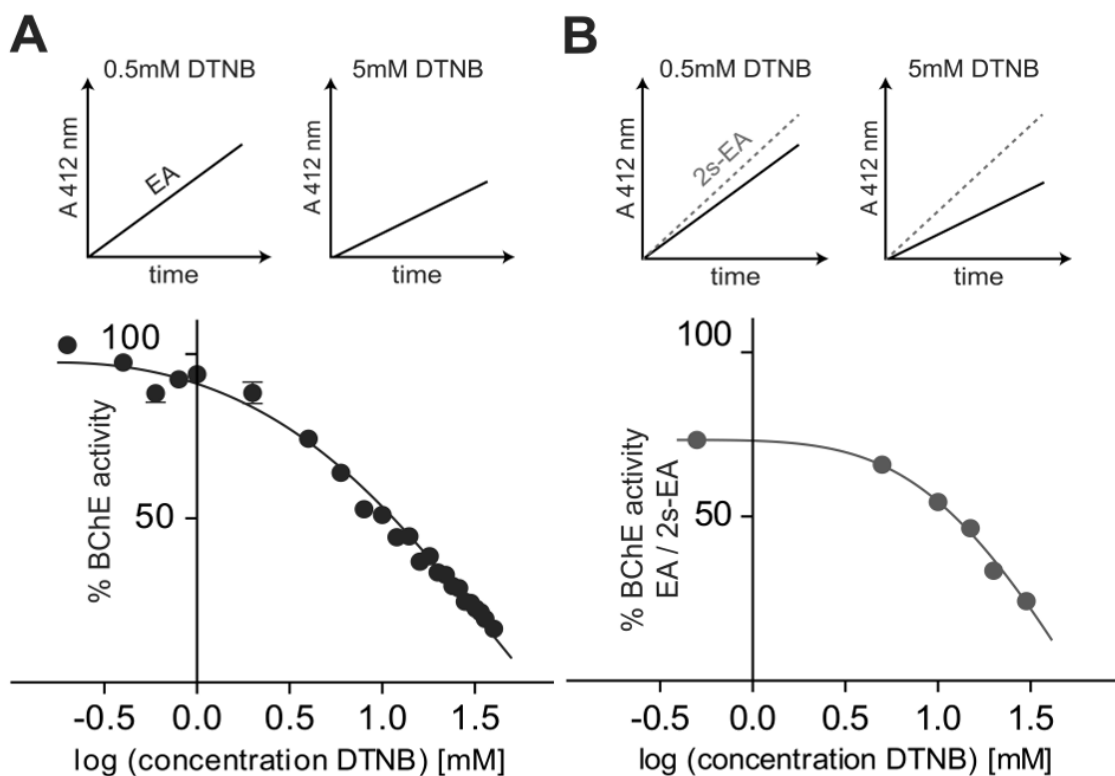


Figure 20: Interaction of DTNB with rhBChE: Effect of increasing concentrations of DTNB on rhBChE activity using standard EA (A) and 2s-EA (B). In both cases, 50 % of rhBChE activity is decreased in the presence of 10 mM DTNB. The figures are constructed from the mean values of triplicates. Results were confirmed in 10 (A) and 3 (B) independent experiments. The commonly used DTNB concentration is 0.5 mM (log -0.3 on the scale).

Direct interaction of DTNB with hBChE was confirmed by isothermal titration calorimetry that measures changes in heat that occur during complex formation. The thermogram describing the binding of DTNB to hBChE was compared with the control experiment in which the heat of dilution of DTNB into the buffer was followed (Figure 21). The interaction of DTNB with the enzyme was exothermic, releasing heat during complex formation. The magnitude of each peak diminished with progression of the titration, suggesting that interaction was taking place. In contrast, injections of DTNB into the buffer generated peaks of constant magnitude within the titration, reflecting the heat of dilution of ligand into buffer.

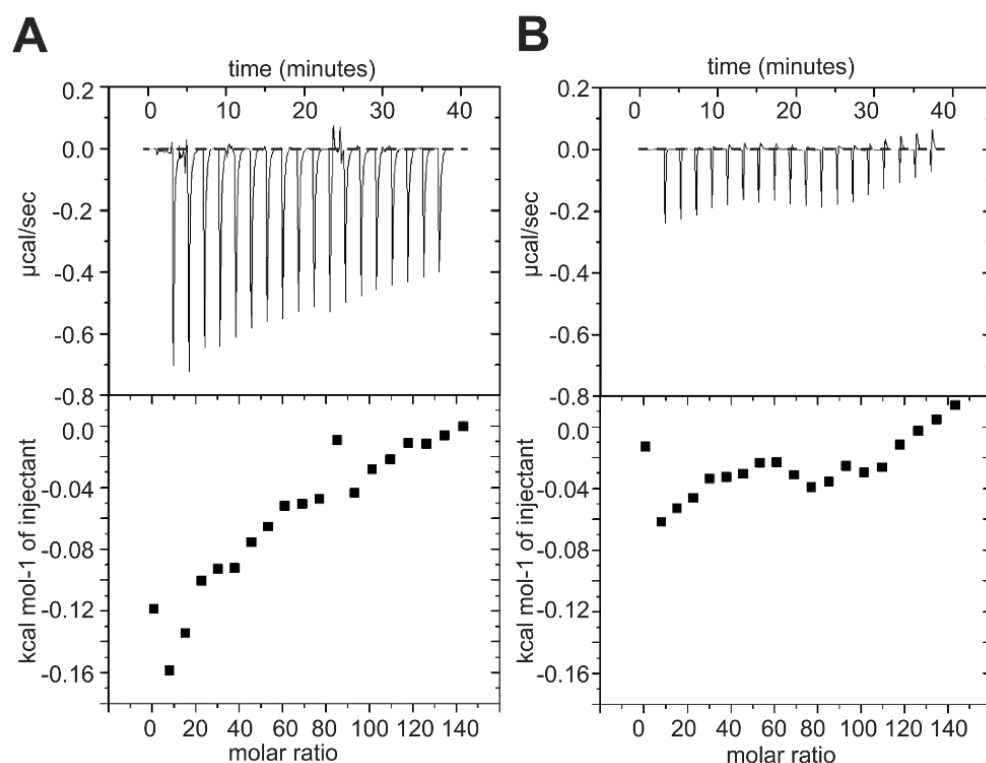


Figure 21: Data from the isothermal titration calorimetry for (left) the DTNB/hBChE interaction and (right) DTNB/phosphate buffer dilution: The upper panel shows the rate of heat release as a function of time from repeated $2 \mu\text{L}$ injections of 2 mM DTNB titrated into a cell containing $200 \mu\text{l}$ of $27 \mu\text{M}$ hBChE, measured at $25 \text{ }^\circ\text{C}$. The lower panel shows the integrated areas under the respective peaks in the top panel plotted against the molar ratio of DTNB titrated into the enzyme.

4.1.1.4 Enzyme-linked immunosorbent assay

To improve the detection of BChE activity in tissue extracts, we tested ELISA for this application. Selective binding of BChE to immobilized antibody in ELISA yields a relatively "pure" BChE sample that is depleted of free SH groups that react with DTNB. This step decreases background absorbance and allows detection of low ChE activity in biological samples.

While 80 μ l of mouse diaphragm extract was out of detection range when measured by EA, the increase of absorbance over time was possible to follow in ELISA (Figure 22). When a smaller amount of mouse diaphragm extract (30 μ l) was used, the course of the absorbance increase versus time was comparable in EA and ELISA, with higher absolute values for the former method (Figure 22). This method, therefore, could be useful for measuring low ChE activities in biological samples containing a high content of free SH groups (and thus high background) where dilution of the sample would lead to undetectable signal (e.g., tissues from AChE or BChE heterozygous animals).

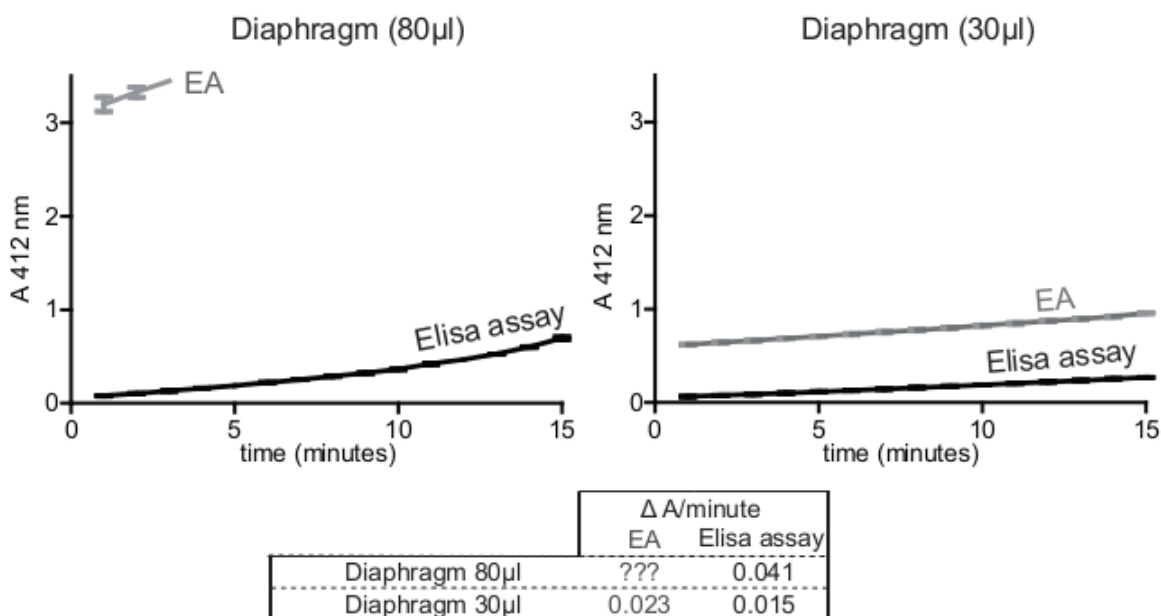


Figure 22: High background in biological samples. ELISA (■) and regular EA (▒) were performed in 80 or 30 μ l of mouse diaphragm extract using 1 mM BTC as a substrate. High background prevents detection of 80 μ l extract using EA. Figure panels depict the average values obtained from triplicates. Results were confirmed by repeating the experiment 10 times.

4.1.2 ACTIVITY OF CHOLINESTERASES IN HEART

We used modified 2s-EA for precise determination of AChE (Figure 23A,B) and BChE (Figure 23C,D) activities in the extracts of individual compartments of Langendorff-perfused mouse heart: the right atrium, the left atrium, the right ventricle, the left ventricle, the septum, the apex and the base of the heart. The extracts contained the same amount of the total protein.

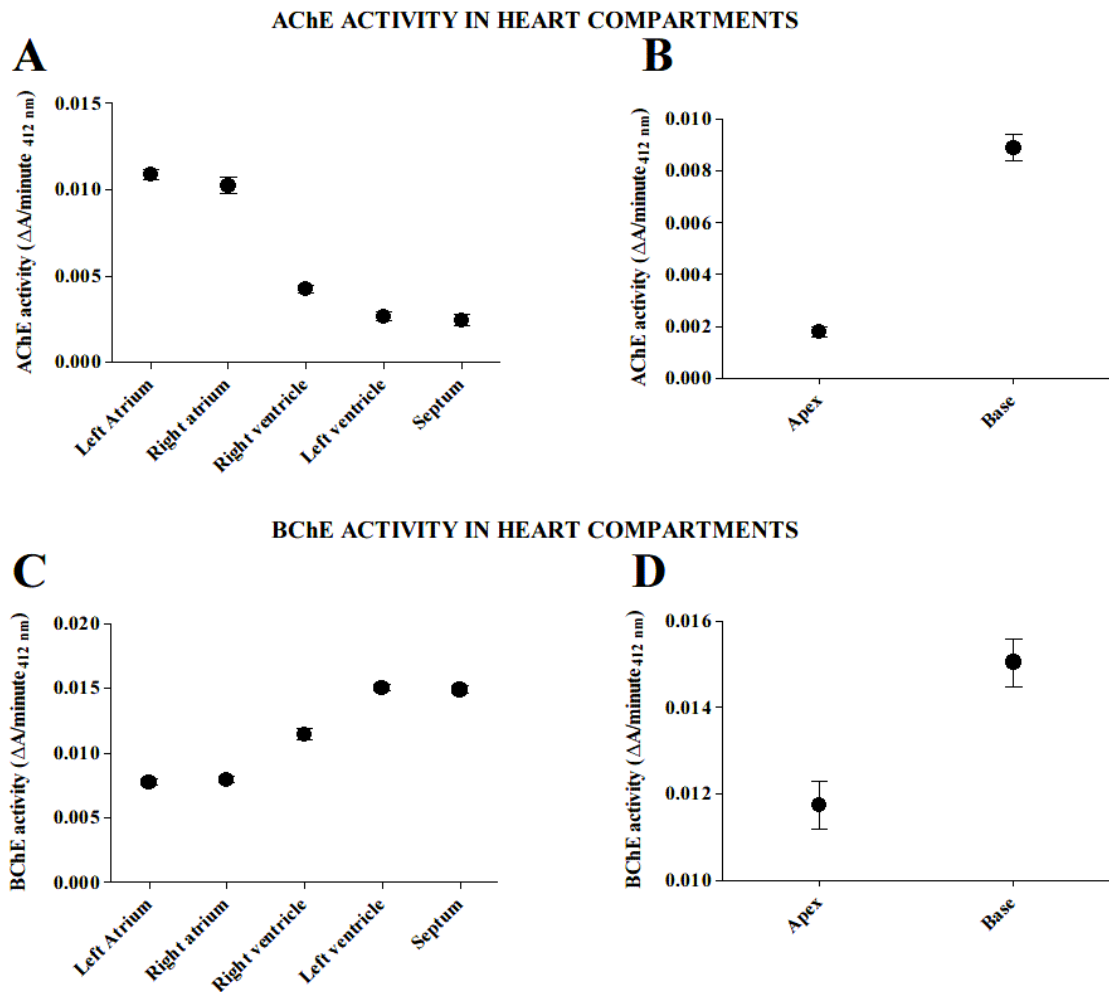


Figure 23: AChE and BChE activities in heart compartments. (A) Activity pattern of AChE activity is following: the left atrium \approx the right atrium $>$ the right ventricle $>$ the left ventricle \approx the septum. (C) BChE activities were determined in subsequent activity order: the left atrium \approx the right atrium $<$ the right ventricle $<$ the left ventricle \approx the septum. Higher AChE (B) and BChE (D) activities were observed on the base of the heart than in apex. This experiment was performed with the same amount of protein in each sample and repeated three times.

We detected the highest AChE activity in the atria. AChE activities of left and right atria were comparable with slightly higher content of activity in the left part. We observed notably lower AChE activity in the ventricles in comparison to atria. The lowest activity was determined in the septum and the left ventricle. Activity in the right ventricle was slightly higher than in the septum and the left ventricle, but still 2.5-fold lower than in the atria (Figure 23A). When AChE activities in the apex and on the base of the heart were observed, more than 4-fold higher activity was determined on the base of the heart (Figure 23B).

In contrary to AChE activities, the lowest BChE activities were detected in the atria. Higher activity was observed in the right ventricle and the highest activities were detected in the left ventricle and the septum (Figure 23C). Similarly to AChE activity, BChE activity was higher on the base of the heart than in apex, however only 1.3-fold higher (Figure 23D).

4.2 MOLECULAR FORMS OF CHOLINESTERASES IN THE HEART

We used method of sucrose gradient (as described in the chapter 3.3.3 SUCROSE GRADIENTS) to clarify which molecular forms of ChE are present in the mouse heart. Moreover, we quantitatively determined contribution of each molecular form in the mouse heart compartments: the right atrium, the left atrium, the right ventricle, the left ventricle, the septum, the apex and the base.

4.2.1 ACETYLCHOLINESTERASE IN THE HEART

To find out which AChE molecular forms are present in the mouse heart, we analyzed hearts from WT, ColQ^{-/-} and PRiMA^{-/-} mice using the method of sucrose gradient (Figure 24).

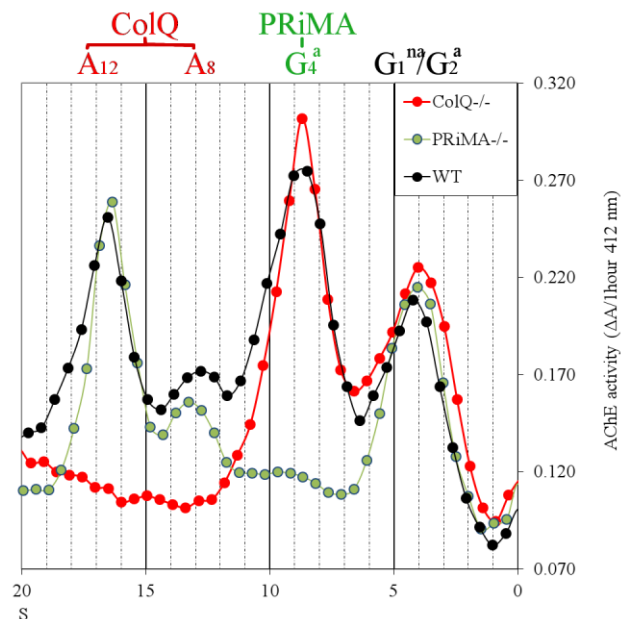


Figure 24: Molecular forms of AChE in the Langendorff-perfused mouse heart. Peaks of AChE activity characterize presence of AChE molecular forms depicted above the figure. Peak around 4S corresponds to presence of G_1^{na}/G_2^a , 9S to PRiMA AChE, 12.5 and 16.1S to ColQ AChE. Gradients were performed in BRIJ detergent and high salt (0.8M NaCl) that solubilize anchored forms from membrane and basal lamina. Experiments were repeated two times for knockout mice and at least three times for WT mice.

In WT mice, AChE was distributed into four peaks. Peak around 4S corresponds to the presence of G_1^{na}/G_2^a and was present in the WT, ColQ^{-/-} and also PRiMA^{-/-} mice. Peak around 9S (in gradient containing BRIJ) corresponds to the presence of amphiphilic tetramer G_4^a , which is known as PRiMA AChE. This peak was observed only in WT and ColQ^{-/-} mice and was completely absent in heart of PRiMA^{-/-} mice. Peaks of AChE around 12.5S and 16S are known as peaks of asymmetric forms. They were absent in ColQ^{-/-} mice and preserved in WT and PRiMA^{-/-} mice. These peaks correspond to presence of ColQ AChE. Quantitatively, ColQ AChE and PRiMA AChE are present in the mouse heart approximately at ratio 1:1.

We discovered that amount of G_1^{na}/G_2^a forms in the heart is highly dependent on the quality of the perfusion. When non-perfused heart was used for analysis, the size of the peak at 4S, caused by high activity of GPI AChE on the erythrocyte membrane, was so high that it made other molecular forms almost undetectable (Figure 25). This peak markedly decreased when heart was thoroughly perfused (Figure 24). The perfusion is therefore a critical step to quantify AChE and BChE in highly vascularized tissues, such as heart.

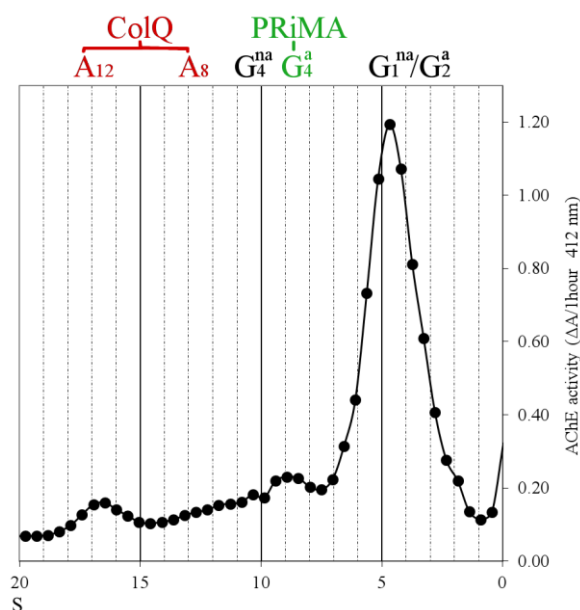


Figure 25: Molecular forms of AChE in the non-perfused heart of WT mice. Peaks of AChE activity characterize presence of AChE molecular forms depicted above the figure. In non-perfused heart, peak 4S that corresponds to presence of G_1^{na}/G_2^a was so high, that peaks at 9S (PRiMA AChE) and 12.5S; 16.1S (ColQ AChE) were almost undetectable. Gradients were performed in BRIJ detergent.

To reduce the number of used mutant mice, further we performed gradients in BRIJ and CHAPS detergents to distinguish amphiphilic and non-amphiphilic molecular forms in the individual heart compartments of WT mice. Amphiphilic tetramers (e.g PRiMA AChE) associate with the BRIJ detergent, producing a characteristic shift in sedimentation coefficient when compared to CHAPS detergent. Non-amphiphilic forms do not interact with detergent thus positions of peaks in BRIJ and CHAPS detergents are the same (Bernard et al., 2011; Bon et al., 1988). We did not analyze in detail the nature of the G_2^a of AChE. Its origin of AChE_T and AChE_H could only be distinguished by the enzymatic digestion of the GPI.

The solubilization of the ChE and the conversion of the molecular forms by the proteases cause a significant problem when activity of AChE and BChE molecular forms is evaluated. In fact, ColQ and PRiMA complexes are easily converted in G_4^{na} . A single step extraction in buffer containing high concentrations of salts, CHAPS as detergent (in place of Triton) and EDTA associated with the fast solubilization in a Mixer Mill reduces dramatically the quantity of G_4^{na} of ChE.

4.2.1.1 Acetylcholinesterase in the Atria

In both atria (Figure 26), we detected presence of G_1^{na}/G_2^a , PRiMA AChE and ColQ AChE. The anchored forms of AChE formed the predominant part. However, content of PRiMA AChE was slightly higher than that of ColQ AChE (ratio 1:1.2). Results in right and left atria were almost identical.

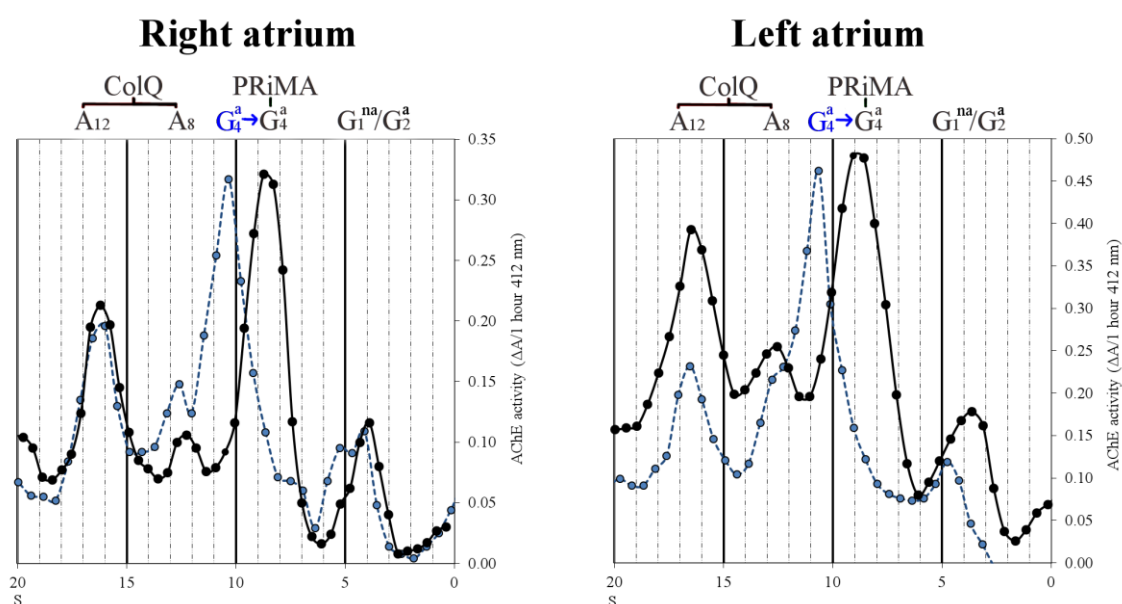


Figure 26: Molecular forms of AChE in the right and the left atrium of WT mice. Peaks correspond to presence of G_1^{na}/G_2^a , PRiMA AChE and ColQ AChE. Gradients were performed in detergent BRIJ (●) and CHAPS (●). Shift between detergents confirms presence of amphiphilic forms. Experiment was repeated at least three times.

4.2.1.2 Acetylcholinesterase in the Ventricles and the Septum

Detected AChE activity in the ventricles and the septum was lower than the activity in the atria. We observed presence of G_1^{na}/G_2^a , PRiMA AChE and ColQ AChE in the right ventricle, the left ventricle and the septum (Figure 27).

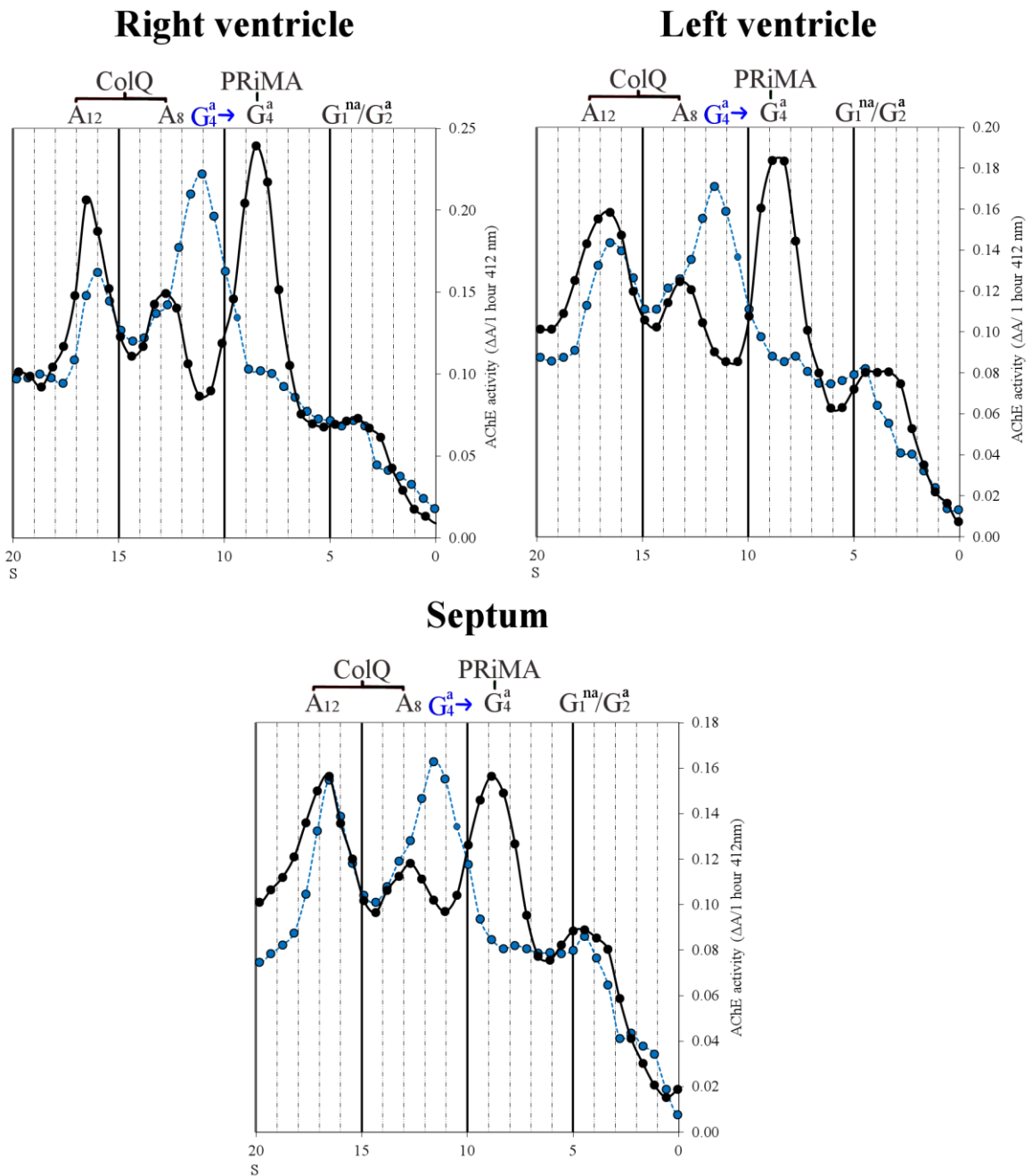


Figure 27: Molecular forms of AChE in the ventricles and the septum of WT mice. Peaks correspond to presence of G_1^{na}/G_2^a , PRiMA AChE and ColQ AChE. Gradients were performed in detergent BRIJ (●) and CHAPS (●). Experiment was repeated at least three times.

Anchored forms of AChE were present in the major quantity in these compartments. However, we noticed slight difference in content of PRiMA AChE and ColQ AChE. While in the right ventricle, ratio of these forms was 1:1, in the left ventricle and the septum we detected slightly higher content of ColQ AChE (ColQ AChE: PRiMA AChE = 1:0.8).

4.2.1.3 Acetylcholinesterase in the Apex and on the Base of the Heart

When the heart base and the apex were compared (Figure 28), different ratios of PRiMA AChE and ColQ AChE were observed. In apex, we observed slightly higher content of ColQ AChE than PRiMA AChE. In contrary, we observed higher amount of PRiMA AChE than ColQ AChE on the base of the heart. Nevertheless, as discussed above, AChE activity is higher on the base than in the apex, regardless the molecular forms (thus both, ColQ AChE and PRiMA AChE activities are higher on base than in apex).

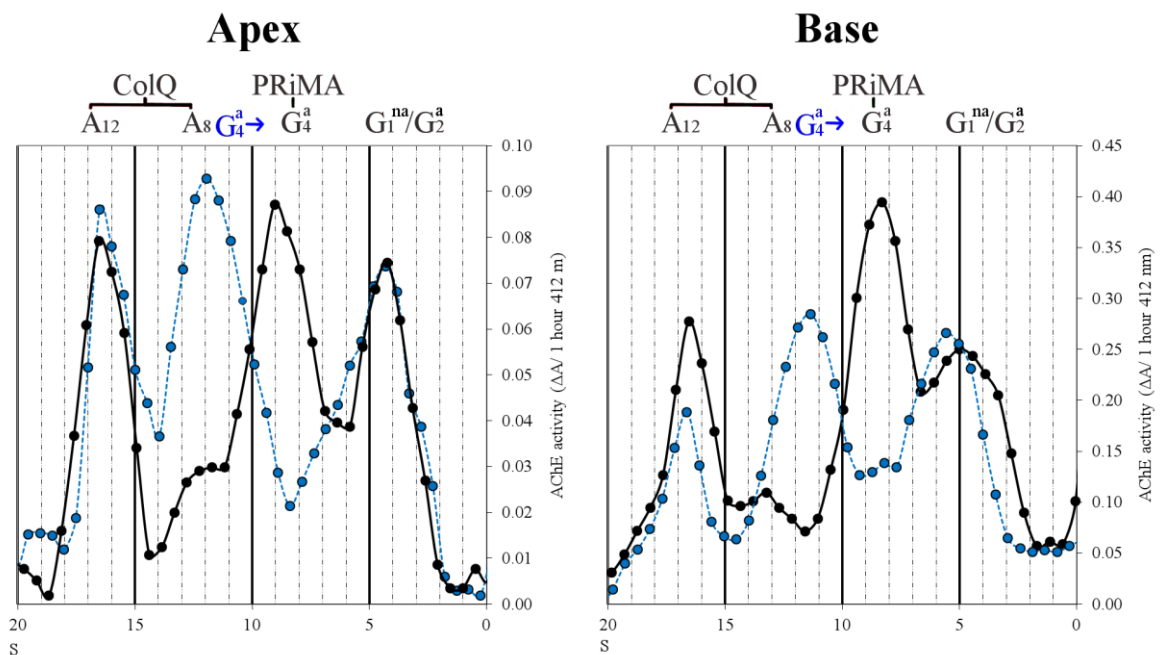


Figure 28: Molecular forms of AChE in the apex and on the base of the heart of WT mice. Peaks correspond to presence of G_1^{na}/G_2^a , PRiMA AChE and ColQ AChE. Note the difference in the scale of the Y axes. Gradients were performed in detergent BRIJ (●) and CHAPS (●). Experiment was repeated at least three times.

4.2.2 BUTYRYLCHOLINESTERASE IN THE HEART

Molecular forms of BChE in the mouse heart from WT, ColQ^{-/-} and PRiMA^{-/-} mice were also analyzed by method of sucrose gradient (Figure 29). Globular G₁^a and G₄^{na} forms of BChE were present in heart of all three studied genotypes, in comparable quantities. This reveals that no anchored forms of BChE are present in the heart. Major part of BChE molecular forms in perfused heart was formed by G₁^a forms.

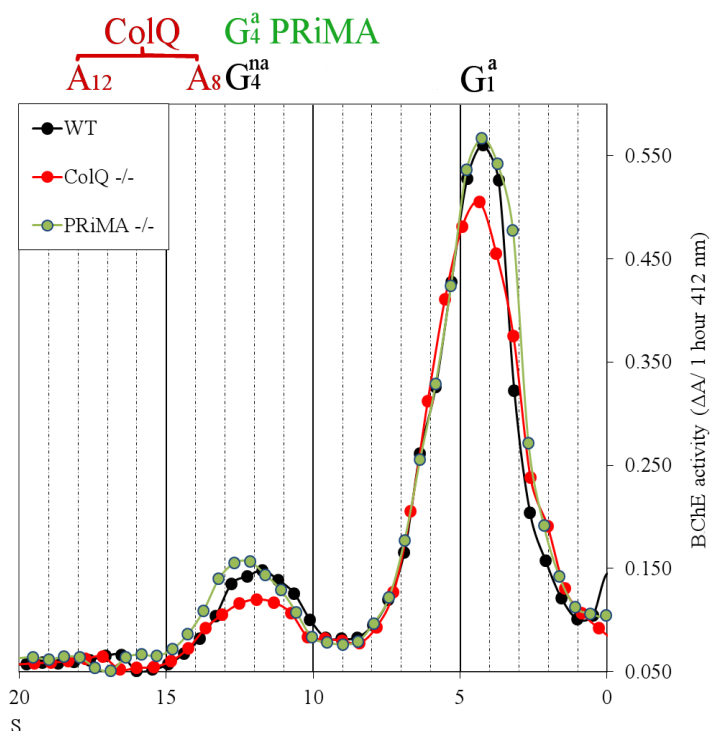


Figure 29: Molecular forms of BChE in the mouse heart. Peaks characterize presence of molecular forms depicted above the figure. Peak around 4.5S corresponds to presence of G₁^a and 12.5S to G₄^{na}. Gradients were performed in BRIJ detergent and repeated two times for knockout mice and at least three times for WT mice.

Content of soluble tetramers (G₄^{na}) is highly dependent on the tissue perfusion due to the high activity of this form in the serum. We observed that the quantity of G₄^{na} in non-perfused heart (Figure 30) is higher than that of G₁^a and substantially decreased after perfusion (Figure 29).

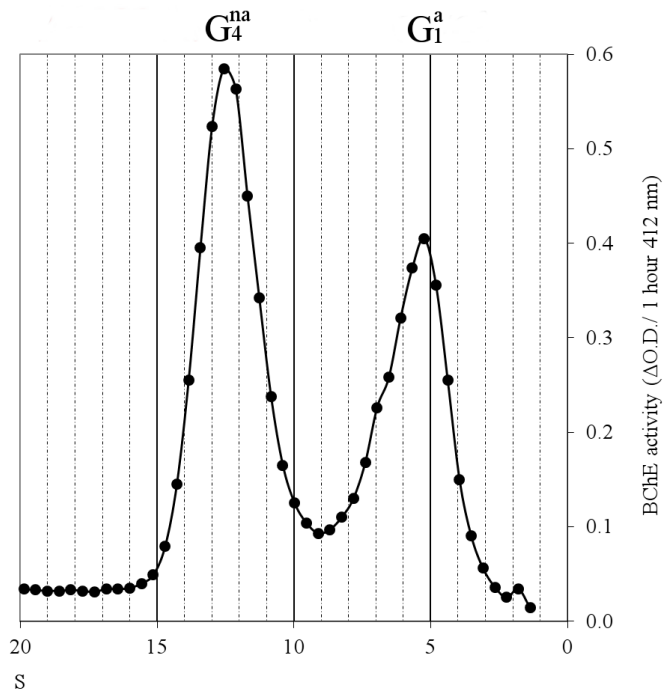


Figure 30: Molecular forms of BChE in the non-perfused heart of WT mice. Peaks characterize presence of molecular forms depicted above the figure. Peak around 12.5S corresponds to presence of G_4^{na} . In non-perfused heart, activity of G_4^{na} is higher than that of G_1^a (4.5S). Gradients were performed in BRIJ detergent.

Similarly to analysis of AChE forms, BRIJ detergent and CHAPS detergent were used to distinguish amphiphilic and non-amphiphilic molecular forms in the heart compartments of WT mice.

4.2.2.1 Butyrylcholinesterase in the Heart Compartments

In all studied parts of the heart, we detected only G_1^a and G_4^{na} molecular forms of BChE (Figure 31), while the ratio of these forms was similar in all compartments. As we detected shift in peak at 4.5S between gradients performed in CHAPS and BRIJ detergents, we can conclude that the majority of BChE in heart is represented by G_1^a forms.

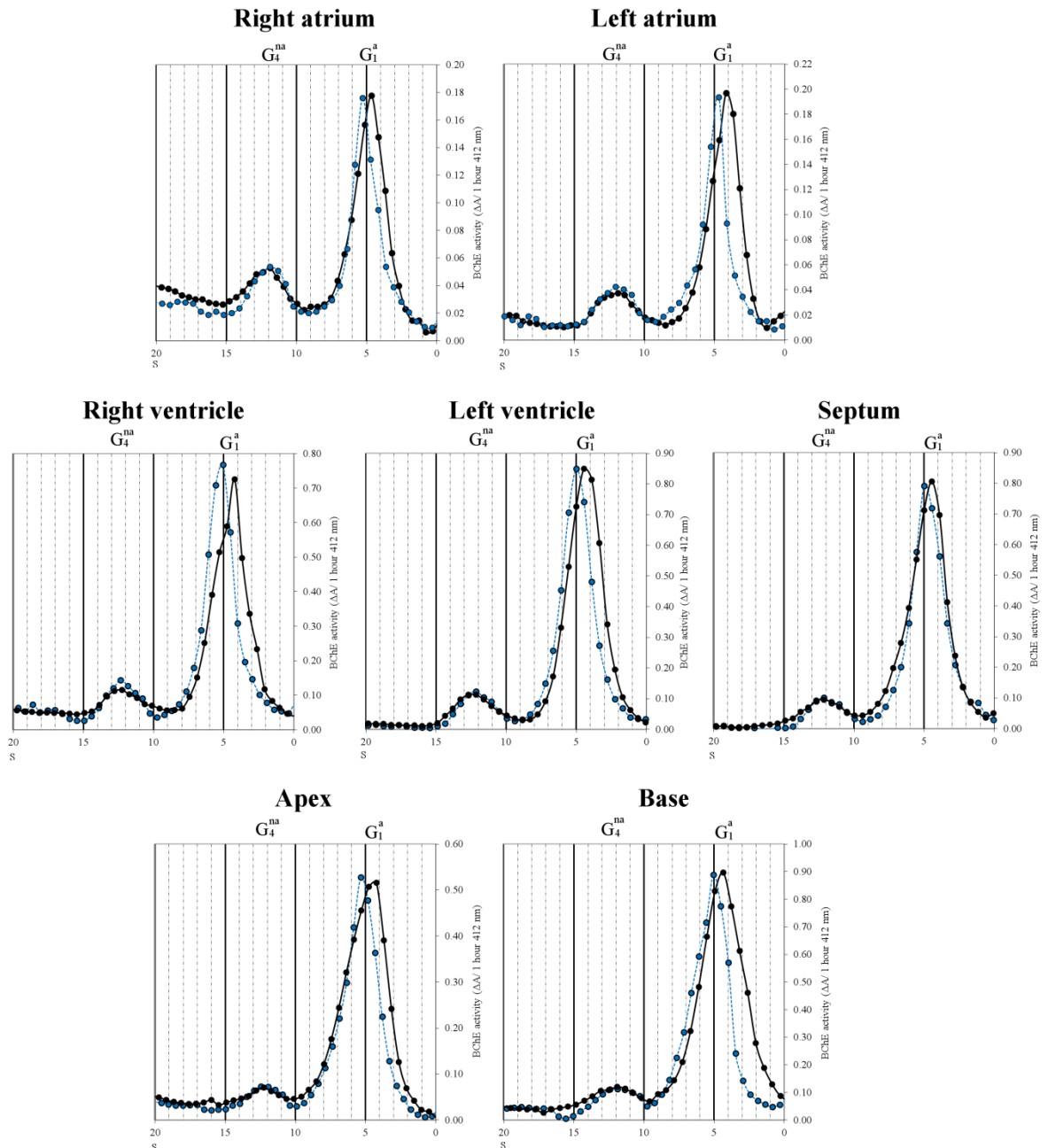


Figure 31: Distribution of peaks characterizing molecular forms of BChE in heart compartments. In all parts, only G_1^a and G_4^{na} were detected. Gradients were performed in BRIJ (●) and CHAPS (●) detergent. Experiment was repeated at least three times.

4.3 LOCALIZATION OF CHOLINESTERASES IN THE HEART

4.3.1 BASIC MORPHOLOGY OF THE HEART

To examine an impact of lack of different molecular forms of ChE on overall heart morphology, we performed hematoxyline and eosin staining in transversal sections of perfused heart of WT mice, AChE del E 5+6^{-/-}, BChE^{-/-}, PRiMA^{-/-} and ColQ^{-/-} mice. Diameter of cardiomyocytes was measured and compared between genotypes (Figure 32).

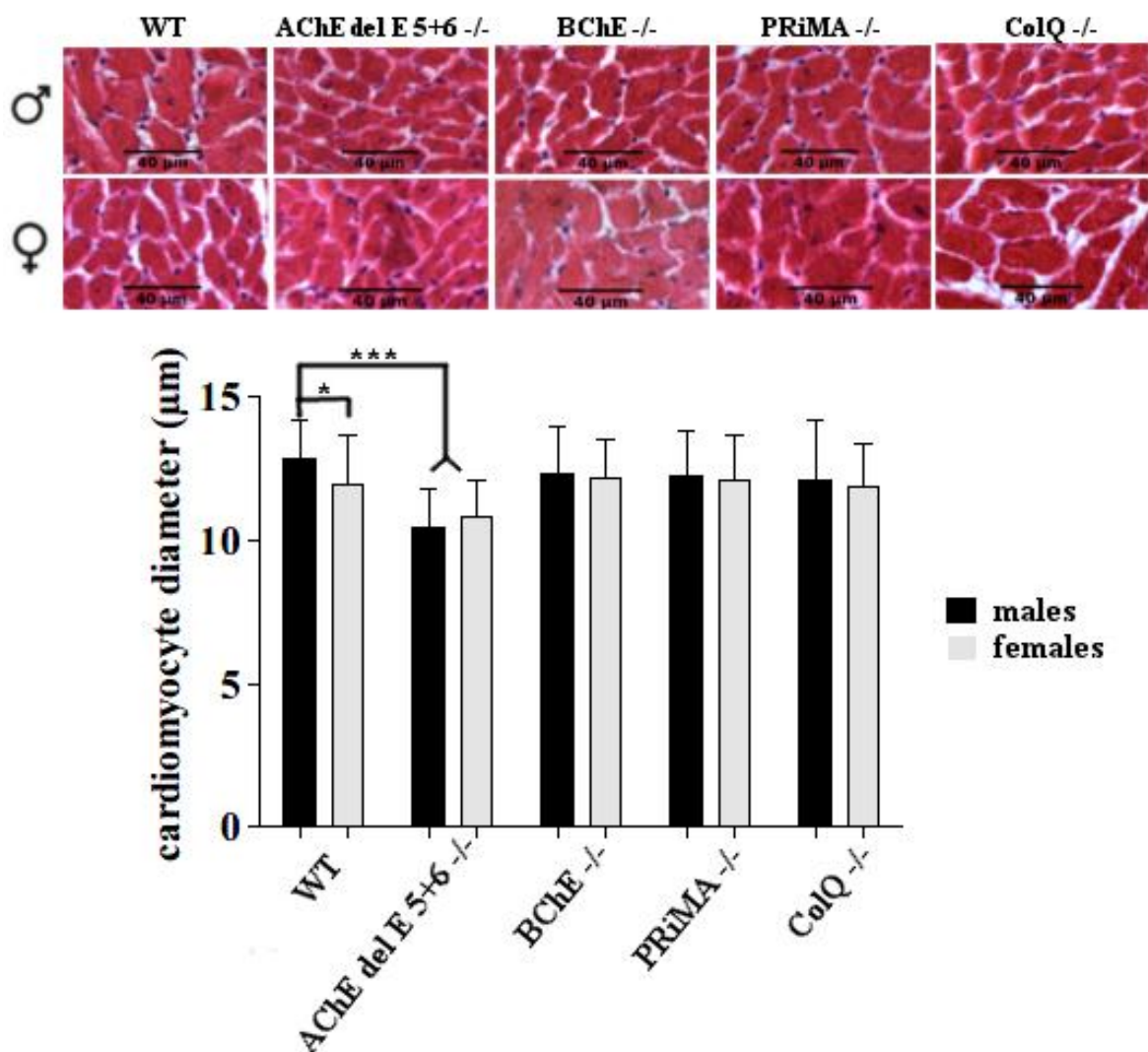


Figure 32: Average cardiomyocyte diameters in hearts of WT and ChE knockout mice. Significant differences were observed in the values of AChE del E 5+6^{-/-} mice and WT mice ($p < 0.001$) and in the values of females and males WT mice ($p < 0.05$). Experiment was repeated two times for each genotype and sex.

We detected significantly lower ($p < 0.001$) cardiomyocyte diameter in AChE del E 5+6^{-/-} mice when compared to WT mice. This relationship was confirmed for males and females. We did not observe other significant differences in cardiomyocyte diameter between WT and other genotypes. However, difference was revealed between males and females in WT mice. Females had significantly lower cardiomyocyte diameter ($p < 0.05$) than males. In other genotypes, no intersex differences were observed.

4.3.2 CHOLINESTERASES ON THE BASE OF THE HEART

Previous studies showed that cardiac plexus, which consists of parasympathetic and sympathetic nerves, is localized on the heart base. To facilitate the visualization of the epicardial surface of the heart, we inflated the heart by gelatin injection into the all heart chambers (as described in details in the section 3.2.1.1 Heart Tissue Preparation). Using the ChE activity staining method, we evaluated ChE activity in the mutant mice (AChE del E 5+6^{-/-}, BChE^{-/-}, PRiMA^{-/-} and ColQ^{-/-}). We were thus able to characterize localization of AChE, BChE and their molecular forms (ColQ and PRiMA AChE) in this region (Figure 33).

On the heart base of WT mice, we observed strong, homogenously distributed ChE activity. Similar results were acquired in BChE mutant mice, indicating that anchored AChE is predominant in this part of the heart. In AChE del E 5+6^{-/-} mice, only one markedly stained lining, which disappeared after treatment with BChE inhibitor, was observed. This confirms the major localization of AChE on the heart base. Comparable strong staining was preserved in both, ColQ^{-/-} and PRiMA^{-/-} hearts. We can conclude that both, PRiMA AChE and ColQ AChE are localized on the heart base.

In higher magnification, clear difference in coloration was observed between the genotypes in the heart hilum, where the veins input and output are localized. In WT, BChE^{-/-} and ColQ^{-/-} mice, strongly colored structures and also small branching were stained. However, small branching was not visible in AChE del E 5+6^{-/-} and PRiMA^{-/-} mice. This suggests that subtle branching on the heart base is formed by PRiMA AChE.

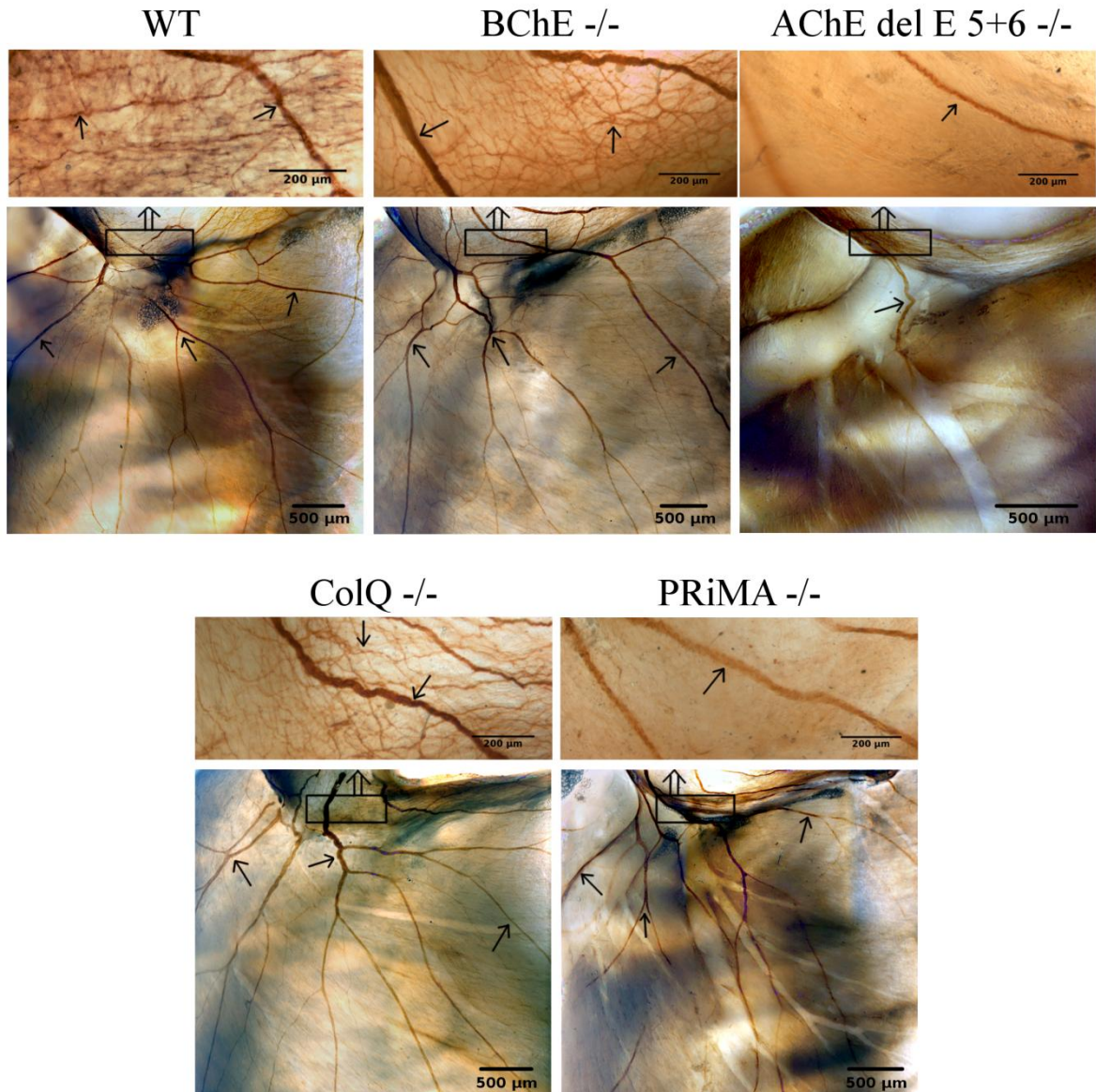


Figure 33: Localization of ChE on the heart base. ChE activity was revealed for 3 hours with ATC as a substrate. ChE activity is marked by black arrows. Strong ChE activity was detected in WT, BChE^{-/-}, ColQ^{-/-}, PRiMA^{-/-} mice, but not in AChE del E 5+6^{-/-} mice, where only one colored lining was present. Majority of coloration on the heart base was formed by ColQ AChE and PRiMA AChE. Higher magnification revealed presence of AChE anchored by PRiMA in subtle branching on the heart hilum. This coloration is present in WT, BChE^{-/-}, ColQ^{-/-}, but not in AChE del E 5+6^{-/-} and PRiMA^{-/-} mice.

4.3.3 CHOLINESTERASES IN THE VENTRICLES

Transversal and longitudinal sections of the ventricles of WT and mutant mice were stained for AChE and BChE activity. We did not detect any AChE activity in the ventricular myocardium in any of the studied hearts, even after prolonged incubation.

However, we observed stronger diffuse staining in the WT mice than in BChE^{-/-} mice, when BChE activity was revealed (Figure 34). This staining was not affected by the perfusion process. This suggests that BChE is probably found intracellularly.

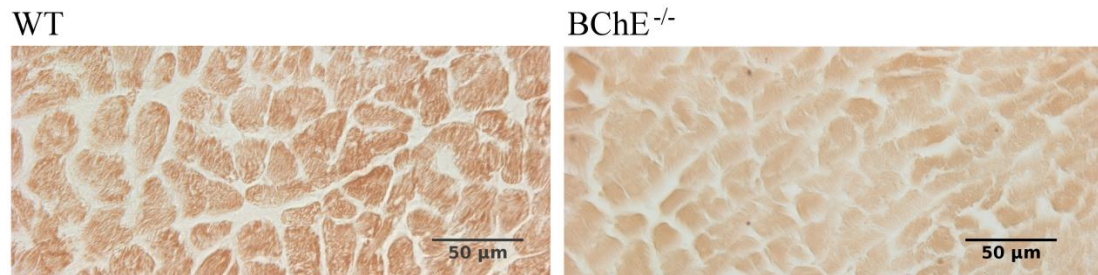


Figure 34: BChE activity in the transversal sections of myocardium of the ventricles. In WT mice and BChE^{-/-} mice, activity of BChE was revealed in the presence of BW with ATC or with BTC as substrate. Background color is stronger in the WT mice, which suggests diffusely distributed BChE in the myocardium. Experiment was repeated at least three times.

Longitudinal sections of the ventricles were studied also by immunohistochemistry. We used biotinylated 4H1 BChE antibody and streptavidine 488 to visualize BChE in the heart of WT and BChE^{-/-} mice (Figure 35). We did not detect any localized BChE protein in these sections.

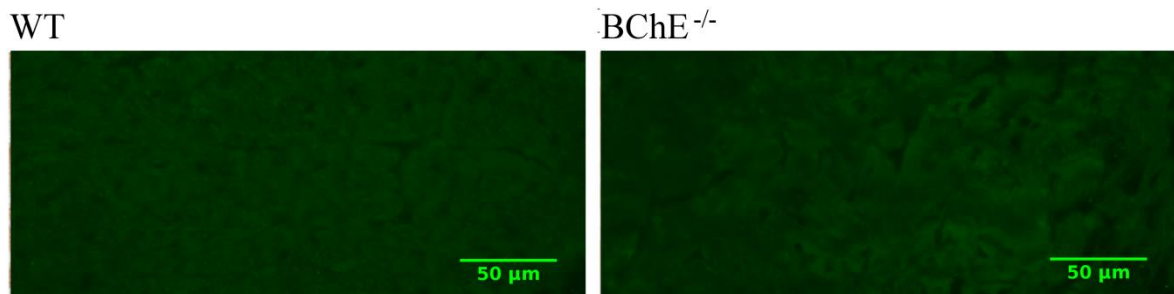


Figure 35: Immunohistochemistry performed with biotinylated 4H1 and avidine 488 on the longitudinal sections of hearts of WT and BChE^{-/-} mice. We did not detect any fluorescent signal.

Localized AChE activity was observed in the epicardium of transversal sections of heart (Figure 36). Localization corresponds to strongly colored lining identified on the base of the heart. Intense coloration was observed in the WT, BChE^{-/-}, ColQ^{-/-} and PRiMA^{-/-} mice. No coloration was detected in the AChE del E 5+6^{-/-} mice. Thus, AChE anchored by PRiMA and ColQ was confirmed in the epicardium of heart base.

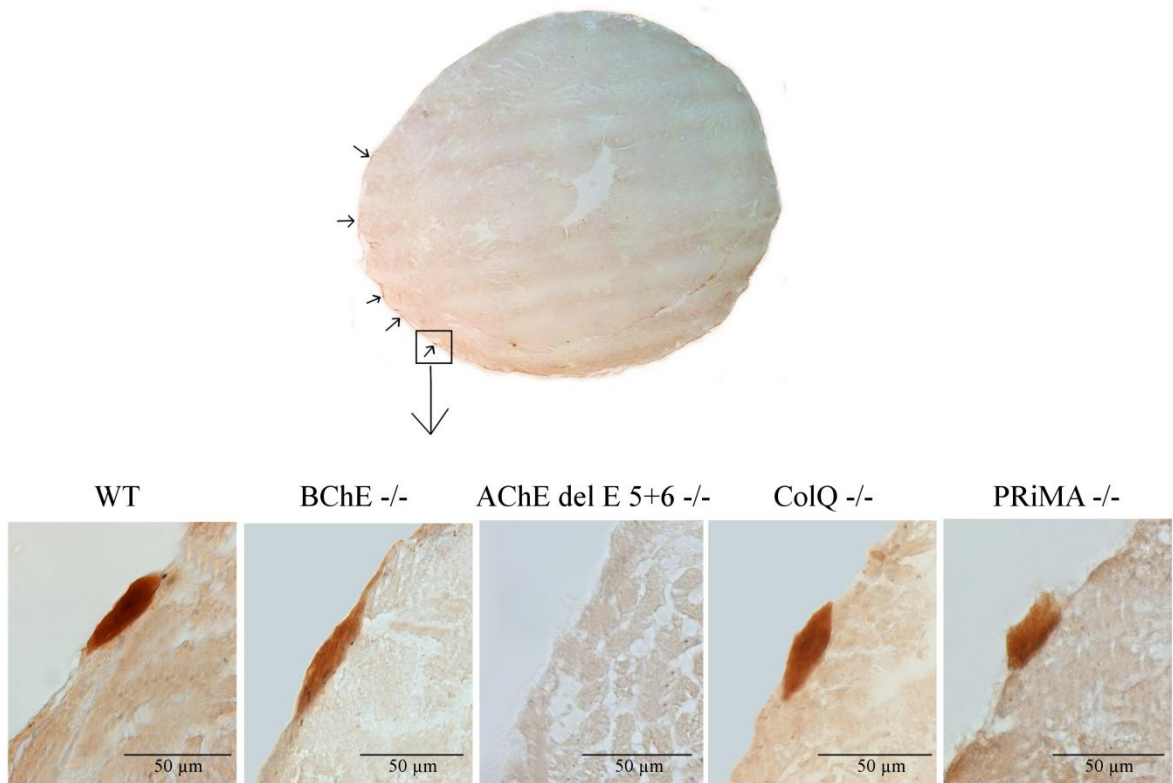


Figure 36: Transversal section of the ventricles. Strong staining was identified in the epicardium of WT, BChE^{-/-}, ColQ^{-/-} and PRiMA^{-/-} mice. No coloration was detected in the Del E 5+6^{-/-} mice. Experiment was repeated five times.

Immunohistochemistry using specific anti-AChE antibody, antibody against neuronal marker TUJ1 and endothelial marker PECAM1 was performed in the transversal sections of the ventricle (Figure 37).

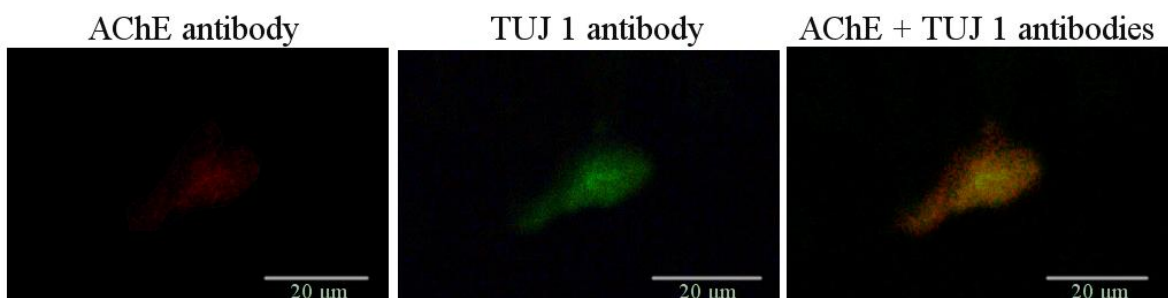


Figure 37: Localization of AChE and neuronal marker (TUJ1) in the epicardium by immunohistochemistry. Fluorescent signal of AChE antibody and TUJ1 antibody were co-localized. Experiment was repeated three times.

In agreement with previous results, we detected AChE protein in the epicardium. Fluorescent signal of AChE antibody was co-localized with TUJ1 antibody, but not with anti-PECAM1. This suggests that strong coloration present on the base of the heart is linked to the neuronal cells.

4.3.4 CHOLINESTERASES IN THE ATRIA

Localization of ChE was examined in both, cryosections of atrial myocardium and epicardium of atria of gelatin filled whole-mounted heart (Figure 38).

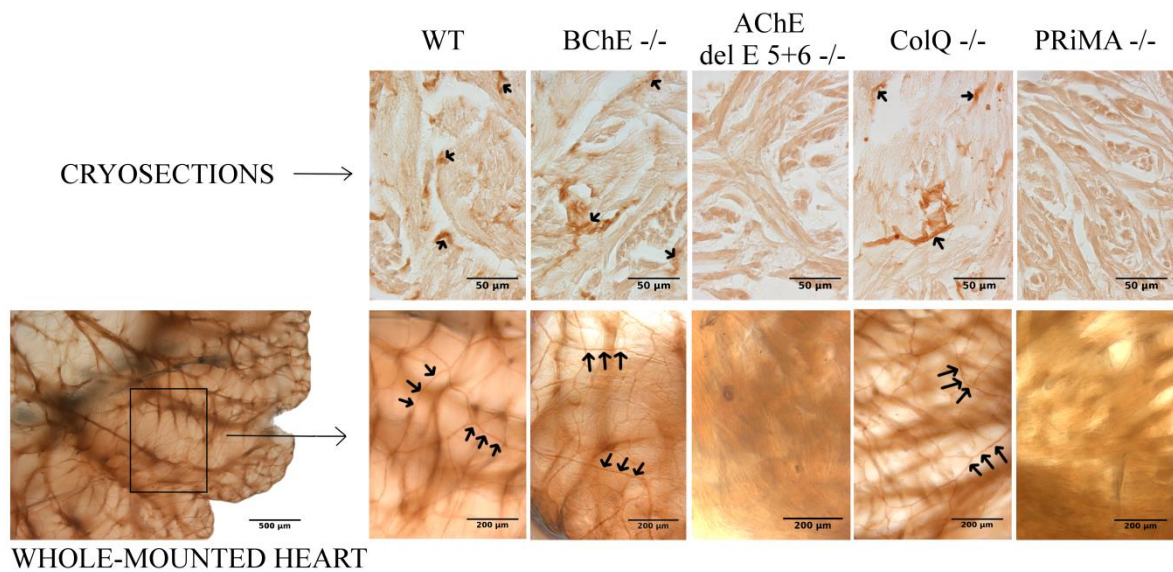


Figure 38: Localization of ChE in cryosections of atria and in the atria of whole-mounted heart. ChE activity is marked by black arrows. ChE activity was detected in the WT, BChE^{-/-} and ColQ^{-/-} mice. No activity was detected in the AChE del E 5+6^{-/-} and PRiMA^{-/-} mice. Experiments were repeated at least three times.

In both myocardium and epicardium of atria, results were similar. We detected activity in the WT, BChE^{-/-} and ColQ^{-/-} mice. Activity staining was absent in the AChE del E 5+6^{-/-} and PRiMA^{-/-} mice. Thus, in the atria, AChE anchored by PRiMA was localized in the myocardium and also in the epicardium.

We performed immunohistochemistry using specific anti-AChE antibody, antibody against neuronal marker TUJ1 and antibody against endothelial marker PECAM1 in the sections of the atria (Figure 39). Fluorescent signal of AChE antibody was co-localized with TUJ1 antibody, but not with anti-PECAM1. This suggests that coloration presents in the atria is linked to neuronal cells.

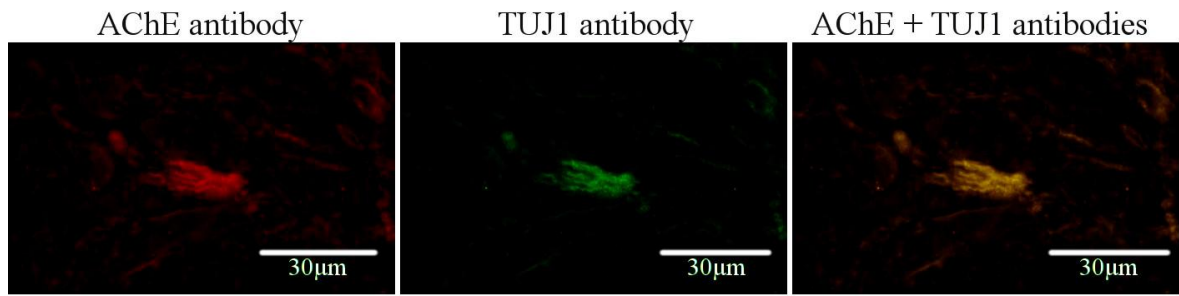


Figure 39: Localization of AChE and neuronal marker (TUJ1) in the atria by immunohistochemistry. Fluorescent signal of AChE antibody and TUJ1 antibody were co-localized. Experiment was repeated three times.

5 DISCUSSION

Study of cholinergic system in the heart has been neglected for a long time. In the last decade, however, increasing amount of papers dealing with study of the neuronal and non-neuronal cholinergic system in the heart has been published. Cholinergic neuronal control of the heart is provided by *nervus vagus* (Abramochkin et al., 2010; Coiado et al., 2015; Pauza et al., 2000; Rysevaite et al., 2011a; Saburkina et al., 2014). Non-neuronal cholinergic system in the heart was described only recently and it has been shown to play a crucial role in regulating heart functions (Kakinuma et al., 2013, 2012, 2009; Lara et al., 2010; Rana et al., 2010; Rocha-Resende et al., 2012; Roy et al., 2013).

The mentioned papers were focused on the study of ACh (Abramochkin et al., 2012, 2010; Borodinova et al., 2013; Kakinuma et al., 2009; Oberhauser et al., 2001; Rana et al., 2010; Rocha-Resende et al., 2012; Roy et al., 2013), cholinacetyltransferase (Kakinuma et al., 2013, 2009; Rana et al., 2010; Roy et al., 2013; Rysevaite et al., 2011b), ChT (English et al., 2010; Kakinuma et al., 2009; Neumann et al., 2005; Rana et al., 2010), vesicular transporter (Lara et al., 2010; Rana et al., 2010; Roy et al., 2013, 2012; Yasuhara et al., 2007) or ACh receptors in the heart (Brodde and Michel, 1999; Dunlap et al., 2003; Oberhauser et al., 2001; Olshansky et al., 2008). ChE, especially AChE, were used mainly as tools to identify cholinergic neurons in heart (Pauza et al., 2000, Rysevaite et al., 2011, Saburkina et al., 2010, Pauza et al., 1997b, Pauza et al., 1999, Saburkina et al., 2014) and authors did not focus on the study of ChE as enzymes regulating ACh action. Detailed information about ChE in the heart was missing. In this work, complex information about ChE activity, localization and precise characterization of their molecular forms are presented for the first time.

Modified EA enables to study low ChE activities in biological samples

The study of ChE activity in heart required adjustment of the popular Ellman's method (Ellman et al., 1961). This optimization has been designed to acquire precise information about AChE and BChE activities in the biological samples, including heart, where low ChE activities are measured (Dingova et al., 2014).

Due to the character of *in vitro* studies, pure enzymes in high quantities (micromolar range; e.g., (Groner et al., 2007; Hrabovská et al., 2006a) are usually used for the analyses by enzymologist. In the body, however, the concentration of ChE varies between tissues (Li et al., 2000), ranging from high (e.g., AChE in striatum (Dobbertin et

al., 2009), BChE in liver (Li et al., 2000)) to low (e.g., AChE in heart (Li et al., 2000), BChE in striatum (Dobbertin et al., 2009)). Moreover, different scientific approaches (e.g., genetic manipulations) may further decrease the level of the protein to the detection limits. Prolonged incubation is often needed to record very low activities. For example, histochemistry with 30 minute of incubation leads to a typical AChE staining of the WT neuromuscular junction but gives no staining in mutant mice with deletion of ColQ AChE forms. However, increased incubation time (to 3 hours or even over-night) reveals low activity of residual PRiMA AChE (Bernard et al., 2011). Use of the same approach (with prolonged incubation) for detection of low ChE activities by Ellman's method is limited, because of instability of DTNB in the commonly used phosphate buffer. We confirm that DTNB is unstable in phosphate buffer and that stability of DNTB in liquid depends inversely on pH. However, the presence of 5.0 mM HEPES buffer in the solution increases the stability of DTNB over time, as does a decrease of the pH to 7.0. The presence of HEPES buffer has no effect on enzyme hydrolysis but slightly increases the stability of intermediate products (TCh) or end products (TNB). This information can be used to increase the stability of the stock solution of DTNB as well as in assays that require prolonged recording time of enzyme hydrolysis.

Another problem that must be faced when studying ChE activities in biological samples is the occurrence of free SH groups in many biomolecules. Interaction with DTNB gives a significant background that can interfere with detection of product formation (e.g., AChE detection in liver (Xie et al., 2000) vs. (Li et al., 2000)). Authors try to solve the problem by a 20 minutes pre-incubation of biological enzyme sample with DTNB prior to the addition of substrate (Wang et al., 2004). In such conditions, however, DTNB instability in phosphate buffer (pH 8.0), protease action and DTNB effect on enzyme activity may make it impossible to detect low activities of the enzyme. We have observed an interaction of DTNB with BChE activity. Although it may be of no importance when high BChE activities are being followed, low BChE activities may be masked, especially when high background is present. An inhibitory effect on BChE, but not on AChE, was observed for Triton X-100 previously as well (Gómez et al., 1999; Li et al., 2000; Moral-Naranjo et al., 1996). Triton X-100 is an efficient protein extraction agent that has been commonly used for tissue ChE extraction. Its inhibitory action toward BChE is species specific. This was explained by different amino acid lining of the acyl-binding pocket within the active site gorge (Boeck et al., 2002; Li et al., 2000) (Figure 40).

```

      1          10          20          30          40          50
human BChE - NP_000046.1 - EDDIIITATKNGKVRGMNLTVPGGTVAFLGIPYAQPPLGRRLRFRKKPQSLT
mouse BChE - NP_033868.3 - EEDFIITTKTGRVRLSMPVLLGGTVAFLGIPYAQPPLGSLRFRKKPQPLN
rat BChE - NP_075231.1 - EEDVITTKTGRVRLSMPVLLGGTVAFLGIPYAQPPLGSLRFRKKPQPLN
dog BChE - XP_545267.2 - EEDIIVITTKNGKVRGMNLEVLGGTVAFLGIPYAQPPLGRRLRFRKKPQLT

      60          70          80          90          100
human BChE - NP_000046.1 - KWSDIWNATKYANSCCQNIHQSFPGFHGSEMWNPNNTDLSEDCLYLNWVWIP
mouse BChE - NP_033868.3 - KWFDIHNATQYANSCYQNIHQAFPGFQGSEMWNPNNTLSEDCLYLNWVWIP
rat BChE - NP_075231.1 - KWEDVYNATKYANSCYQNIHQAFPGFQGSEMWNPNNTLSEDCLYLNWVWIP
dog BChE - XP_545267.2 - KWSDIWNATKYANSCYQNIHQSFPGFHGSEMWNPNNTDLSEDCLYLNWVWIP

      110         120         130         140         150
human BChE - NP_000046.1 - APKPKNATVLIWIYGGGFQGTSSLVHVDGKFLARVERVIVVSMNYRVGA
mouse BChE - NP_033868.3 - VPKPKNATVMVWIYGGGFQGTSSLVVDGKFLARVERVIVVSMNYRVGA
rat BChE - NP_075231.1 - VPKPKNATVMVWIYGGGFQGTSSLVVDGKFLTRVERVIVVSMNYRVGA
dog BChE - XP_545267.2 - TPKPKNATVMWIYGGGFQGTSSLVVDGKFLARVERVIVVSMNYRVGA

      160         170         180         190         200
human BChE - NP_000046.1 - LGFLALPGNPEAPGNMGLFDQQLALQWVQKNIAAFGGNPKSVTLFGESAG
mouse BChE - NP_033868.3 - LGFLALPGNPDAPGNMGLFDQQLALQWVQRNIAAFGGNPKSVTLFGESAG
rat BChE - NP_075231.1 - LGFLALPGNSEAPGNMGLFDQQLALQWVQRNIAAFGGNPKSVTLFGESAG
dog BChE - XP_545267.2 - LGFLALPGNPEAPGNLGLFDQQLALQWVQKNIAAFGGNPKSVTLFGESAG

      210         220         230         240         250
human BChE - NP_000046.1 - AASVSLHLLSPGSHLFTTRAILQSGSFNAPWAVTSLYEARNRRTLNLAKLT
mouse BChE - NP_033868.3 - AASVSLHLLCPQSYPLFTRAILESGSSNAPWAVKHPFEARNRRTLAKLFT
rat BChE - NP_075231.1 - AASVSLHLLCPQSYPLFTRAILESGSSNAPWAVKHPFEARNRRTLAKLFT
dog BChE - XP_545267.2 - AGSVGLHLLSPRSQPLFTRAILQSGSSNAPWAVMSLFEARNRRTLAKLFT

      260         270         280         290         300
human BChE - NP_000046.1 - GCSRENETEIIKCLRNDKDPQEILLNEAFVVPYGTPLSVNFGPPTVDGDFTL
mouse BChE - NP_033868.3 - GCSKENEMEMIKCLRNDKDPQEILLNERFVLPDSDSILSINFGPPTVDGDFTL
rat BChE - NP_075231.1 - GCSKENEKKEIITCLRNDKDPQEILLNEKLVLPDSDSIRSNFGPPTVDGDFTL
dog BChE - XP_545267.2 - GCSRENETEIIKCLRNDKDPQEILLNEVLVLPDSDTLLSVNFGPPTVDGDFTL

      310         320         330         340         350
human BChE - NP_000046.1 - DMPDILLELGGQFKKQILVGVNKDEGTAFLVYGAPGFSKDNNSIITRKEF
mouse BChE - NP_033868.3 - DMPHTLLQLGKVKKAQILVGVNKDEGTAFLVYGAPGFSKDNDSLITRKEF
rat BChE - NP_075231.1 - DMPHTLLQLGKVKTAQILVGVNKDEGTAFLVYGAPGFSKDNDSLITRKEF
dog BChE - XP_545267.2 - DMPDHTLLQLGQFKKAQILVGVNKDEGTAFLVYRAGPFSKDNDSIITRKEF

      360         370         380         390         400
human BChE - NP_000046.1 - QEGLKIFPFGVSEFGKESILFHYTDWVDDQRPENYREALGDVVGDYNFIC
mouse BChE - NP_033868.3 - QEGLNMYFPGVSRILGKEAVLFYVDWLGESQSPVYRDALDDVIGDYNIIIC
rat BChE - NP_075231.1 - QEGLNMYFPGVSLGKEAILFYYVDWLGDTPEVYREAFDDIIGDYNIIIC
dog BChE - XP_545267.2 - QEGLKMYFPGVSEFGRESILFYYVDLDDQREKRYRDALDDVIGDYNIIIC

      410         420         430         440         450
human BChE - NP_000046.1 - PALEFTKKFSEWGNNAFFYYFEHRSSKLPWPPEWGMVHGHEIEFVFGGLPL
mouse BChE - NP_033868.3 - PALEFTKKFAELNNNAFFYYFEHRSSKLPWPPEWGMVHGHEIEFVFGGLPL
rat BChE - NP_075231.1 - PALEFTKKFAELINNAFFYYFEHRSSKLPWPPEWGMVHGHEIEFVFGGLPL
dog BChE - XP_545267.2 - PALEFTKKFSELGNNAFFYYFEHRSSQLPWPKWMGMVHGHEIEFVFGGLPL

      460         470         480         490         500
human BChE - NP_000046.1 - ERRDNYTKAEELSRISIVKRWANFAKYGNPNETQNNSTSWPVPFKSTEQKY
mouse BChE - NP_033868.3 - GRRVNYTRAEEIISRSIMKTWANFAKYGHPNGTQGNSTMWVPVFTSTEQKY
rat BChE - NP_075231.1 - ERRVNYTRAEEIISRSIMKTWANFAKYGHPNGTQGNSTVWVPVFTSTEQKY
dog BChE - XP_545267.2 - ERRANYTKAEELSRISIMKTWATFAKYGHPDGTQNNSTRWPAFENTDQKY

      510         520         530         540         550
human BChE - NP_000046.1 - LTLNTESTRIMTKLRAQQCRFWTSFFPKVLEMTGNIDEAEWEWKAGFHRW
mouse BChE - NP_033868.3 - LTLNTEKSKIYSKLRAEQCFWRLLFFPKVLEMTGDIDETEQEWKAGFHRW
rat BChE - NP_075231.1 - LTLNTEKSKINSKLRAEQCFWRLLFFPKVLEITGDIDEREQEWKAGFHRW
dog BChE - XP_545267.2 - LTLNTDSERVYTKLRAQQCRFWTLFFPKVLEMTGNIDEAEREWRAGFYRW

      560         570         580         590         600
human BChE - NP_000046.1 - NNYMMDWKNQFN DYTSKKESC VGL
mouse BChE - NP_033868.3 - SNYMMDWQNQFN DYTSKKESC TAL
rat BChE - NP_075231.1 - SNYMMDWKNQFN DYTSKKECTDL
dog BChE - XP_545267.2 - NNYMMDWKNQFN DYTSKKESCAGL

```

Figure 40: Aligned sequences of human, mouse, rat and dog BChEs viewed by Multiple sequence viewer tool in Maestro. Position 278 is highlighted in a box.

Based on the sequence alignment, residues at positions 250 and 278 (numbering in human BChE) may be responsible for interaction of DTNB in the case of human and mouse BChE, but not in the case of rat and dog BChE. In human and mouse proteins Thr is present at position 250, whereas in rat and dog BChE Ile is at this position. At position 278, Phe is present in human and mouse BChE, whereas Val is present in rat and dog enzymes. Residues at position 250 are located on the surface of proteins, but far from the active site. Residues at position 278 are located at the entrance of the active site in the peripheral anionic site, offering the possibility of binding DTNB by means of π - π interaction of its aromatic phenyl ring with Phe, while avoiding such interaction in the case of Val. DTNB bound on entrance could quell supplies of substrate. Inactivation of Cys residues by DTNB was reported in the literature to decrease the activity of some proteins such as *Pseudomonas mevalonii* 3-hydroxy-3-methylglutaryl-CoRA reductase (Jordan-Starck and Rodwell, 1989), native lecithin-cholesterol acyltransferase (Francone and Fielding, 1991), human immunodeficiency virus protease (D'Ettorre and Levine, 1994), insect ChE (Rowland et al., 2008), and AChE in *Torpedo californica* (Steinberg et al., 1990). The mechanism of the DTNB inhibition of *Torpedo* AChE was explained by an interaction with the free SH group of Cys away from the active site at position 231. Nevertheless, DTNB was less potent than other SH agents. For BChE, the free SH group of Cys is available in human at position 66 and in mouse and rat at position 239, although there is none in dog enzyme. Therefore, it is very unlikely that the effect of DTNB on activity of mouse and human BChE, but not on rat and dog BChE, is facilitated through the free Cys SH group. Moreover, DTNB changes the thermal stability of the *Torpedo* enzyme by a still unknown mechanism probably involving other site(s) than just the free SH group (Wilson et al., 1996).

To overcome the limitations of the standard EA, we propose a modified 2s-EA in which ATC or BTC is hydrolyzed by AChE and BChE with no DTNB present in the reaction mixture. Production of TCh (which is stable over time in our experimental conditions, as discussed above) is visualized at different time points by adding DTNB, followed by immediate measurement of yellow color. This modification troubleshoots the most important problems arising from the study of low ChE activities in biological samples. In the modified method, there is no change of the background arising from DTNB instability over time and no inhibition of ChE activity by DTNB. This 2s-EA method is an alternative to Johnson and Russell's method (Johnson and Russell, 1975) that overcomes

the radioactivity issue. The second approach to study low activities of BChE in biological samples is the use of ELISA. The advantage is that the enzyme is selectively captured and isolated from other biomolecules. As we have confirmed here, results obtained with captured enzyme are comparable to those obtained with enzyme in solution. Efficiency of this method, however, depends on the binding characteristic of antibodies and protein. Avidity, sensitivity, efficiency and selectivity in protein capturing, therefore, should always be assessed (Mrvova et al., 2013). ELISA enables one to study very low activities in biological samples, because these are not masked by the background resulting from DTNB interaction with free SH groups. Moreover, pre-incubation of the sample with DTNB is not needed and, thus, no interference with DTNB is present.

Based on our results, we have performed activity study in the heart in HEPES buffer pH 7.5 using modified 2s-EA. The modification of method enables more sensitive detection. This has been very useful especially in the right and left atria, where the lowest activities of the BChE have been detected. Due to higher sensitivity of the modified method, pooling several tissues of atria to determine BChE activity has not been necessary. Thus, our suggested optimization of the method also enables a decrease in the consumption of biological material.

Molecular forms of AChE and BChE present in the mouse heart

Overall activity study has shown that AChE activity in the entire heart is a few-fold lower than BChE activity. Our results are in line with the previously published data. It was shown that BChE activity predominates over AChE activity in the heart of mice (Gómez et al., 1999; Li et al., 2000), rats (Nyquist-Battie et al., 1987; Stanley et al., 1978) and human (Chow et al., 2001).

We have observed high AChE activity in the left atrium and the right atrium of mice (Figure 41), which is in agreement with previous observations acquired from human, dog (Sinha et al., 1976) and rat tissues (Nyquist-Battie and Trans-Saltzmann, 1989). Moreover, we have shown presence of PRiMA AChE and ColQ AChE in both atria, with the slightly higher content of the first one. The lowest AChE activity has been determined in the left ventricle and the septum. Majority of its activity has been formed by anchored AChE forms. However, here, ColQ AChE has been found in the slightly higher amount

than PRiMA AChE. Medium activity has been detected in the right ventricle, where the ratio of PRiMA AChE and ColQ AChE has been 1:1.

We have found the reversed activity pattern (Figure 41) of BChE in the studied heart compartments. This type of study has not been performed so far. The only similar experiment was performed in dogs, where the authors claimed higher BChE activity in the ventricles than in the atria (Sinha et al., 1976) that we have also confirmed in mice. Our results suggest non-uniform distribution of BChE activity in the heart. The lowest activity level has been detected in the right and left atria. The highest activity has been observed in the left ventricle and the septum, while activity in the right ventricle has been approximately 22 % lower. In all heart compartments, BChE has been found mainly as G_1^a (80 – 89 % of the total activity). Rest of the activity has been formed by G_4^{na} .

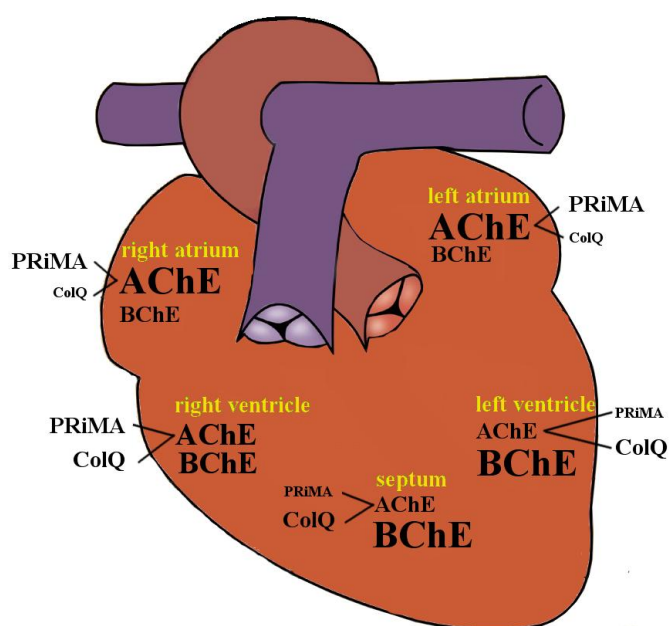


Figure 41: Activity pattern of AChE and BChE in the mouse heart. The size of the font relates to the amount of activity detected in the heart compartments. High AChE activities, predominantly anchored by PRiMA protein, have been determined in the atria. Lower activity has been observed in the right ventricle anchored by PRiMA and ColQ in the ratio 1:1. The lowest AChE activities have been detected in the left ventricle and the septum, anchored by PRiMA and ColQ, with the slightly higher content of the former. In case of BChE, activity, the pattern has been completely reversed. In all compartments, BChE has been found in form of G_1^a (80-89 %) and G_4^{na} (11-20 %).

In the myocardium of the atria, we have visualized clear AChE activity, but no BChE activity. As mentioned above, results from the biochemical analysis have shown that PRiMA AChE and ColQ AChE are present in these compartments. While we have precisely localized PRiMA AChE, we were not able to detect ColQ AChE. It is possible, that ColQ AChE is not concentrated in one structure or cell type, but it is more dispersed within the tissue and thus signal is under detection limit. Recently, a similar discrepancy between biochemical and microscopic analysis was observed in the skeletal muscles. It was shown that quantity of PRiMA AChE and ColQ AChE were similar, but only ColQ AChE was visible at the neuromuscular junction (Bernard et al., 2011). Finally, the authors discovered diffusely distributed PRiMA AChE along the muscle in the extrajunctional regions (Bernard et al., 2011). Other explanation of inconsistent results between these two techniques can be prolonged tissue handling in microscopy analysis and thus possible degradation of ColQ AChE.

In the myocardium of the ventricles, we have not detected any AChE activity, but we have observed BChE staining. Reports in literature are quite contradictory when it comes to BChE localization in ventricular myocardium. Chow et al. (Chow et al., 2001) reported massive BChE staining in the sinoatrial and atrioventricular nodes in infants, which gradually disappeared till adulthood. There are no studies dealing with localization of BChE in mice. We have visualized diffusely distributed BChE activity in the myocardium. This can be caused by high level (80 – 89 % of the total activity) of intracellularly localized G_1^a . However, the precise cellular localization of this pool is questionable. As previously published, monomeric and dimeric forms of ChE were found in the endoplasmic reticulum of different tissues (De Jaco et al., 2006; Eichler and Silman, 1995; Liesi et al., 1980; Somogyi et al., 1975) and their importance for the assembly of AChE and BChE was confirmed (Brockman et al., 1986; Eichler and Silman, 1995). Thus, we suggest that observed pool of inactive BChE enzyme could be localized in the endoplasmic reticulum and serves as the precursor for formation of soluble tetrameric BChE protein. Other possibility is that BChE G_1^a is present in the sarcoplasmic reticulum as published previously in rat (Karnovsky, 1964) and rabbit heart (Hagopian and Tennyson, 1971). Rotundo et al. (Rotundo et al., 1989) showed that AChE molecules can be chased into the sarcoplasmic reticulum prior to degradation. Moreover, potential role of sarcoplasmic reticulum in protein synthesis and folding is discussed (Glembotski, 2012).

This hypothesis suggests similar function of endoplasmic and sarcoplasmic reticulum in the assembly of ChE.

In the epicardium of heart, we have visualized dense AChE staining on the base of the heart, which extended epicardially to the atria, where we have identified PRiMA AChE. On the heart base, apart from strongly-colored linings, we have also noticed subtle branches. Molecular forms of AChE on the heart base have never been researched before. Here, we for the first time, report that strong epicardial AChE staining on the base of the heart consists of ColQ AChE and also PRiMA AChE. Staining of subtle branches has disappeared in the PRiMA deficient mice. This suggests that PRiMA AChE is responsible for this subtle coloration. As published before, staining from the heart base prolonged by the left dorsal, dorsal right atrial, right ventral and ventral left atrial routes (Rysevaite et al., 2011a). The structural organization of the staining matched to that obtained from human hearts (Pauza et al., 2000). This makes mouse heart a suitable model for studying human epicardial AChE.

In case of BChE, we have been able to detect only one strongly-colored lining on the base of the heart and no epicardial staining on the apex. These results are in line with outcomes gained from biochemical analysis, where higher activity has been detected on the base of the heart than in the region of apex. The nature of this activity is, however, questionable. The fact, that the activity is precisely localized, suggests presence of anchored forms of BChE. But it is contradictory to our biochemical experiments, where no such forms have been detected. We cannot rule out that this activity belongs to G_1^a . However, available information about this form in the organism is poor. The other possibility is the presence of the amphiphilic G_4 BChE. Gomez et al. (Gómez et al., 1999) have shown small amount (3 %) of this form in the mouse heart. Amphiphilic G_4 corresponds to the PRiMA anchored BChE. However, in our experiment we have used PRiMA deficient mice and the results are comparable to hearts of WT littermates. We have also used two detergents, BRIJ and CHAPS, to distinguish between amphiphilic and non-amphiphilic forms, while no amphiphilic G_4 have been observed. Thus, we are more prone to believe that activity belongs to the G_1^a or G_4^{na} , which presence in the heart was proved within this study.

Neuronal vs. non-neuronal system in the heart

It is well-known that AChE hydrolyses ACh in the synapses of cholinergic ganglia and also ACh released from parasympathetic postganglionic intracardiac neurons in the heart (Abramochkin et al., 2012, 2010; Borodinova et al., 2013; Dunlap et al., 2003; Olshansky et al., 2008). For decades, scientists have been considering AChE as a neuronal marker (Batulevicius et al., 2003; Marron et al., 1995; Pauza et al., 2002, 2000; Rysevaite et al., 2011a; Saburkina et al., 2014, 2014, 2010; Vaitkevicius et al., 2009). Thus, co-localization of AChE with cholinergic nerves on the heart base could be expected.

We report, that in the myocardium of atria, fluorescent signal of the PRiMA AChE has been co-localized with the signal of neuronal marker TUJ1. This suggests neuronal character of PRiMA AChE in the atria (Figure 42A).

At the time of writing this thesis, we have not been able to set suitable conditions for visualization of fluorescent signal in the gelatin-filled heart with specific anti-AChE antibody and antibody against neuronal marker TUJ1. Therefore, we have used a different approach to study the source of AChE localized on the heart base. We have performed transversal sections of the ventricles in the region of the heart base and then we have localized PRiMA AChE, ColQ AChE and neurons in the epicardium. Based on the obtained results, we report, that strongly-colored structures (representing PRiMA AChE and ColQ AChE) on the base of the heart have neuronal character (Figure 42A). In these sections, colored subtle branches seen in activity stained hearts filled with gelatin, representing only PRiMA AChE (see above), have not been visible and thus we cannot definitely conclude character of this staining. However, it was shown that PRiMA gene encodes the AChE anchor in the mammalian brain and that AChE is anchored by PRiMA on the cells membranes of the cholinergic neurons (Dobbertin et al., 2009b; Perrier et al., 2002, 2003). Moreover, PRiMA AChE was shown to be produced by motoneurons (Bernard et al., 2011). Thus, it is possible that this staining, identified as PRiMA AChE, has also neuronal character.

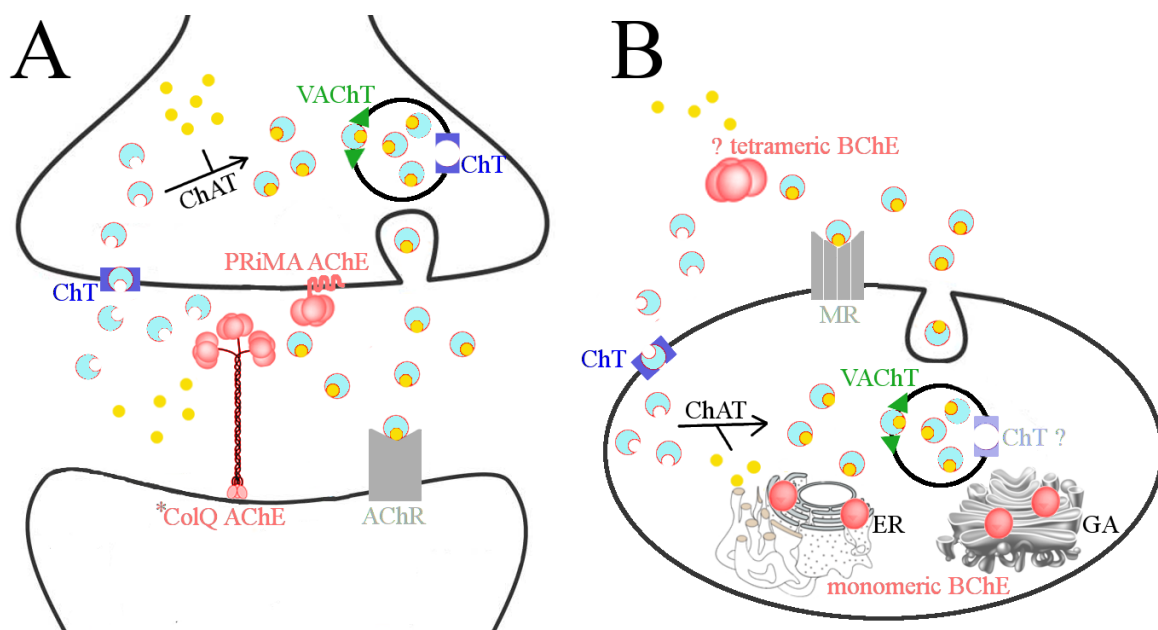


Figure 42: Neuronal (A) and non-neuronal (B) cholinergic system in the heart. A: Choline (●) is transported into the presynaptic nerve by choline transporter (ChT) where it reacts with acetyl Co-A (●) and ACh (●) is produced. This reaction is catalyzed by the action of cholinacetyltransferase (ChAT). ACh is transported into the vesicles by vesicular ACh transporter (VAcHT). Subsequently, ACh is released into the synaptic cleft where it stimulates ACh receptors. ACh is hydrolyzed by anchored AChE into choline and acetyl. PRiMA AChE is co-localized with the cholinergic postganglionic nerves in atria and ventricles. (*) ColQ AChE was confirmed to co-localize with neurons only on the heart base, while its origin in atria remains questionable. B: In cardiomyocytes, ACh is synthesized and released by the same pathway as in the case of neuron. However, ACh is probably hydrolyzed by BChE tetramer. We propose that the tetramer could be produced from G_1^a BChE in the endoplasmic reticulum (ER) and passes the secretion cascade through Golgi apparatus (GA).

AChE does not only fulfill function in the neurotransmission, synaptogenesis (Silman and Sussman, 2005) or neurite growth (Sharma et al., 2001), but also modulates haematopoietic differentiation (Deutsch et al., 2002) and plays a role in embryogenesis (Hanneman and Westerfield, 1989). Moreover, our results suggest that AChE may also play a role in the cardiomyogenesis. In the AChE del 5+6^{-/-} mice, which are typical for the absence of anchored forms of AChE, we have observed significantly lower cardiomyocyte diameter than in the WT mice. AChE del 5+6^{-/-} mice are smaller and weaker than WT mice. Thus, logical explanation can be that due to the lower body and heart weights, also cardiomyocyte diameter is decreased. However, previous investigations showed no changes in the total length or the mean diameter of cardiomyocytes due to changes in food intake and caloric restriction even if the body, heart and left ventricular weights were significantly reduced (Gruber et al., 2012). Thus, effect of body weight on the

cardiomyocyte diameter is excluded. Other studies revealed that administration of selective AChE inhibitor, pyridostigmine, led to the reduced diameter of cardiomyocytes (Lataro et al., 2013) and prevented the cellular hypertrophy induced by adrenergic overstimulation (Rocha-Resende et al., 2012). These observations strongly support our hypothesis, that anchored AChE affects cardiomyocyte diameter.

Recently, it has been shown that cardiomyocytes have properties of the non-neuronal cholinergic nervous system. These cells possess all components necessary for the ACh synthesis and release (Kakinuma et al., 2009; Lara et al., 2010; Rocha-Resende et al., 2012). Similarly to cholinergic neurons, ACh is synthesized by cholinacetyltransferase, choline is transported to the cytoplasm through the ChT and ACh is packed into the vesicles by vesicular ACh transporter (for review see Roy et al., 2014). However, it looks that the release of ACh is controlled differently. In the neurons, the fusion of the vesicles is triggered by the membrane depolarization that opens voltage gated calcium channel. Because the voltage gated calcium channels control the shape of the action potential that triggers the muscle contraction, it is improbable that ACh is released at each contraction (Abramochkin et al., 2010). Indeed it was observed that the vesicles are not localized close to the plasma membrane but around the nucleus. This suggests that even if the molecular actors involved in the packaging of ACh are identical, the release of ACh is differently controlled. As a consequence, the degradation of ACh in the cardiomyocytes could also be differently controlled than in the nervous system where AChE and BChE are specifically anchored (Dobbertin et al., 2009; Perrier et al., 2002, 2003; Tsim and Soreq, 2013). A fundamental difference between the synaptic neurotransmission and the function of ACh released by the cardiomyocytes is the timing. During the synaptic neurotransmission, the duration of ACh function is in the range of milliseconds (Ordentlich et al., 1998; Rosenberry, 1975), thus AChE must be already present, i.e., anchored by ColQ or PRiMA. In the cardiomyocytes, the timing appears to be different. The best example is when comparing the cardiac function in presence or in absence of ACh in the cardiomyocytes (Roy et al., 2013). After acute, brief exercise, heart rate recovers in 30 minutes when ACh is produced by the cardiomyocytes, however, it requires more than one hour when cardiomyocytes cannot produce ACh (Roy et al., 2013). At the physiological level, if ACh functions have to be ended during this period, an efficient way could be the release of BChE tetramer. This could be done by the production of PRAD and the maturation of G₁^a BChE that is present intracellularly, probably in the endoplasmic reticulum (Figure 42B).

During the past years, BChE was found to contain a PRAD as organizer of the tetramer (Altamirano and Lockridge, 1999; H. Li et al., 2008). We propose that secreted BChE tetramer could play a role in the degradation of non-neuronal ACh (Figure 42B). However, release of tetramer into extracellular location is not clear. Here, a question arises if this tetramer is being continuously released or it is released in specific conditions, when ACh level has to be controlled.

Alternatively, intracellular BChE can also have a function in cardiomyocyte, similarly to the $\alpha 7$ nicotinic receptors in mouse liver mitochondria (Kalashnyk et al., 2012). It was shown that intracellular receptors regulates mitochondrial pore formation and early pro-apoptotic events like cytochrome C release (Gergalova et al., 2014, 2012). Also other proteins might have intracellular and extracellular roles, too e.g., epimorphin/syntaxin 2, amphoterin/high mobility group protein B1 and tissue transglutaminase (Radisky et al., 2009).

**CONCLUSION AND
PRACTICAL
IMPLEMENTATION OF
RESULTS**

ChE perform an important role in cholinergic system of the heart. However, knowledge about this subject has until now been very poor and thus it deserves more attention. We have provided a complex study of ChE in the heart. Activities of AChE (Table 3) and BChE (Table 4) in the heart compartments have been determined and molecular forms present in these parts have been described. We have performed localization study of AChE (Table 3) and BChE (Table 4) in the epicardium and myocardium of heart and we have studied the origin of these ChE. Moreover, we have assessed effect of lack of ChE and their molecular forms on the diameter of cardiomyocytes.

We have observed the highest AChE activity in the atria, anchored by both, PRiMA and ColQ protein. PRiMA AChE is localized in the myocardium and epicardium of the atria and its presence is linked to the neuronal cells. While no AChE has been localized in the myocardium of the ventricles, PRiMA and ColQ AChE are clearly distributed epicardially on the heart base. Using neuronal marker, we have identified that epicardial AChE are linked to the intracardiac neurons. Apart from intracardiac neurons, PRiMA AChE forms subtle branching on the heart base.

In the study we have used mouse mutant strains with specific deletion of ChE or their molecular forms. We have found that when anchored AChE is missing, diameter of cardiomyocytes is significantly lowered.

Table 3: Summary of results about AChE activity, molecular forms and their localization in the heart

Tissue	AChE Activity level	PRiMA AChE				ColQ AChE			
		Identified by biochemical analysis	Localized by microscopy		Co-localized with nerve cells	Identified by biochemical analysis	Localized by microscopy		Co-localized with nerve cells
			myo	epi			myo	epi	
RA	↑	✓	✓	✓	✓	✓	×	×	?
LA	↑	✓	✓	✓	✓	✓	×	×	?
RV	↕	✓	×	✓	✓	✓	×	✓	✓
LV+SE	↓	✓	×	✓	✓	✓	×	✓	✓
Base	↑	✓	×	✓	✓	✓	×	✓	✓
Apex	↓	✓	×	✓	?	✓	×	✓	?

RA- right atrium, LA- left atrium, RV – right ventricle, LV – left ventricle, SE – septum, myo – myocardium, epi – epicardium, ↑ high activity, ↕ medium activity, ↓ low activity.

Activity of BChE in the heart has been found to be higher than that of AChE. In all studied heart compartments, major form of BChE are monomers. The rest of the activity belongs to the non-amphiphilic tetramers. The highest BChE activity has been determined in the ventricles, specifically the left ventricle and the septum. However, in the myocardium, we could not precisely localize its activity. We have detected diffusely distributed BChE within the heart. In the epicardium, we have localized one strong staining, suggesting presence of BChE activity.

Table 4: Summary of results about BChE activity, molecular forms and their localization in the heart

Tissue	BChE Activity level	Identified by biochemical analysis	G ₁ ^a		Co-localized with nerve cells
			Localized by microscopy myo	epi	
RA	↓	✓	×	×	?
LA	↓	✓	×	×	?
RV	↕	✓	✓	×	?
LV+SE	↑	✓	✓	×	?
Base	↑	✓	✓	✓	✓
Apex	↕	✓	✓	×	?

RA - right atrium, LA- left atrium, RV – right ventricle, LV – left ventricle, SE – septum, myo – myocardium, epi – epicardium, ↑ high activity, ↕ medium activity, ↓ low activity.

In the presented work, we filled the missing information about ChE in the heart. These results can be very helpful, since ChE control the level of ACh in the tissue and protective effect of ACh was observed in the heart diseases e.g., heart failure, atrial and ventricular fibrillation (for review see Roy et al., 2014). Potential targets in pharmacotherapy of mentioned disorders are ChE. Recent studies showed that donepezil, selective AChE inhibitor, reduces cardiac remodeling and markedly improves the long-term survival in chronic heart failure (Handa et al., 2009) and in chronic heart failure followed by the extensive myocardial infarction (Li et al., 2013). Other AChE inhibitor, pyridostigmine, showed positive effects on cardiac remodeling, attenuating left ventricular dysfunction in the onset of heart failure following myocardial infarction (Lataro et al., 2013) and also in the model of sympathetic hyperactivity inducing cardiac dysfunction (Gavioli et al., 2014). Other studies also confirmed beneficial effect of pyridostigmine in patients with heart failure. They showed that pyridostigmine reduces ventricular

arrhythmia density (Behling et al., 2003), improves hemodynamic profile during dynamic exercise (Serra et al., 2009) and increases heart rate recovery after exercise (Androne et al., 2003). Moreover, effect of pyridostigmine bromide on the heart failure is currently tested in the phase 2 of clinical trials (clinicaltrials.gov NCT01415921).

Our results provide deep information about ChE in the heart. We have precisely determined their activity, molecular forms and localization. One of the most interesting observations claim, that AChE is localized mainly in the atria and its presence is linked to the neuronal cells. On the contrary, BChE is localized mainly in the ventricles, where probably plays a role in the non-neuronal system of cardiomyocytes. Thus these results can help to selectively affect ChE in specific heart compartments and thus enable selective pharmaceutical intervention. These investigations can help to better characterize relationship between heart disease and effect of ChE inhibitors with respect to their selectivity and thus may result in production of a new, more effective pharmacotherapy in future that may reduce morbidity and mortality in patients with heart diseases. Apart from the clinical point of view, our results can be widely used in the experimental practice e.g., in the study of the heart morphology, anatomy and physiology of the heart.

Within this study we also optimized EA. This method is one of the most widely used methods for determination of ChE activity. It is commonly used in the biological monitoring of agriculturalists or human who comes in contact with organophosphates, carbamates or other ChE inhibitors (London et al., 1995). In clinical practice, EA is used for prediction of prolonged apnea after succinylcholine administration (Alexander DR, 2015; Dietz et al., 1973). Moreover, in the experimental procedures, activities of AChE and BChE are studied more and more extensively, especially due to their link to pathologies, e.g., diabetes mellitus (Iwasaki et al., 2007; Rao et al., 2007; Sato et al., 2014), obesity (Alcântara et al., 2003; Dantas et al., 2011; Lima et al., 2013), liver diseases (Ramachandran et al., 2014; Steinebrunner et al., 2014), Alzheimer disease (Alkalay et al., 2013; Appleyard and McDonald, 1992; García-Ayllón et al., 2010), Parkinson disease (Bawaskar et al., 2015; Hiraoka et al., 2012), Lewy-body disease (Shimada et al., 2009; Wang et al., 2015), coronary artery disease (Alcântara et al., 2002).

In all mentioned areas, where EA is routinely used, biological samples are analyzed. Our modification of method was designed especially for studying ChE activity in

biological samples. Moreover, it is notably useful when low activities of ChE are determined. We recommend performing prolonged (hours-long) activity assays of ChE in HEPES buffer. If phosphate buffer is required for the experiment, pH 7.0 or 7.5 should be used to increase DTNB stability and lower the background over the time of measurement. Low ChE activities in biological samples should be followed by the modified 2s-EA in which interaction of DTNB is abolished. We also found out that the more time-consuming ELISA may be used if the background needs to be eliminated. Use of ELISA may be limited by the availability of monoclonal antibodies to detect ChE from different species (Dingova et al., 2014).

BIBLIOGRAPHY

- Abramochkin, D.V., Borodinova, A.A., Rosenshtraukh, L.V., Nikolsky, E.E., 2012. Both neuronal and non-neuronal acetylcholine take part in non-quantal acetylcholine release in the rat atrium. *Life Sci.* 91, 1023–1026.
- Abramochkin, D.V., Nurullin, L.F., Borodinova, A.A., Tarasova, N.V., Sukhova, G.S., Nikolsky, E.E., Rosenshtraukh, L.V., 2010. Non-quantal release of acetylcholine from parasympathetic nerve terminals in the right atrium of rats. *Exp. Physiol.* 95, 265–273.
- Alberts Bruce, Dennis Bray, Julian Lewis, Martin Raff, Keith Roberts, James Watson, 1989. *Molecular biology of the cell*. Garland Publishing, Inc.
- Alcântara, V.M., Chautard-Freire-Maia, E.A., Scartezini, M., Cerci, M.S.J., Braun-Prado, K., Picheth, G., 2002. Butyrylcholinesterase activity and risk factors for coronary artery disease. *Scand. J. Clin. Lab. Invest.* 62, 399–404.
- Alcântara, V.M., Oliveira, L.C., Réa, R.R., Suplicy, H.L., Chautard-Freire-Maia, E.A., 2003. Butyrylcholinesterase and obesity in individuals with the CHE2 C5+ and CHE2 C5- phenotypes. *Int. J. Obes. Relat. Metab. Disord. J. Int. Assoc. Study Obes.* 27, 1557–1564.
- Alexander DR, 2015. Pseudocholinesterase Deficiency Workup. *Medscape Drugs & Diseases*.
- Alisaraie, L., Fels, G., 2006. Molecular docking study on the “back door” hypothesis for product clearance in acetylcholinesterase. *J. Mol. Model.* 12, 348–354.
doi:10.1007/s00894-005-0051-5
- Alkalay, A., Rabinovici, G.D., Zimmerman, G., Agarwal, N., Kaufer, D., Miller, B.L., Jagust, W.J., Soreq, H., 2013. Plasma acetylcholinesterase activity correlates with intracerebral β -amyloid load. *Curr. Alzheimer Res.* 10, 48–56.
- Altamirano, C.V., Lockridge, O., 1999. Conserved aromatic residues of the C-terminus of human butyrylcholinesterase mediate the association of tetramers. *Biochemistry (Mosc.)* 38, 13414–13422.
- Anderson RM, 1993. *The Gross Physiology of the Cardiovascular System*, 2nd ed. Racquet Press.
- Ando, M., Katare, R.G., Kakinuma, Y., Zhang, D., Yamasaki, F., Muramoto, K., Sato, T., 2005. Efferent vagal nerve stimulation protects heart against ischemia-induced arrhythmias by preserving connexin43 protein. *Circulation* 112, 164–170.
- Androne, A.S., Hryniewicz, K., Goldsmith, R., Arwady, A., Katz, S.D., 2003. Acetylcholinesterase inhibition with pyridostigmine improves heart rate recovery after maximal exercise in patients with chronic heart failure. *Heart Br. Card. Soc.* 89, 854–858.
- Ankle, M.R., Joshi, P.S., 2011. A study to evaluate the efficacy of xylene-free hematoxylin and eosin staining procedure as compared to the conventional hematoxylin and eosin staining: An experimental study. *J. Oral Maxillofac. Pathol. JOMFP* 15, 161–167.
- Appleton, C.P., Kovács, S.J., 2009. The Role of Left Atrial Function in Diastolic Heart Failure. *Circ. Cardiovasc. Imaging* 2, 6–9.
- Appleyard, M.E., McDonald, B., 1992. Acetylcholinesterase and butyrylcholinesterase activities in cerebrospinal fluid from different levels of the neuraxis of patients with dementia of the Alzheimer type. *J. Neurol. Neurosurg. Psychiatry* 55, 1074–1078.
- Armour, J.A., 2008. Potential clinical relevance of the “little brain” on the mammalian heart. *Exp. Physiol.* 93, 165–176.
- Armour, J.A., 2004. Cardiac neuronal hierarchy in health and disease. *Am. J. Physiol. Regul. Integr. Comp. Physiol.* 287, R262–271.

- Armour, J.A., Murphy, D.A., Yuan, B.X., Macdonald, S., Hopkins, D.A., 1997. Gross and microscopic anatomy of the human intrinsic cardiac nervous system. *Anat. Rec.* 247, 289–298.
- Armour, J.A., Richer, L.-P., Pagé, P., Vinet, A., Kus, T., Vermeulen, M., Nadeau, R., Cardinal, R., 2005. Origin and pharmacological response of atrial tachyarrhythmias induced by activation of mediastinal nerves in canines. *Auton. Neurosci. Basic Clin.* 118, 68–78. doi:10.1016/j.autneu.2005.01.006
- Arpagaus, M., Kott, M., Vatsis, K.P., Bartels, C.F., La Du, B.N., Lockridge, O., 1990. Structure of the gene for human butyrylcholinesterase. Evidence for a single copy. *Biochemistry (Mosc.)* 29, 124–131.
- Axelsen, P.H., Harel, M., Silman, I., Sussman, J.L., 1994. Structure and dynamics of the active site gorge of acetylcholinesterase: synergistic use of molecular dynamics simulation and X-ray crystallography. *Protein Sci. Publ. Protein Soc.* 3, 188–197.
- Badiou, A., Froment, M.T., Fournier, D., Masson, P., Belzunces, L.P., 2008. Hysteresis of insect acetylcholinesterase. *Chem. Biol. Interact.* 175, 410–412. doi:10.1016/j.cbi.2008.05.039
- Bajgar, J., Kuca, K., Jun, D., Bartosova, L., Fusek, J., 2007. Cholinesterase reactivators: the fate and effects in the organism poisoned with organophosphates/nerve agents. *Curr. Drug Metab.* 8, 803–809.
- Baldwin, H.S., Shen, H.M., Yan, H.C., DeLisser, H.M., Chung, A., Mickanin, C., Trask, T., Kirschbaum, N.E., Newman, P.J., Albelda, S.M., 1994. Platelet endothelial cell adhesion molecule-1 (PECAM-1/CD31): alternatively spliced, functionally distinct isoforms expressed during mammalian cardiovascular development. *Dev. Camb. Engl.* 120, 2539–2553.
- Baraka, A.S., Haroun-Bizri, S.T., Nawfal, M.F., Gerges, F.J., Nasr, V.G., 2005. Does pancuronium or cisatracurium delay the rate of arousal following remifentanyl-based anesthesia? *Middle East J. Anaesthesiol.* 18, 477–484.
- Barakat, N.H., Zheng, X., Gilley, C.B., MacDonald, M., Okolotowicz, K., Cashman, J.R., Vyas, S., Beck, J.M., Hadad, C.M., Zhang, J., 2009. Chemical synthesis of two series of nerve agent model compounds and their stereoselective interaction with human acetylcholinesterase and human butyrylcholinesterase. *Chem. Res. Toxicol.* 22, 1669–1679
- Barak, D., Kronman, C., Ordentlich, A., Ariel, N., Bromberg, A., Marcus, D., Lazar, A., Velan, B., Shafferman, A., 1994. Acetylcholinesterase peripheral anionic site degeneracy conferred by amino acid arrays sharing a common core. *J. Biol. Chem.* 269, 6296–6305.
- Bartolini, M., Bertucci, C., Cavrini, V., Andrisano, V., 2003. beta-Amyloid aggregation induced by human acetylcholinesterase: inhibition studies. *Biochem. Pharmacol.* 65, 407–416.
- Batulevicius, D., Pauziene, N., Pauza, D.H., 2005. Architecture and age-related analysis of the neuronal number of the guinea pig intrinsic cardiac nerve plexus. *Ann. Anat. - Anat. Anz.* 187, 225–243.
- Batulevicius, D., Pauziene, N., Pauza, D.H., 2003. Topographic morphology and age-related analysis of the neuronal number of the rat intracardiac nerve plexus. *Ann. Anat. Anat. Anz. Off. Organ Anat. Ges.* 185, 449–459.
- Batulevicius, D., Skripka, V., Pauziene, N., Pauza, D.H., 2008. Topography of the porcine epicardiac nerve plexus as revealed by histochemistry for acetylcholinesterase. *Auton. Neurosci. Basic Clin.* 138, 64–75.

- Bawaskar, H.S., Bawaskar, P.H., Bawaskar, P.H., 2015. RBC acetyl cholinesterase: A poor man's early diagnostic biomarker for familial alzheimer's and Parkinson's disease dementia. *J. Neurosci. Rural Pract.* 6, 33–38.
- Behling, A., Moraes, R.S., Rohde, L.E., Ferlin, E.L., Nóbrega, A.C.L., Ribeiro, J.P., 2003. Cholinergic stimulation with pyridostigmine reduces ventricular arrhythmia and enhances heart rate variability in heart failure. *Am. Heart J.* 146, 494–500.
- Bernard, V., Girard, E., Hrabovska, A., Camp, S., Taylor, P., Plaud, B., Krejci, E., 2011. Distinct localization of collagen Q and PRiMA forms of acetylcholinesterase at the neuromuscular junction. *Mol. Cell. Neurosci.* 46, 272–281.
- Blong, R.M., Bedows, E., Lockridge, O., 1997. Tetramerization domain of human butyrylcholinesterase is at the C-terminus. *Biochem. J.* 327, 747–757.
- Blusztajn, J.K., Liscovitch, M., Mauron, C., Richardson, U.I., Wurtman, R.J., 1987. Phosphatidylcholine as a precursor of choline for acetylcholine synthesis. *J. Neural Transm. Suppl.* 24, 247–259.
- Boeck, A.T., Schopfer, L.M., Lockridge, O., 2002. DNA sequence of butyrylcholinesterase from the rat: expression of the protein and characterization of the properties of rat butyrylcholinesterase. *Biochem. Pharmacol.* 63, 2101–2110.
- Bon, S., Coussen, F., Massoulié, J., 1997. Quaternary associations of acetylcholinesterase. II. The polyproline attachment domain of the collagen tail. *J. Biol. Chem.* 272, 3016–3021.
- Bon, S., Toutant, J.P., Méflah, K., Massoulié, J., 1988. Amphiphilic and nonamphiphilic forms of Torpedo cholinesterases: I. Solubility and aggregation properties. *J. Neurochem.* 51, 776–785.
- Borodinova, A.A., Abramochkin, D.V., Sukhova, G.S., 2013. Non-quantal release of acetylcholine in rat atrial myocardium is inhibited by noradrenaline. *Exp. Physiol.* 98, 1659–1667.
- Boron, W.F., 2003. *Medical Physiology: A Cellular and Molecular Approach*. W.B. Saunders.
- Boudinot, E., Bernard, V., Camp, S., Taylor, P., Champagnat, J., Krejci, E., Foutz, A.S., 2009. Influence of differential expression of acetylcholinesterase in brain and muscle on respiration. *Respir. Physiol. Neurobiol.* 165, 40–48.
- Bourne, Y., Radic, Z., Sulzenbacher, G., Kim, E., Taylor, P., Marchot, P., 2006. Substrate and product trafficking through the active center gorge of acetylcholinesterase analyzed by crystallography and equilibrium binding. *J. Biol. Chem.* 281, 29256–29267.
- Boyett, M.R., Honjo, H., Kodama, I., 2000. The sinoatrial node, a heterogeneous pacemaker structure. *Cardiovasc. Res.* 47, 658–687. doi:10.1016/S0008-6363(00)00135-8
- Brockman, S.K., Usiak, M.F., Younkin, S.G., 1986. Assembly of monomeric acetylcholinesterase into tetrameric and asymmetric forms. *J. Biol. Chem.* 261, 1201–1207.
- Brodde, O.E., Michel, M.C., 1999. Adrenergic and muscarinic receptors in the human heart. *Pharmacol. Rev.* 51, 651–690.
- Brutsaert, D.L., 2003. Cardiac Endothelial-Myocardial Signaling: Its Role in Cardiac Growth, Contractile Performance, and Rhythmicity. *Physiol. Rev.* 83, 59–115. doi:10.1152/physrev.00017.2002
- Brutsaert, D.L., Franssen, P., Andries, L.J., Keulenaer, G.W.D., Sys, S.U., 1998. Cardiac endothelium and myocardial function. *Cardiovasc. Res.* 38, 281–290.
- Burton, R.A.B., Plank, G., Schneider, J.E., Grau, V., Ahammer, H., Keeling, S.L., Lee, J., Smith, N.P., Gavaghan, D., Trayanova, N., Kohl, P., 2006. Three-Dimensional

- Models of Individual Cardiac Histoanatomy: Tools and Challenges. *Ann. N. Y. Acad. Sci.* 1080, 301–319.
- Calderon-Margalit, R., Adler, B., Abramson, J.H., Gofin, J., Kark, J.D., 2006. Butyrylcholinesterase activity, cardiovascular risk factors, and mortality in middle-aged and elderly men and women in Jerusalem. *Clin. Chem.* 52, 845–852.
- Camp, S., Zhang, L., Marquez, M., de la Torre, B., Long, J.M., Bucht, G., Taylor, P., 2005. Acetylcholinesterase (AChE) gene modification in transgenic animals: functional consequences of selected exon and regulatory region deletion. *Chem. Biol. Interact.* 157-158, 79–86.
- Cardiff, R.D., Miller, C.H., Munn, R.J., 2014. Manual hematoxylin and eosin staining of mouse tissue sections. *Cold Spring Harb. Protoc.* 2014, 655–658.
- Cartaud, A., Strohlic, L., Guerra, M., Blanchard, B., Lambergeon, M., Krejci, E., Cartaud, J., Legay, C., 2004. MuSK is required for anchoring acetylcholinesterase at the neuromuscular junction. *J. Cell Biol.* 165, 505–515.
- Cauet, G., Friboulet, A., Thomas, D., 1987. Substrate activation and thermal denaturation kinetics of the tetrameric and the trypsin-generated monomeric forms of horse serum butyrylcholinesterase. *Biochim. Biophys. Acta* 912, 338–342.
- Chang, J.Y.F., Kessler, H.P., 2008. Masson trichrome stain helps differentiate myofibroma from smooth muscle lesions in the head and neck region. *J. Formos. Med. Assoc. Taiwan Yi Zhi* 107, 767–773.
- Chatonnet, F., Boudinot, E., Chatonnet, A., Taysse, L., Daulon, S., Champagnat, J., Foutz, A.S., 2003. Respiratory survival mechanisms in acetylcholinesterase knockout mouse. *Eur. J. Neurosci.* 18, 1419–1427.
- Chen, V.P., Luk, W.K.W., Chan, W.K.B., Leung, K.W., Guo, A.J.Y., Chan, G.K.L., Xu, S.L., Choi, R.C.Y., Tsim, K.W.K., 2011. Molecular Assembly and Biosynthesis of Acetylcholinesterase in Brain and Muscle: the Roles of t-peptide, FHB Domain, and N-linked Glycosylation. *Front. Mol. Neurosci.* 4, 36.
- Chen, V.P., Xie, H.Q., Chan, W.K.B., Leung, K.W., Chan, G.K.L., Choi, R.C.Y., Bon, S., Massoulié, J., Tsim, K.W.K., 2010. The PRiMA-linked cholinesterase tetramers are assembled from homodimers: hybrid molecules composed of acetylcholinesterase and butyrylcholinesterase dimers are up-regulated during development of chicken brain. *J. Biol. Chem.* 285, 27265–27278.
- Chitlaru, T., Kronman, C., Velan, B., Shafferman, A., 2001. Effect of human acetylcholinesterase subunit assembly on its circulatory residence. *Biochem. J.* 354, 613–625.
- Choate, J.K., Klemm, M., Hirst, G.D., 1993. Sympathetic and parasympathetic neuromuscular junctions in the guinea-pig sino-atrial node. *J. Auton. Nerv. Syst.* 44, 1–15.
- Chow, L.T., Chow, S.S., Anderson, R.H., Gosling, J.A., 2001. Autonomic innervation of the human cardiac conduction system: changes from infancy to senility--an immunohistochemical and histochemical analysis. *Anat. Rec.* 264, 169–182.
- Chung MK, Rich MW, 1990. Introduction to the cardiovascular system. *Alcohol Health and Research World* 14, 269–276.
- Cifelli, C., Rose, R.A., Zhang, H., Voigtlaender-Bolz, J., Bolz, S.-S., Backx, P.H., Heximer, S.P., 2008. RGS4 regulates parasympathetic signaling and heart rate control in the sinoatrial node. *Circ. Res.* 103, 527–535.
- Coiado, O., Buiochi, E., O'Brien, W., 2015. Ultrasound-induced heart rate decrease: role of the vagus nerve. *IEEE Trans. Ultrason. Ferroelectr. Freq. Control* 62, 329–336.

- Colletier, J.-P., Fournier, D., Greenblatt, H.M., Stojan, J., Sussman, J.L., Zaccari, G., Silman, I., Weik, M., 2006. Structural insights into substrate traffic and inhibition in acetylcholinesterase. *EMBO J.* 25, 2746–2756.
- Cook, D.J., 2006. Cellular Pathology, second edition, 2Rev Ed edition. ed. Scion Publishing Ltd, Bloxham, Oxfordshire.
- Cousin, X., Bon, S., Massoulié, J., Bon, C., 1998. Identification of a novel type of alternatively spliced exon from the acetylcholinesterase gene of *Bungarus fasciatus*. Molecular forms of acetylcholinesterase in the snake liver and muscle. *J. Biol. Chem.* 273, 9812–9820.
- Dantas, V.G.L., Furtado-Alle, L., Souza, R.L.R., Chautard-Freire-Maia, E.A., 2011. Obesity and variants of the GHRL (ghrelin) and BCHE (butyrylcholinesterase) genes. *Genet. Mol. Biol.* 34, 205–207.
- De Jaco, A., Comoletti, D., Kovarik, Z., Gaietta, G., Radic, Z., Lockridge, O., Ellisman, M.H., Taylor, P., 2006. A mutation linked with autism reveals a common mechanism of endoplasmic reticulum retention for the alpha,beta-hydrolase fold protein family. *J. Biol. Chem.* 281, 9667–9676.
- Dejana, E., Del Maschio, A., 1995. Molecular organization and functional regulation of cell to cell junctions in the endothelium. *Thromb. Haemost.* 74, 309–312.
- Deprez, P., Inestrosa, N.C., Krejci, E., 2003. Two different heparin-binding domains in the triple-helical domain of ColQ, the collagen tail subunit of synaptic acetylcholinesterase. *J. Biol. Chem.* 278, 23233–23242.
- D’Ettorre, C., Levine, R.L., 1994. Reactivity of cysteine-67 of the human immunodeficiency virus-1 protease: studies on a peptide spanning residues 59 to 75. *Arch. Biochem. Biophys.* 313, 71–76.
- Deutsch, V.R., Pick, M., Perry, C., Grisaru, D., Hemo, Y., Golan-Hadari, D., Grant, A., Eldor, A., Soreq, H., 2002. The stress-associated acetylcholinesterase variant AChE-R is expressed in human CD34(+) hematopoietic progenitors and its C-terminal peptide ARP promotes their proliferation. *Exp. Hematol.* 30, 1153–1161.
- Dietz, A.A., Rubinstein, H.M., Lubrano, T., 1973. Colorimetric determination of serum cholinesterase and its genetic variants by the propionylthiocholine-dithiobis(nitrobenzoic acid) procedure. *Clin. Chem.* 19, 1309–1313.
- Dingova, D., Leroy, J., Check, A., Garaj, V., Krejci, E., Hrabovska, A., 2014. Optimal detection of cholinesterase activity in biological samples: modifications to the standard Ellman’s assay. *Anal. Biochem.* 462, 67–75.
- Dobbertin, A., Hrabovska, A., Dembele, K., Camp, S., Taylor, P., Krejci, E., Bernard, V., 2009. Targeting of acetylcholinesterase in neurons in vivo: a dual processing function for the proline-rich membrane anchor subunit and the attachment domain on the catalytic subunit. *J. Neurosci. Off. J. Soc. Neurosci.* 29, 4519–4530.
- Doevendans, P.A., Daemen, M.J., Muinck, E.D. de, Smits, J.F., 1998. Cardiovascular phenotyping in mice. *Cardiovasc. Res.* 39, 34–49.
- Doganavsargil, B., Buberl, G.E., Toz, H., Sarsik, B., Pehlivanoglu, B., Sezak, M., Sen, S., 2015. Digitally reinforced hematoxylin-eosin polarization technique in diagnosis of rectal amyloidosis. *World J. Gastroenterol. WJG* 21, 1827–1837.
- Drake, C.J., Fleming, P.A., 2000. Vasculogenesis in the day 6.5 to 9.5 mouse embryo. *Blood* 95, 1671–1679.
- Dunlap, M.E., Bibevski, S., Rosenberry, T.L., Ernsberger, P., 2003. Mechanisms of altered vagal control in heart failure: influence of muscarinic receptors and acetylcholinesterase activity. *Am. J. Physiol. Heart Circ. Physiol.* 285, H1632–1640.

- Dvir, H., Harel, M., Bon, S., Liu, W.-Q., Vidal, M., Garbay, C., Sussman, J.L., Massoulié, J., Silman, I., 2004. The synaptic acetylcholinesterase tetramer assembles around a polyproline II helix. *EMBO J.* 23, 4394–4405.
- Dvir, H., Silman, I., Harel, M., Rosenberry, T.L., Sussman, J.L., 2010. Acetylcholinesterase: From 3D Structure to Function. *Chem. Biol. Interact.* 187, 10–22.
- Eckenstein, F., Baughman, R.W., 1984. Two types of cholinergic innervation in cortex, one co-localized with vasoactive intestinal polypeptide. *Nature* 309, 153–155.
- Eichler, J., Silman, I., 1995. The activity of an endoplasmic reticulum-localized pool of acetylcholinesterase is modulated by heat shock. *J. Biol. Chem.* 270, 4466–4472.
- Eisele, J.C., Schaefer, I.-M., Nyengaard, J.R., Post, H., Liebetanz, D., Brüel, A., Mühlfeld, D.C., 2007. Effect of voluntary exercise on number and volume of cardiomyocytes and their mitochondria in the mouse left ventricle. *Basic Res. Cardiol.* 103, 12–21.
- Ellman, G.L., 1959. Tissue sulfhydryl groups. *Arch. Biochem. Biophys.* 82, 70–77.
- Ellman, G.L., Courtney, K.D., Andres, V., Feather-Stone, R.M., 1961. A new and rapid colorimetric determination of acetylcholinesterase activity. *Biochem. Pharmacol.* 7, 88–95.
- English, B.A., Appalsamy, M., Diedrich, A., Ruggiero, A.M., Lund, D., Wright, J., Keller, N.R., Louderback, K.M., Robertson, D., Blakely, R.D., 2010. Tachycardia, reduced vagal capacity, and age-dependent ventricular dysfunction arising from diminished expression of the presynaptic choline transporter. *Am. J. Physiol. Heart Circ. Physiol.* 299, H799–810.
- Evers, A.S., Maze, M., Kharasch, E.D., 2011. *Anesthetic Pharmacology: Basic Principles and Clinical Practice.* Cambridge University Press.
- Farar, V., Hrabovska, A., Krejci, E., Myslivecek, J., 2013. Developmental adaptation of central nervous system to extremely high acetylcholine levels. *PloS One* 8, e68265.
- Farb, A., Burke, A.P., Virmani, R., 1992. Anatomy and pathology of the right ventricle (including acquired tricuspid and pulmonic valve disease). *Cardiol. Clin.* 10, 1–21.
- Fekonja, O., Zorec-Karlovsek, M., El Kharbili, M., Fournier, D., Stojan, J., 2007. Inhibition and protection of cholinesterases by methanol and ethanol. *J. Enzyme Inhib. Med. Chem.* 22, 407–415.
- Feng, G., Krejci, E., Molgo, J., Cunningham, J.M., Massoulié, J., Sanes, J.R., 1999. Genetic analysis of collagen Q: roles in acetylcholinesterase and butyrylcholinesterase assembly and in synaptic structure and function. *J. Cell Biol.* 144, 1349–1360.
- Ferguson, S.M., Bazalakova, M., Savchenko, V., Tapia, J.C., Wright, J., Blakely, R.D., 2004. Lethal impairment of cholinergic neurotransmission in hemicholinium-3-sensitive choline transporter knockout mice. *Proc. Natl. Acad. Sci. U. S. A.* 101, 8762–8767.
- Ferguson, S.M., Blakely, R.D., 2004. The choline transporter resurfaces: new roles for synaptic vesicles? *Mol. Interv.* 4, 22–37.
- Fischer, A.H., Jacobson, K.A., Rose, J., Zeller, R., 2008. Hematoxylin and eosin staining of tissue and cell sections. *CSH Protoc.* 2008, pdb.prot4986.
- Flynn, C.J., Wecker, L., 1986. Elevated choline levels in brain. A non-cholinergic component of organophosphate toxicity. *Biochem. Pharmacol.* 35, 3115–3121.
- Forbes, M.S., 2001. Chapter 5 - Ultrastructure of Cardiac Muscle and Blood Vessels, in: Cohen, N.S.K.T.V. (Ed.), *Heart Physiology and Pathophysiology (Fourth Edition).* Academic Press, San Diego, pp. 71–98.

- Francone, O.L., Fielding, C.J., 1991. Effects of site-directed mutagenesis at residues cysteine-31 and cysteine-184 on lecithin-cholesterol acyltransferase activity. *Proc. Natl. Acad. Sci. U. S. A.* 88, 1716–1720.
- García-Ayllón, M.-S., Riba-Llena, I., Serra-Basante, C., Alom, J., Boopathy, R., Sáez-Valero, J., 2010. Altered levels of acetylcholinesterase in Alzheimer plasma. *PLoS One* 5, e8701.
- García-Ayllón, M.S., Sáez-Valero, J., Muñoz-Delgado, E., Vidal, C.J., 2001. Identification of hybrid cholinesterase forms consisting of acetyl- and butyrylcholinesterase subunits in human glioma. *Neuroscience* 107, 199–208.
- Garlanda, C., Dejana, E., 1997. Heterogeneity of Endothelial Cells Specific Markers. *Arterioscler. Thromb. Vasc. Biol.* 17, 1193–1202.
- Garvey, W., 1984. Modified elastic tissue-Masson trichrome stain. *Stain Technol.* 59, 213–216.
- Gavioli, M., Lara, A., Almeida, P.W.M., Lima, A.M., Damasceno, D.D., Rocha-Resende, C., Ladeira, M., Resende, R.R., Martinelli, P.M., Melo, M.B., Brum, P.C., Fontes, M.A.P., Souza Santos, R.A., Prado, M.A.M., Guatimosim, S., 2014. Cholinergic signaling exerts protective effects in models of sympathetic hyperactivity-induced cardiac dysfunction. *PLoS One* 9, e100179.
- Gentile, C., Muise-Helmericks, R.C., Drake, C.J., 2013. VEGF-mediated phosphorylation of eNOS regulates angioblasts and embryonic endothelial cell proliferation. *Dev. Biol.* 373, 163–175.
- George, K.M., Schule, T., Sandoval, L.E., Jennings, L.L., Taylor, P., Thompson, C.M., 2003. Differentiation between acetylcholinesterase and the organophosphate-inhibited form using antibodies and the correlation of antibody recognition with reactivation mechanism and rate. *J. Biol. Chem.* 278, 45512–45518.
- George, P.M., Abernethy, M.H., 1983. Improved Ellman procedure for erythrocyte cholinesterase. *Clin. Chem.* 29, 365–368.
- Gergalova, G., Lykhmus, O., Kalashnyk, O., Koval, L., Chernyshov, V., Kryukova, E., Tsetlin, V., Komisarenko, S., Skok, M., 2012. Mitochondria express $\alpha 7$ nicotinic acetylcholine receptors to regulate Ca^{2+} accumulation and cytochrome c release: study on isolated mitochondria. *PLoS One* 7, e31361.
- Gergalova, G., Lykhmus, O., Komisarenko, S., Skok, M., 2014. $\alpha 7$ nicotinic acetylcholine receptors control cytochrome c release from isolated mitochondria through kinase-mediated pathways. *Int. J. Biochem. Cell Biol.* 49, 26–31.
- Getman, D.K., Eubanks, J.H., Camp, S., Evans, G.A., Taylor, P., 1992. The human gene encoding acetylcholinesterase is located on the long arm of chromosome 7. *Am. J. Hum. Genet.* 51, 170–177.
- Giacobini, E. (Ed.), 2003a. *Butyrylcholinesterase: Its Function and Inhibitors*. Martin Dunitz.
- Giacobini, E., 2003b. Cholinergic function and Alzheimer's disease. *Int. J. Geriatr. Psychiatry* 18, S1–5.
- Gibson, K.M., Chan, C., Chapuis, P.H., Dent, O.F., Bokey, L., 2014. Mural and extramural venous invasion and prognosis in colorectal cancer. *Dis. Colon Rectum* 57, 916–926.
- Glembotski, C.C., 2012. Roles for the Sarco-/Endoplasmic Reticulum in Cardiac Myocyte Contraction, Protein Synthesis, and Protein Quality Control. *Physiology* 27, 343–350.
- Gómez, J.L., Moral-Naranjo, M.T., Campoy, F.J., Vidal, C.J., 1999. Characterization of acetylcholinesterase and butyrylcholinesterase forms in normal and dystrophic Lama2dy mouse heart. *J. Neurosci. Res.* 56, 295–306.

- Groner, E., Ashani, Y., Schorer-Apelbaum, D., Sterling, J., Herzig, Y., Weinstock, M., 2007. The kinetics of inhibition of human acetylcholinesterase and butyrylcholinesterase by two series of novel carbamates. *Mol. Pharmacol.* 71, 1610–1617.
- Gruber, C., Nink, N., Nikam, S., Magdowski, G., Kripp, G., Voswinckel, R., Mühlfeld, C., 2012. Myocardial remodelling in left ventricular atrophy induced by caloric restriction. *J. Anat.* 220, 179–185.
- Gutstein, D.E., 2003. The organization of adherens junctions and desmosomes at the cardiac intercalated disc is independent of gap junctions. *J. Cell Sci.* 116, 875–885.
- Haddad, F., Hunt, S.A., Rosenthal, D.N., Murphy, D.J., 2008. Right Ventricular Function in Cardiovascular Disease, Part I Anatomy, Physiology, Aging, and Functional Assessment of the Right Ventricle. *Circulation* 117, 1436–1448.
- Hagopian, M., Tennyson, V.M., 1971. Cytochemical localization of cholinesterase activity in adult rabbit heart. *J. Histochem. Cytochem. Off. J. Histochem. Soc.* 19, 376–381.
- Hamann, J.J., Ruble, S.B., Stolen, C., Wang, M., Gupta, R.C., Rastogi, S., Sabbah, H.N., 2013. Vagus nerve stimulation improves left ventricular function in a canine model of chronic heart failure. *Eur. J. Heart Fail.* 15, 1319–1326.
- Hamers, T., Molin, K.R., Koeman, J.H., Murk, A.J., 2000. A small-volume bioassay for quantification of the esterase inhibiting potency of mixtures of organophosphate and carbamate insecticides in rainwater: development and optimization. *Toxicol. Sci. Off. J. Soc. Toxicol.* 58, 60–67.
- Handa, T., Katare, R.G., Kakinuma, Y., Arikawa, M., Ando, M., Sasaguri, S., Yamasaki, F., Sato, T., 2009. Anti-Alzheimer's drug, donepezil, markedly improves long-term survival after chronic heart failure in mice. *J. Card. Fail.* 15, 805–811.
- Hanneman, E., Westerfield, M., 1989. Early expression of acetylcholinesterase activity in functionally distinct neurons of the zebrafish. *J. Comp. Neurol.* 284, 350–361.
- Hara, H., Virmani, R., Ladich, E., Mackey-Bojack, S., Titus, J., Reisman, M., Gray, W., Nakamura, M., Mooney, M., Poulouse, A., Schwartz, R.S., 2005. Patent Foramen Ovale: Current Pathology, Pathophysiology, and Clinical Status. *J. Am. Coll. Cardiol.* 46, 1768–1776.
- Hardwick, J.C., Baran, C.N., Southerland, E.M., Ardell, J.L., 2009. Remodeling of the guinea pig intrinsic cardiac plexus with chronic pressure overload. *Am. J. Physiol. - Regul. Integr. Comp. Physiol.* 297, R859–R866. doi:10.1152/ajpregu.00245.2009
- Hartmann, J., Kiewert, C., Duysen, E.G., Lockridge, O., Greig, N.H., Klein, J., 2007. Excessive hippocampal acetylcholine levels in acetylcholinesterase-deficient mice are moderated by butyrylcholinesterase activity. *J. Neurochem.* 100, 1421–1429.
- Hasan, W., 2013. Autonomic cardiac innervation: development and adult plasticity. *Organogenesis* 9, 176–193.
- Helm, P.A., Younes, L., Beg, M.F., Ennis, D.B., Leclercq, C., Faris, O.P., McVeigh, E., Kass, D., Miller, M.I., Winslow, R.L., 2006. Evidence of Structural Remodeling in the Dyssynchronous Failing Heart. *Circ. Res.* 98, 125–132.
- Henderson, Z., Matto, N., John, D., Nalivaeva, N.N., Turner, A.J., 2010. Co-localization of PRiMA with acetylcholinesterase in cholinergic neurons of rat brain: an immunocytochemical study. *Brain Res.* 1344, 34–42.
- He, X., Zhao, M., Bi, X., Sun, L., Yu, X., Zhao, M., Zang, W., 2014. Novel strategies and underlying protective mechanisms of modulation of vagal activity in cardiovascular diseases. *Br. J. Pharmacol.*
- Hiraoka, K., Okamura, N., Funaki, Y., Hayashi, A., Tashiro, M., Hisanaga, K., Fujii, T., Takeda, A., Yanai, K., Iwata, R., Mori, E., 2012. Cholinergic deficit and response

- to donepezil therapy in Parkinson's disease with dementia. *Eur. Neurol.* 68, 137–143.
- Hockfield, S., Pintar, J., Hockfield, S., 1993. *Selected Methods for Antibody and Nucleic Acid Probes*. Cold Spring Harbor Laboratory Press, Plainview, N.Y.
- Ho, D., Zhao, X., Gao, S., Hong, C., Vatner, D.E., Vatner, S.F., 2011. Heart Rate and Electrocardiography Monitoring in Mice. *Curr. Protoc. Mouse Biol.* 1, 123–139.
- Hofer, P., Fringeli, U.P., 1981. Acetylcholinesterase kinetics. *Biophys. Struct. Mech.* 8, 45–59.
- Holas, O., Musilek, K., Pohanka, M., Kuca, K., 2012. The progress in the cholinesterase quantification methods. *Expert Opin. Drug Discov.* 7, 1207–1223.
- Hopkins, D.A., Macdonald, S.E., Murphy, D.A., Armour, J.A., 2000. Pathology of intrinsic cardiac neurons from ischemic human hearts. *Anat. Rec.* 259, 424–436.
- Ho, S.Y., 2009. Anatomy and myoarchitecture of the left ventricular wall in normal and in disease. *Eur. Heart J. - Cardiovasc. Imaging* 10, iii3–iii7.
- Ho, S.Y., Nihoyannopoulos, P., 2006. Anatomy, echocardiography, and normal right ventricular dimensions. *Heart* 92, i2–i13.
- Hrabovska, A., Bernard, V., Krejci, E., 2010. A novel system for the efficient generation of antibodies following immunization of unique knockout mouse strains. *PloS One* 5, e12892.
- Hrabovská, A., Debouzy, J.-C., Froment, M.-T., Devínsky, F., Pauliková, I., Masson, P., 2006a. Rat butyrylcholinesterase-catalysed hydrolysis of N-alkyl homologues of benzoylcholine. *FEBS J.* 273, 1185–1197.
- Hrabovska, A., Krejci, E., 2014. Reassessment of the role of the central cholinergic system. *J. Mol. Neurosci.* MN 53, 352–358.
- Hrabovská, A., Pauliková, I., Kovács, P., 2006b. Súčasný poznatky v oblasti štúdia cholinesteráz. *Českoslov. Fyziologie* 55, 30–38.
- Hu, Y.-F., Dawkins, J.F., Cho, H.C., Marbán, E., Cingolani, E., 2014. Biological pacemaker created by minimally invasive somatic reprogramming in pigs with complete heart block. *Sci. Transl. Med.* 6, 245ra94–245ra94.
- Hwang, S.-J., Ballantyne, C.M., Sharrett, A.R., Smith, L.C., Davis, C.E., Gotto, A.M., Boerwinkle, E., 1997. Circulating Adhesion Molecules VCAM-1, ICAM-1, and E-selectin in Carotid Atherosclerosis and Incident Coronary Heart Disease Cases The Atherosclerosis Risk In Communities (ARIC) Study. *Circulation* 96, 4219–4225.
- Iacobellis, G., Willens, H.J., 2009. Echocardiographic epicardial fat: a review of research and clinical applications. *J. Am. Soc. Echocardiogr. Off. Publ. Am. Soc. Echocardiogr.* 22, 1311–1319; quiz 1417–1418.
- Igisu, H., Matsumura, H., Matsuoka, M., 1994. [Acetylcholinesterase in the erythrocyte membrane]. *J. UOEH* 16, 253–262.
- Incardona, J.P., Rosenberry, T.L., 1996. Construction and characterization of secreted and chimeric transmembrane forms of *Drosophila* acetylcholinesterase: a large truncation of the C-terminal signal peptide does not eliminate glycoinositol phospholipid anchoring. *Mol. Biol. Cell* 7, 595–611.
- Iwasaki, T., Yoneda, M., Nakajima, A., Terauchi, Y., 2007. Serum butyrylcholinesterase is strongly associated with adiposity, the serum lipid profile and insulin resistance. *Intern. Med. Tokyo Jpn.* 46, 1633–1639.
- Izant, J.G., McIntosh, J.R., 1980. Microtubule-associated proteins: a monoclonal antibody to MAP2 binds to differentiated neurons. *Proc. Natl. Acad. Sci. U. S. A.* 77, 4741–4745.

- Jankowska-Kulawy, A., Bielarczyk, H., Pawełczyk, T., Wróblewska, M., Szutowicz, A., 2010. Acetyl-CoA and acetylcholine metabolism in nerve terminal compartment of thiamine deficient rat brain. *J. Neurochem.* 115, 333–342.
- Jayam Trouth, A., Dabi, A., Solieman, N., Kurukumbi, M., Kalyanam, J., 2012. Myasthenia gravis: a review. *Autoimmune Dis.* 2012, 874680.
- Jbilo, O., Bartels, C.F., Chatonnet, A., Toutant, J.P., Lockridge, O., 1994. Tissue distribution of human acetylcholinesterase and butyrylcholinesterase messenger RNA. *Toxicol. Off. J. Int. Soc. Toxinology* 32, 1445–1457.
- Johnson, C.D., Russell, R.L., 1975. A rapid, simple radiometric assay for cholinesterase, suitable for multiple determinations. *Anal. Biochem.* 64, 229–238.
- Jordan-Starck, T.C., Rodwell, V.W., 1989. Role of cysteine residues in *Pseudomonas mevalonii* 3-hydroxy-3-methylglutaryl-CoA reductase. Site-directed mutagenesis and characterization of the mutant enzymes. *J. Biol. Chem.* 264, 17919–17923.
- Jun, D., Musilova, L., Kuca, K., Kassa, J., Bajgar, J., 2008. Potency of several oximes to reactivate human acetylcholinesterase and butyrylcholinesterase inhibited by paraoxon in vitro. *Chem. Biol. Interact.* 175, 421–424.
- Kakinuma, Y., Akiyama, T., Okazaki, K., Arikawa, M., Noguchi, T., Sato, T., 2012. A non-neuronal cardiac cholinergic system plays a protective role in myocardium salvage during ischemic insults. *PloS One* 7, e50761.
- Kakinuma, Y., Akiyama, T., Sato, T., 2009. Cholinoceptive and cholinergic properties of cardiomyocytes involving an amplification mechanism for vagal efferent effects in sparsely innervated ventricular myocardium. *FEBS J.* 276, 5111–5125.
- Kakinuma, Y., Tsuda, M., Okazaki, K., Akiyama, T., Arikawa, M., Noguchi, T., Sato, T., 2013. Heart-specific overexpression of choline acetyltransferase gene protects murine heart against ischemia through hypoxia-inducible factor-1 α -related defense mechanisms. *J. Am. Heart Assoc.* 2, e004887.
- Kalashnyk, O.M., Gergalova, G.L., Komisarenko, S.V., Skok, M.V., 2012. Intracellular localization of nicotinic acetylcholine receptors in human cell lines. *Life Sci.* 91, 1033–1037.
- Kalow, W., 1964. The influence of pH on the hydrolysis of benzoylcholine by pseudocholinesterase of human PLASMA. *Can. J. Physiol. Pharmacol.* 42, 161–168.
- Kanazawa, H., Ieda, M., Kimura, K., Arai, T., Kawaguchi-Manabe, H., Matsushashi, T., Endo, J., Sano, M., Kawakami, T., Kimura, T., Monkawa, T., Hayashi, M., Iwanami, A., Okano, H., Okada, Y., Ishibashi-Ueda, H., Ogawa, S., Fukuda, K., 2010. Heart failure causes cholinergic transdifferentiation of cardiac sympathetic nerves via gp130-signaling cytokines in rodents. *J. Clin. Invest.* 120, 408–421.
- Kapoor, N., Liang, W., Marbán, E., Cho, H.C., 2013. Direct conversion of quiescent cardiomyocytes to pacemaker cells by expression of Tbx18. *Nat. Biotechnol.* 31, 54–62.
- Karnovsky, M.J., 1964. The localization of cholinesterase activity in rat cardiac muscle by electron microscopy. *J. Cell Biol.* 23, 217–232.
- Karnovsky, M.J., Roots, L., 1964. A “direct-coloring” thiocholine method for cholinesterases. *J. Histochem. Cytochem. Off. J. Histochem. Soc.* 12, 219–221.
- Karpel, R., Ben Aziz-Aloya, R., Sternfeld, M., Ehrlich, G., Ginzberg, D., Tarroni, P., Clementi, F., Zakut, H., Soreq, H., 1994. Expression of three alternative acetylcholinesterase messenger RNAs in human tumor cell lines of different tissue origins. *Exp. Cell Res.* 210, 268–277.

- Karpel, R., Sternfeld, M., Ginzberg, D., Guhl, E., Graessmann, A., Soreq, H., 1996. Overexpression of alternative human acetylcholinesterase forms modulates process extensions in cultured glioma cells. *J. Neurochem.* 66, 114–123.
- Katz AM, 2010. *Physiology of the Heart*, Fifth edition. ed. LWW, Philadelphia, PA.
- Katz, A.M., Katz, P.B., 1989. Homogeneity out of heterogeneity. *Circulation* 79, 712–717.
- Kawashima, K., Fujii, T., 2008. Basic and clinical aspects of non-neuronal acetylcholine: overview of non-neuronal cholinergic systems and their biological significance. *J. Pharmacol. Sci.* 106, 167–173.
- Kawashima, T., 2005. The autonomic nervous system of the human heart with special reference to its origin, course, and peripheral distribution. *Anat. Embryol. (Berl.)* 209, 425–438.
- Kayalar, N., Burkhart, H.M., Dearani, J.A., Cetta, F., Schaff, H.V., 2009. Congenital coronary anomalies and surgical treatment. *Congenit. Heart Dis.* 4, 239–251.
- Kayser, O., Warzecha, H., 2012. *Pharmaceutical Biotechnology: Drug Discovery and Clinical Applications*. John Wiley & Sons.
- Kiernan, J., Rajakumar, R., 2013. *Barr's The Human Nervous System: An Anatomical Viewpoint*. Lippincott Williams & Wilkins.
- Kimura, K., Ieda, M., Fukuda, K., 2012. Development, maturation, and transdifferentiation of cardiac sympathetic nerves. *Circ. Res.* 110, 325–336.
- Kitzman, D.W., Edwards, W.D., 1990. Age-related changes in the anatomy of the normal human heart. *J. Gerontol.* 45, M33–39.
- Koelle, G.B., 1951. The elimination of enzymatic diffusion artifacts in the histochemical localization of cholinesterases and a survey of their cellular distributions. *J. Pharmacol. Exp. Ther.* 103, 153–171.
- Koelle, G.B., 1950. The histochemical differentiation of types of cholinesterases and their localizations in tissues of the cat. *J. Pharmacol. Exp. Ther.* 100, 158–179.
- Koelle, G.B., Friedenwald, J.A., 1949. A histochemical method for localizing cholinesterase activity. *Proc. Soc. Exp. Biol. Med. Soc. Exp. Biol. Med. N. Y.* N 70, 617–622.
- Kohl, P., 2004. Cardiac cellular heterogeneity and remodelling. *Cardiovasc. Res.* 64, 195–197.
- Kohl, P., 2003. Heterogeneous Cell Coupling in the Heart An Electrophysiological Role for Fibroblasts. *Circ. Res.* 93, 381–383.
- Kohl, P., Hunter, P., Noble, D., 1999. Stretch-induced changes in heart rate and rhythm: clinical observations, experiments and mathematical models. *Prog. Biophys. Mol. Biol.* 71, 91–138.
- Koistinaho, J., Wadhvani, K.C., Rapoport, S.I., 1989. Increased density of perivascular adrenergic innervation in tibial and vagus nerves of spontaneously hypertensive rats. *J. Neurosci. Res.* 24, 424–430.
- Krejci, E., Legay, C., Thomine, S., Sketelj, J., Massoulié, J., 1999. Differences in expression of acetylcholinesterase and collagen Q control the distribution and oligomerization of the collagen-tailed forms in fast and slow muscles. *J. Neurosci. Off. J. Soc. Neurosci.* 19, 10672–10679.
- Krejci, E., Thomine, S., Boschetti, N., Legay, C., Sketelj, J., Massoulié, J., 1997. The mammalian gene of acetylcholinesterase-associated collagen. *J. Biol. Chem.* 272, 22840–22847.
- Kukanova, B., Mravec, B., 2006. Complex intracardiac nervous system. *Bratisl. Lekárske Listy* 107, 45–51.
- Kurt, M., Wang, J., Torre-Amione, G., Nagueh, S.F., 2009. Left Atrial Function in Diastolic Heart Failure. *Circ. Cardiovasc. Imaging* 2, 10–15.

- Lara, A., Damasceno, D.D., Pires, R., Gros, R., Gomes, E.R., Gavioli, M., Lima, R.F., Guimarães, D., Lima, P., Bueno, C.R., Vasconcelos, A., Roman-Campos, D., Menezes, C.A.S., Sirvente, R.A., Salemi, V.M., Mady, C., Caron, M.G., Ferreira, A.J., Brum, P.C., Resende, R.R., Cruz, J.S., Gomez, M.V., Prado, V.F., de Almeida, A.P., Prado, M.A.M., Guatimosim, S., 2010. Dysautonomia due to reduced cholinergic neurotransmission causes cardiac remodeling and heart failure. *Mol. Cell. Biol.* 30, 1746–1756.
- Lataro, R.M., Silva, C.A.A., Fazan, R., Rossi, M.A., Prado, C.M., Godinho, R.O., Salgado, H.C., 2013. Increase in parasympathetic tone by pyridostigmine prevents ventricular dysfunction during the onset of heart failure. *Am. J. Physiol. Regul. Integr. Comp. Physiol.* 305, R908–916.
- Lemieux, H., Hoppel, C.L., 2009. Mitochondria in the human heart. *J. Bioenerg. Biomembr.* 41, 99–106.
- Lenz, D.E., Yeung, D., Smith, J.R., Sweeney, R.E., Lumley, L.A., Cerasoli, D.M., 2007. Stoichiometric and catalytic scavengers as protection against nerve agent toxicity: a mini review. *Toxicology* 233, 31–39.
- Levin, H.S., Rodnitzky, R.L., 1976. Behavioral effects of organophosphate in man. *Clin. Toxicol.* 9, 391–403.
- Li, B., Duysen, E.G., Carlson, M., Lockridge, O., 2008a. The butyrylcholinesterase knockout mouse as a model for human butyrylcholinesterase deficiency. *J. Pharmacol. Exp. Ther.* 324, 1146–1154.
- Li, B., Duysen, E.G., Lockridge, O., 2008b. The butyrylcholinesterase knockout mouse is obese on a high-fat diet. *Chem. Biol. Interact.* 175, 88–91.
- Li, B., Duysen, E.G., Saunders, T.L., Lockridge, O., 2006. Production of the butyrylcholinesterase knockout mouse. *J. Mol. Neurosci.* MN 30, 193–195.
- Li, B., Stribley, J.A., Ticu, A., Xie, W., Schopfer, L.M., Hammond, P., Brimijoin, S., Hinrichs, S.H., Lockridge, O., 2000. Abundant tissue butyrylcholinesterase and its possible function in the acetylcholinesterase knockout mouse. *J. Neurochem.* 75, 1320–1331.
- Liesi, P., Panula, P., Rechartd, L., 1980. Ultrastructural localization of acetylcholinesterase activity in primary cultures of rat substantia nigra. *Histochemistry* 70, 7–18.
- Li, H., Schopfer, L.M., Masson, P., Lockridge, O., 2008. Lamellipodin proline rich peptides associated with native plasma butyrylcholinesterase tetramers. *Biochem. J.* 411, 425–432.
- Li, J., Inada, S., Schneider, J.E., Zhang, H., Dobrzynski, H., Boyett, M.R., 2014. Three-Dimensional Computer Model of the Right Atrium Including the Sinoatrial and Atrioventricular Nodes Predicts Classical Nodal Behaviours. *PLoS ONE* 9, e112547.
- Li, L., Miano, J.M., Cserjesi, P., Olson, E.N., 1996. SM22 α , a Marker of Adult Smooth Muscle, Is Expressed in Multiple Myogenic Lineages During Embryogenesis. *Circ. Res.* 78, 188–195.
- Lima, J.K., Leite, N., Turek, L.V., Souza, R.L.R., da Silva Timossi, L., Osiecki, A.C.V., Osiecki, R., Furtado-Alle, L., 2013. 1914G variant of BCHE gene associated with enzyme activity, obesity and triglyceride levels. *Gene* 532, 24–26.
- Li, M., Zheng, C., Kawada, T., Inagaki, M., Uemura, K., Shishido, T., Sugimachi, M., 2013. Donepezil markedly improves long-term survival in rats with chronic heart failure after extensive myocardial infarction. *Circ. J. Off. J. Jpn. Circ. Soc.* 77, 2519–2525.

- Li, M., Zheng, C., Sato, T., Kawada, T., Sugimachi, M., Sunagawa, K., 2004. Vagal nerve stimulation markedly improves long-term survival after chronic heart failure in rats. *Circulation* 109, 120–124.
- Lockridge, O., Adkins, S., La Du, B.N., 1987a. Location of disulfide bonds within the sequence of human serum cholinesterase. *J. Biol. Chem.* 262, 12945–12952.
- Lockridge, O., Bartels, C.F., Vaughan, T.A., Wong, C.K., Norton, S.E., Johnson, L.L., 1987b. Complete amino acid sequence of human serum cholinesterase. *J. Biol. Chem.* 262, 549–557.
- Loe, M.J., Edwards, W.D., 2004. A light-hearted look at a lion-hearted organ (or, a perspective from three standard deviations beyond the norm) Part 1 (of two parts). *Cardiovasc. Pathol.* 13, 282–292.
- London, L., Thompson, M.L., Sacks, S., Fuller, B., Bachmann, O.M., Myers, J.E., 1995. Repeatability and validity of a field kit for estimation of cholinesterase in whole blood. *Occup. Environ. Med.* 52, 57–64.
- MacQueen, J., Plaut, D., Borges, J., Anido, G., 1971. Manual colorimetric methods for pseudocholinesterase and red cell (true) cholinesterase. *Clin. Chem.* 17, 481–485.
- Malone, D.M., Lindsay, J., 2007. Cholinesterase inhibitors and cardiovascular disease: a survey of old age psychiatrists' practice. *Age Ageing* 36, 331–333.
- Marron, K., Wharton, J., Sheppard, M.N., Fagan, D., Royston, D., Kuhn, D.M., de Leval, M.R., Whitehead, B.F., Anderson, R.H., Polak, J.M., 1995. Distribution, morphology, and neurochemistry of endocardial and epicardial nerve terminal arborizations in the human heart. *Circulation* 92, 2343–2351.
- Mason, H.J., Waine, E., Stevenson, A., Wilson, H.K., 1993. Aging and spontaneous reactivation of human plasma cholinesterase activity after inhibition by organophosphorus pesticides. *Hum. Exp. Toxicol.* 12, 497–503.
- Masson, P., 2012. Time-dependent kinetic complexities in cholinesterase-catalyzed reactions. *Biochem. Biokhimiia* 77, 1147–1161.
- Masson, P., Froment, M.T., Fortier, P.L., Visicchio, J.E., Bartels, C.F., Lockridge, O., 1998. Butyrylcholinesterase-catalysed hydrolysis of aspirin, a negatively charged ester, and aspirin-related neutral esters. *Biochim. Biophys. Acta* 1387, 41–52.
- Masson, P., Froment, M.T., Fort, S., Ribes, F., Bec, N., Balny, C., Schopfer, L.M., 2002a. Butyrylcholinesterase-catalyzed hydrolysis of N-methylindoxyl acetate: analysis of volume changes upon reaction and hysteretic behavior. *Biochim. Biophys. Acta* 1597, 229–243.
- Masson, P., Goldstein, B.N., Debouzy, J.-C., Froment, M.-T., Lockridge, O., Schopfer, L.M., 2004. Damped oscillatory hysteretic behaviour of butyrylcholinesterase with benzoylcholine as substrate. *Eur. J. Biochem. FEBS* 271, 220–234.
- Masson, P., Lockridge, O., 2010. Butyrylcholinesterase for protection from organophosphorus poisons: catalytic complexities and hysteretic behavior. *Arch. Biochem. Biophys.* 494, 107–120.
- Masson, P., Nachon, F., Bartels, C.F., Froment, M.-T., Ribes, F., Matthews, C., Lockridge, O., 2003. High activity of human butyrylcholinesterase at low pH in the presence of excess butyrylthiocholine. *Eur. J. Biochem. FEBS* 270, 315–324.
- Masson, P., Schopfer, L.M., Bartels, C.F., Froment, M.-T., Ribes, F., Nachon, F., Lockridge, O., 2002b. Substrate activation in acetylcholinesterase induced by low pH or mutation in the pi-cation subsite. *Biochim. Biophys. Acta* 1594, 313–324.
- Masson, P., Schopfer, L.M., Froment, M.-T., Debouzy, J.-C., Nachon, F., Gillon, E., Lockridge, O., Hrabovska, A., Goldstein, B.N., 2005. Hysteresis of butyrylcholinesterase in the approach to steady-state kinetics. *Chem. Biol. Interact.* 157–158, 143–152.

- Massoulié, J., 2002. The origin of the molecular diversity and functional anchoring of cholinesterases. *Neurosignals* 11, 130–143.
- Massoulié, J., Bon, S., Perrier, N., Falasca, C., 2005. The C-terminal peptides of acetylcholinesterase: cellular trafficking, oligomerization and functional anchoring. *Chem. Biol. Interact.* 157-158, 3–14.
- Massoulié, J., Perrier, N., Nouredine, H., Liang, D., Bon, S., 2008. Old and new questions about cholinesterases. *Chem. Biol. Interact.* 175, 30–44.
- Massoulié, J., Pezzementi, L., Bon, S., Krejci, E., Vallette, F.M., 1993. Molecular and cellular biology of cholinesterases. *Prog. Neurobiol.* 41, 31–91.
- Masuda, Y., 2004. Cardiac effect of cholinesterase inhibitors used in Alzheimer's disease--from basic research to bedside. *Curr. Alzheimer Res.* 1, 315–321.
- Matsunaga, S., Kishi, T., Iwata, N., 2014. Combination Therapy with Cholinesterase Inhibitors and Memantine for Alzheimer's disease: A Systematic Review and Meta-analysis. *Int. J. Neuropsychopharmacol. Off. Sci. J. Coll. Int. Neuropsychopharmacol. CINP.*
- Mattes, C., Bradley, R., Slaughter, E., Browne, S., 1996. Cocaine and butyrylcholinesterase (BChE): determination of enzymatic parameters. *Life Sci.* 58, PL257–261.
- McLellan, G.J., Miller, P.E., 2011. Feline Glaucoma – A Comprehensive Review. *Vet. Ophthalmol.* 14, 15–29.
- Mehrzad, R., Rajab, M., Spodick, D.H., 2014. The Three Integrated Phases of Left Atrial Macrophysiology and Their Interactions. *Int. J. Mol. Sci.* 15, 15146–15160.
- Mettauer, B., Zoll, J., Garnier, A., Ventura-Clapier, R., 2006. Heart failure: a model of cardiac and skeletal muscle energetic failure. *Pflüg. Arch. Eur. J. Physiol.* 452, 653–666.
- Metz, R.P., Patterson, J.L., Wilson, E., 2012. Vascular smooth muscle cells: isolation, culture, and characterization. *Methods Mol. Biol. Clifton NJ* 843, 169–176.
- Michel, V., Yuan, Z., Ramsubir, S., Bakovic, M., 2006. Choline transport for phospholipid synthesis. *Exp. Biol. Med. Maywood NJ* 231, 490–504.
- Milgrom-Hoffman, M., Harrelson, Z., Ferrara, N., Zelzer, E., Evans, S.M., Tzahor, E., 2011. The heart endocardium is derived from vascular endothelial progenitors. *Development* 138, 4777–4787.
- Montenegro, M.F., Ruiz-Espejo, F., Campoy, F.J., Muñoz-Delgado, E., de la Cadena, M.P., Rodríguez-Berrocal, F.J., Vidal, C.J., 2006. Cholinesterases are down-expressed in human colorectal carcinoma. *Cell. Mol. Life Sci. CMLS* 63, 2175–2182.
- Moral-Naranjo, M.T., Cabezas-Herrera, J., Vidal, C.J., 1996. Molecular forms of acetyl- and butyrylcholinesterase in normal and dystrophic mouse brain. *J. Neurosci. Res.* 43, 224–234.
- Moral-Naranjo, M.T., Montenegro, M.F., Muñoz-Delgado, E., Campoy, F.J., Vidal, C.J., 2010. The levels of both lipid rafts and raft-located acetylcholinesterase dimers increase in muscle of mice with muscular dystrophy by merosin deficiency. *Biochim. Biophys. Acta* 1802, 754–764.
- Mrvova, K., Obzerova, L., Girard, E., Krejci, E., Hrabovska, A., 2013. Monoclonal antibodies to mouse butyrylcholinesterase. *Chem. Biol. Interact.* 203, 348–353.
- Nachon, F., Nicolet, Y., Viguié, N., Masson, P., Fontecilla-Camps, J.C., Lockridge, O., 2002. Engineering of a monomeric and low-glycosylated form of human butyrylcholinesterase: expression, purification, characterization and crystallization. *Eur. J. Biochem. FEBS* 269, 630–637.

- Naik NT, 1963. Technical variations in Koelle's histochemical method for demonstrating cholinesterase activity. *Quart J micr Sci* 104, 89.
- Nakamura, T., Ikeda, T., Shimokawa, I., Inoue, Y., Suematsu, T., Sakai, H., Iwasaki, K., Matsuo, T., 1994. Distribution of acetylcholinesterase activity in the rat embryonic heart with reference to HNK-1 immunoreactivity in the conduction tissue. *Anat. Embryol. (Berl.)* 190, 367–373.
- Nakano, S., Muramatsu, T., Nishimura, S., Senbonmatsu, T., 2012. Cardiomyocyte and Heart Failure, in: Sugi, H. (Ed.), *Current Basic and Pathological Approaches to the Function of Muscle Cells and Tissues - From Molecules to Humans*. InTech.
- Nam, J., Onitsuka, I., Hatch, J., Uchida, Y., Ray, S., Huang, S., Li, W., Zang, H., Ruiz-Lozano, P., Mukoyama, Y.-S., 2013. Coronary veins determine the pattern of sympathetic innervation in the developing heart. *Dev. Camb. Engl.* 140, 1475–1485.
- Nese Cokugras A, 2003. Butyrylcholinesterase: Structure and Physiological Importance. *Turk J Biochem* 28, 54–61.
- Neumann, S.A., Lawrence, E.C., Jennings, J.R., Ferrell, R.E., Manuck, S.B., 2005. Heart rate variability is associated with polymorphic variation in the choline transporter gene. *Psychosom. Med.* 67, 168–171.
- Nicolet, Y., Lockridge, O., Masson, P., Fontecilla-Camps, J.C., Nachon, F., 2003. Crystal structure of human butyrylcholinesterase and of its complexes with substrate and products. *J. Biol. Chem.* 278, 41141–41147.
- Nyquist-Battie, C., 1990. Changes in the expression of acetylcholinesterase molecular forms during rat heart development. *Int. J. Dev. Neurosci. Off. J. Int. Soc. Dev. Neurosci.* 8, 327–335.
- Nyquist-Battie, C., Hodges-Savola, C., Fernandez, H.L., 1987. Acetylcholinesterase molecular forms in rat heart. *J. Mol. Cell. Cardiol.* 19, 935–943.
- Nyquist-Battie, C., Trans-Saltzman, K., 1989. Regional distribution of the molecular forms of acetylcholinesterase in adult rat heart. *Circ. Res.* 65, 55–62.
- Oberhauser, V., Schwertfeger, E., Rutz, T., Beyersdorf, F., Rump, L.C., 2001. Acetylcholine release in human heart atrium: influence of muscarinic autoreceptors, diabetes, and age. *Circulation* 103, 1638–1643.
- Odell, I.D., Cook, D., 2013. Immunofluorescence Techniques. *J. Invest. Dermatol.* 133, e4.
- Ogert, R.A., Gentry, M.K., Richardson, E.C., Deal, C.D., Abramson, S.N., Alving, C.R., Taylor, P., Doctor, B.P., 1990. Studies on the topography of the catalytic site of acetylcholinesterase using polyclonal and monoclonal antibodies. *J. Neurochem.* 55, 756–763.
- Olshansky, B., Sabbah, H.N., Hauptman, P.J., Colucci, W.S., 2008. Parasympathetic nervous system and heart failure: pathophysiology and potential implications for therapy. *Circulation* 118, 863–871.
- Opie, L.H., 2004. *Heart Physiology: From Cell to Circulation*. Lippincott Williams & Wilkins.
- O'Rahilly R, 2008. *Basic Human Anatomy*. Dartmouth Medical School.
- Ordentlich, A., Barak, D., Kronman, C., Ariel, N., Segall, Y., Velan, B., Shafferman, A., 1998. Functional characteristics of the oxyanion hole in human acetylcholinesterase. *J. Biol. Chem.* 273, 19509–19517.
- Paranya, G., Vineberg, S., Dvorin, E., Kaushal, S., Roth, S.J., Rabkin, E., Schoen, F.J., Bischoff, J., 2001. Aortic Valve Endothelial Cells Undergo Transforming Growth Factor- β -Mediated and Non-Transforming Growth Factor- β -Mediated Transdifferentiation in Vitro. *Am. J. Pathol.* 159, 1335–1343.

- Pauza, D.H., Pauziene, N., Tamasauskas, K.A., Stropus, R., 1997a. Hilum of the heart. *Anat. Rec.* 248, 322–324.
- Pauza, D.H., Skripka, V., Pauziene, N., 2002. Morphology of the intrinsic cardiac nervous system in the dog: a whole-mount study employing histochemical staining with acetylcholinesterase. *Cells Tissues Organs* 172, 297–320.
- Pauza, D.H., Skripka, V., Pauziene, N., Stropus, R., 2000. Morphology, distribution, and variability of the epicardiac neural ganglionated subplexuses in the human heart. *Anat. Rec.* 259, 353–382.
- Pauza, D.H., Skripka, V., Pauziene, N., Stropus, R., 1999. Anatomical study of the neural ganglionated plexus in the canine right atrium: implications for selective denervation and electrophysiology of the sinoatrial node in dog. *Anat. Rec.* 255, 271–294.
- Pauza, D.H., Skripkiene, G., Skripka, V., Pauziene, N., Stropus, R., 1997b. Morphological study of neurons in the nerve plexus on heart base of rats and guinea pigs. *J. Auton. Nerv. Syst.* 62, 1–12.
- Pauziene, N., Pauza, D.H., 2003. Electron microscopic study of intrinsic cardiac ganglia in the adult human. *Ann. Anat. Anat. Anz. Off. Organ Anat. Ges.* 185, 135–148.
- Pauziene, N., Pauza, D.H., Stropus, R., 2000. Morphology of human intracardiac nerves: an electron microscope study. *J. Anat.* 197 Pt 3, 437–459.
- Pérez-Guillermo, F., Delgado, E.M., Vidal, C.J., 1987. Inhibition of human serum and rabbit muscle cholinesterase by local anesthetics. *Biochem. Pharmacol.* 36, 3593–3596.
- Perriard, J.-C., Hirschy, A., Ehler, E., 2003. Dilated Cardiomyopathy: A Disease of the Intercalated Disc? *Trends Cardiovasc. Med.* 13, 30–38.
- Perrier, A.L., Massoulié, J., Krejci, E., 2002. PRiMA: the membrane anchor of acetylcholinesterase in the brain. *Neuron* 33, 275–285.
- Perrier, N.A., Khérif, S., Perrier, A.L., Dumas, S., Mallet, J., Massoulié, J., 2003. Expression of PRiMA in the mouse brain: membrane anchoring and accumulation of “tailed” acetylcholinesterase. *Eur. J. Neurosci.* 18, 1837–1847.
- Perrier, N.A., Salani, M., Falasca, C., Bon, S., Augusti-Tocco, G., Massoulié, J., 2005. The readthrough variant of acetylcholinesterase remains very minor after heat shock, organophosphate inhibition and stress, in cell culture and in vivo. *J. Neurochem.* 94, 629–638.
- Petroianu, G.A., Nurulain, S.M., Nagelkerke, N., Shafiullah, M., Kassa, J., Kuca, K., 2007. Five oximes (K-27, K-48, obidoxime, HI-6 and trimedoxime) in comparison with pralidoxime: survival in rats exposed to methyl-paraoxon. *J. Appl. Toxicol. JAT* 27, 453–457.
- Petrov, K.A., Girard, E., Nikitashina, A.D., Colasante, C., Bernard, V., Nurullin, L., Leroy, J., Samigullin, D., Colak, O., Nikolsky, E., Plaud, B., Krejci, E., 2014. Schwann cells sense and control acetylcholine spillover at the neuromuscular junction by $\alpha 7$ nicotinic receptors and butyrylcholinesterase. *J. Neurosci. Off. J. Soc. Neurosci.* 34, 11870–11883.
- Pezzementi, L., Chatonnet, A., 2010. Evolution of cholinesterases in the animal kingdom. *Chem. Biol. Interact.* 187, 27–33.
- Pistolozzi, M., Du, H., Wei, H., Tan, W., 2015. Stereoselective inhibition of human butyrylcholinesterase by the enantiomers of bambuterol and their intermediates. *Drug Metab. Dispos. Biol. Fate Chem.* 43, 344–352.
- Pohanka, M., Hrabínova, M., Kuca, K., Simonato, J.-P., 2011. Assessment of acetylcholinesterase activity using indoxylacetate and comparison with the standard Ellman’s method. *Int. J. Mol. Sci.* 12, 2631–2640.

- Prado, M.A.M., Reis, R.A.M., Prado, V.F., de Mello, M.C., Gomez, M.V., de Mello, F.G., 2002. Regulation of acetylcholine synthesis and storage. *Neurochem. Int.* 41, 291–299.
- Primo-Parmo, S.L., Bartels, C.F., Wiersema, B., van der Spek, A.F., Innis, J.W., La Du, B.N., 1996. Characterization of 12 silent alleles of the human butyrylcholinesterase (BCHE) gene. *Am. J. Hum. Genet.* 58, 52–64.
- Rabkin, S.W., 2007. Epicardial fat: properties, function and relationship to obesity. *Obes. Rev. Off. J. Int. Assoc. Study Obes.* 8, 253–261.
- Rachinsky, T.L., Camp, S., Li, Y., Ekström, T.J., Newton, M., Taylor, P., 1990. Molecular cloning of mouse acetylcholinesterase: tissue distribution of alternatively spliced mRNA species. *Neuron* 5, 317–327.
- Rachinsky, T.L., Crenshaw, E.B., Taylor, P., 1992. Assignment of the gene for acetylcholinesterase to distal mouse chromosome 5. *Genomics* 14, 511–514.
- Radisky, D.C., Stallings-Mann, M., Hirai, Y., Bissell, M.J., 2009. Single proteins might have dual but related functions in intracellular and extracellular microenvironments. *Nat. Rev. Mol. Cell Biol.* 10, 228–234.
- Ramachandran, J., Sajith, K.G., Priya, S., Dutta, A.K., Balasubramanian, K.A., 2014. Serum cholinesterase is an excellent biomarker of liver cirrhosis. *Trop. Gastroenterol. Off. J. Dig. Dis. Found.* 35, 15–20.
- Rana, O.R., Schauerte, P., Kluttig, R., Schröder, J.W., Koenen, R.R., Weber, C., Nolte, K.W., Weis, J., Hoffmann, R., Marx, N., Saygili, E., 2010. Acetylcholine as an age-dependent non-neuronal source in the heart. *Auton. Neurosci. Basic Clin.* 156, 82–89.
- Randall, D.C., Brown, D.R., McGuirt, A.S., Thompson, G.W., Armour, J.A., Ardell, J.L., 2003. Interactions within the intrinsic cardiac nervous system contribute to chronotropic regulation. *Am. J. Physiol. Regul. Integr. Comp. Physiol.* 285, R1066–1075.
- Rao, A.A., Sridhar, G.R., Das, U.N., 2007. Elevated butyrylcholinesterase and acetylcholinesterase may predict the development of type 2 diabetes mellitus and Alzheimer's disease. *Med. Hypotheses* 69, 1272–1276.
- Raveh, L., Grunwald, J., Marcus, D., Papier, Y., Cohen, E., Ashani, Y., 1993. Human butyrylcholinesterase as a general prophylactic antidote for nerve agent toxicity. In vitro and in vivo quantitative characterization. *Biochem. Pharmacol.* 45, 2465–2474.
- Red-Horse, K., Ueno, H., Weissman, I.L., Krasnow, M., 2010. Coronary arteries form by developmental reprogramming of venous cells. *Nature* 464, 549–553.
- Reiner, E., Sinko, G., Skrinjarić-Spoljar, M., Simeon-Rudolf, V., 2000. Comparison of protocols for measuring activities of human blood cholinesterases by the Ellman method. *Arh. Hig. Rada Toksikol.* 51, 13–18.
- Renshaw, S. (Ed.), 2005. *Immunohistochemistry: Methods Express Series*, 1st Edition edition. ed. Scion Publishing Ltd., Bloxham, Oxfordshire.
- Ribeiro, F.M., Alves-Silva, J., Volkandt, W., Martins-Silva, C., Mahmud, H., Wilhelm, A., Gomez, M.V., Rylett, R.J., Ferguson, S.S.G., Prado, V.F., Prado, M. a. M., 2003. The hemicholinium-3 sensitive high affinity choline transporter is internalized by clathrin-mediated endocytosis and is present in endosomes and synaptic vesicles. *J. Neurochem.* 87, 136–146.
- Ribeiro, F.M., Black, S.A.G., Prado, V.F., Rylett, R.J., Ferguson, S.S.G., Prado, M.A.M., 2006. The “ins” and “outs” of the high-affinity choline transporter CHT1. *J. Neurochem.* 97, 1–12.

- Rocha-Resende, C., Roy, A., Resende, R., Ladeira, M.S., Lara, A., de Moraes Gomes, E.R., Prado, V.F., Gros, R., Guatimosim, C., Prado, M.A.M., Guatimosim, S., 2012. Non-neuronal cholinergic machinery present in cardiomyocytes offsets hypertrophic signals. *J. Mol. Cell. Cardiol.* 53, 206–216.
- Rosenberry, T.L., 1975. Acetylcholinesterase. *Adv. Enzymol. Relat. Areas Mol. Biol.* 43, 103–218.
- Rossi, M.A., Abreu, M.A., Santoro, L.B., 1998. Connective Tissue Skeleton of the Human Heart A Demonstration by Cell-Maceration Scanning Electron Microscope Method. *Circulation* 97, 934–935.
- Rotundo, R.L., Thomas, K., Porter-Jordan, K., Benson, R.J., Fernandez-Valle, C., Fine, R.E., 1989. Intracellular transport, sorting, and turnover of acetylcholinesterase. Evidence for an endoglycosidase H-sensitive form in Golgi apparatus, sarcoplasmic reticulum, and clathrin-coated vesicles and its rapid degradation by a non-lysosomal mechanism. *J. Biol. Chem.* 264, 3146–3152.
- Rowland, M., Tsigelny, I., Wolfe, M., Pezzementi, L., 2008. Inactivation of an invertebrate acetylcholinesterase by sulfhydryl reagents: a reconsideration of the implications for insecticide design. *Chem. Biol. Interact.* 175, 73–75.
- Roy, A., Fields, W.C., Rocha-Resende, C., Resende, R.R., Guatimosim, S., Prado, V.F., Gros, R., Prado, M.A.M., 2013. Cardiomyocyte-secreted acetylcholine is required for maintenance of homeostasis in the heart. *FASEB J. Off. Publ. Fed. Am. Soc. Exp. Biol.* 27, 5072–5082.
- Roy, A., Guatimosim, S., Prado, V.F., Gros, R., Prado, M.A.M., 2014. Cholinergic activity as a new target in diseases of the heart. *Mol. Med. Camb. Mass.*
- Roy, A., Lara, A., Guimarães, D., Pires, R., Gomes, E.R., Carter, D.E., Gomez, M.V., Guatimosim, S., Prado, V.F., Prado, M.A.M., Gros, R., 2012. An analysis of the myocardial transcriptome in a mouse model of cardiac dysfunction with decreased cholinergic neurotransmission. *PLoS One* 7, e39997.
- Rustemeijer, C., Schouten, J.A., Voerman, H.J., Beynen, A.C., Donker, A.J., Heine, R.J., 2001. Is pseudocholinesterase activity related to markers of triacylglycerol synthesis in Type II diabetes mellitus? *Clin. Sci. Lond. Engl.* 1979 101, 29–35.
- Rysevaite, K., Saburkina, I., Pauziene, N., Noujaim, S.F., Jalife, J., Pauza, D.H., 2011a. Morphologic pattern of the intrinsic ganglionated nerve plexus in mouse heart. *Heart Rhythm Off. J. Heart Rhythm Soc.* 8, 448–454.
- Rysevaite, K., Saburkina, I., Pauziene, N., Vaitkevicius, R., Noujaim, S.F., Jalife, J., Pauza, D.H., 2011b. Immunohistochemical characterization of the intrinsic cardiac neural plexus in whole-mount mouse heart preparations. *Heart Rhythm Off. J. Heart Rhythm Soc.* 8, 731–738.
- Saburkina, I., Gukauskienė, L., Rysevaite, K., Brack, K.E., Pauza, A.G., Pauziene, N., Pauza, D.H., 2014. Morphological pattern of intrinsic nerve plexus distributed on the rabbit heart and interatrial septum. *J. Anat.* 224, 583–593.
- Saburkina, I., Rysevaite, K., Pauziene, N., Mischke, K., Schauerte, P., Jalife, J., Pauza, D.H., 2010. Epicardial neural ganglionated plexus of ovine heart: anatomic basis for experimental cardiac electrophysiology and nerve protective cardiac surgery. *Heart Rhythm Off. J. Heart Rhythm Soc.* 7, 942–950.
- Sacks, H.S., Fain, J.N., 2007. Human epicardial adipose tissue: A review. *Am. Heart J.* 153, 907–917.
- San Mauro MP, Patronelli F, Spinelli E, Cordero A, Covello D, Gorostiaga JA, 2009. Nerves of the heart: a comprehensive review with a clinical point of view. *Neuroanatomy* 8, 26–31.

- Santarpia, L., Grandone, I., Contaldo, F., Pasanisi, F., 2013. Butyrylcholinesterase as a prognostic marker: a review of the literature. *J. Cachexia Sarcopenia Muscle* 4, 31–39.
- Sato, K.K., Hayashi, T., Maeda, I., Koh, H., Harita, N., Uehara, S., Onishi, Y., Oue, K., Nakamura, Y., Endo, G., Kambe, H., Fukuda, K., 2014. Serum butyrylcholinesterase and the risk of future type 2 diabetes: the Kansai Healthcare Study. *Clin. Endocrinol. (Oxf.)* 80, 362–367.
- Schallreuter, K.U., Gibbons, N.C.J., Zothner, C., Elwary, S.M., Rokos, H., Wood, J.M., 2006. Butyrylcholinesterase is present in the human epidermis and is regulated by H₂O₂: more evidence for oxidative stress in vitiligo. *Biochem. Biophys. Res. Commun.* 349, 931–938.
- Serra, S.M., Costa, R.V., Teixeira De Castro, R.R., Xavier, S.S., Nóbrega, A.C.L.D., 2009. Cholinergic stimulation improves autonomic and hemodynamic profile during dynamic exercise in patients with heart failure. *J. Card. Fail.* 15, 124–129.
- Sharma, K.V., Koenigsberger, C., Brimijoin, S., Bigbee, J.W., 2001. Direct evidence for an adhesive function in the noncholinergic role of acetylcholinesterase in neurite outgrowth. *J. Neurosci. Res.* 63, 165–175.
- Sharma, R., Gupta, B., Singh, N., Acharya, J.R., Musilek, K., Kuca, K., Ghosh, K.K., 2014. Development and Structural Modifications of Cholinesterase Reactivators against Chemical Warfare Agents in Last Decade: A Review. *Mini Rev. Med. Chem.*
- Shimada, H., Hirano, S., Shinotoh, H., Aotsuka, A., Sato, K., Tanaka, N., Ota, T., Asahina, M., Fukushi, K., Kuwabara, S., Hattori, T., Suhara, T., Irie, T., 2009. Mapping of brain acetylcholinesterase alterations in Lewy body disease by PET. *Neurology* 73, 273–278.
- Sikorav, J.L., Duval, N., Anselmet, A., Bon, S., Krejci, E., Legay, C., Osterlund, M., Reimund, B., Massoulié, J., 1988. Complex alternative splicing of acetylcholinesterase transcripts in Torpedo electric organ; primary structure of the precursor of the glycolipid-anchored dimeric form. *EMBO J.* 7, 2983–2993.
- Silman, I., Sussman, J.L., 2005. Acetylcholinesterase: “classical” and “non-classical” functions and pharmacology. *Curr. Opin. Pharmacol.* 5, 293–302.
- Simon, S., Krejci, E., Massoulié, J., 1998. A four-to-one association between peptide motifs: four C-terminal domains from cholinesterase assemble with one proline-rich attachment domain (PRAD) in the secretory pathway. *EMBO J.* 17, 6178–6187.
- Sinha, S.N., Keresztes-Nagy, S., Frankfater, A., 1976. Studies on the distribution of cholinesterases: activity in the human and dog heart. *Pediatr. Res.* 10, 754–758.
- Sinha, S.N., Yelich, M.R., Keresztes-Nagy, S., Frankfater, A., 1979. Regional distribution of acetylcholinesterase in the right atria of humans and dogs. *Pediatr. Res.* 13, 1217–1221.
- Sinko, G., Calić, M., Bosak, A., Kovarik, Z., 2007. Limitation of the Ellman method: cholinesterase activity measurement in the presence of oximes. *Anal. Biochem.* 370, 223–227.
- Slavíková, J., Tucek, S., 1982. Choline acetyltransferase in the heart of adult rats. *Pflüg. Arch. Eur. J. Physiol.* 392, 225–229.
- Somogyi, P., Chubb, I.W., Smith, A.D., 1975. A possible structural basis for the extracellular release of acetylcholinesterase. *Proc. R. Soc. Lond. B Biol. Sci.* 191, 271–283.
- Sperelakis, N. (Ed.), 1998. *Cell Physiology Source Book*, Second Edition, 2 edition. ed. Academic Press, San Diego.

- Stanley, R.L., Conatser, J., Dettbarn, W.D., 1978. Acetylcholine, choline acetyltransferase and cholinesterases in the rat heart. *Biochem. Pharmacol.* 27, 2409–2411.
- Steinberg, N., Roth, E., Silman, I., 1990. Torpedo acetylcholinesterase is inactivated by thiol reagents. *Biochem. Int.* 21, 1043–1050.
- Steinebrunner, N., Mogler, C., Vittas, S., Hoyler, B., Sandig, C., Stremmel, W., Eisenbach, C., 2014. Pharmacologic cholinesterase inhibition improves survival in acetaminophen-induced acute liver failure in the mouse. *BMC Gastroenterol.* 14, 148.
- Šteiner I., 2010. kardiopatologie, 1st ed. Galén.
- Stojan, J., 2008. Kinetic evaluation of multiple initial rate data by simultaneous analysis with two equations. *Chem. Biol. Interact.* 175, 242–248.
- Sussman, J.L., Harel, M., Frolow, F., Oefner, C., Goldman, A., Toker, L., Silman, I., 1991. Atomic structure of acetylcholinesterase from *Torpedo californica*: a prototypic acetylcholine-binding protein. *Science* 253, 872–879.
- Taylor, I.M., 1977. The relationship between innervation and the cholinesterases of the rat atrioventricular node. *J. Histochem. Cytochem. Off. J. Histochem. Soc.* 25, 21–26.
- Taylor, I.M., 1976. The cytochemical localization of cholinesterase activity in the developing chick heart. *Histochemistry* 47, 239–246.
- Taylor, P., Brown, J.H., 1999. Synthesis, Storage and Release of Acetylcholine.
- Tripathi, A., Srivastava, U.C., 2010. Acetylcholinesterase :A Versatile Enzyme of Nervous System. *Ann. Neurosci.* 15, 106–111.
- Triposkiadis, F., Karayannis, G., Giamouzis, G., Skoularigis, J., Louridas, G., Butler, J., 2009. The Sympathetic Nervous System in Heart Failure: Physiology, Pathophysiology, and Clinical Implications. *J. Am. Coll. Cardiol.* 54, 1747–1762.
- Trojan S, 2003. *Lékařská fyziologie* (Stanislav Trojan a kol.).
- Tsim, K., Soreq, H., 2013. Acetylcholinesterase: Old Questions and New Developments. *Frontiers E-books*.
- Tsim, K.W., Randall, W.R., Barnard, E.A., 1988a. An asymmetric form of muscle acetylcholinesterase contains three subunit types and two enzymic activities in one molecule. *Proc. Natl. Acad. Sci. U. S. A.* 85, 1262–1266.
- Tsim, K.W., Randall, W.R., Barnard, E.A., 1988b. Synaptic acetylcholinesterase of chicken muscle changes during development from a hybrid to a homogeneous enzyme. *EMBO J.* 7, 2451–2456.
- Tsuboi, M., Furukawa, Y., Nakajima, K., Kurogouchi, F., Chiba, S., 2000. Inotropic, chronotropic, and dromotropic effects mediated via parasympathetic ganglia in the dog heart. *Am. J. Physiol. Heart Circ. Physiol.* 279, H1201–1207.
- Tsuji, S., Larabi, Y., 1983. A modification of thiocholine-ferricyanide method of Karnovsky and Roots for localization of acetylcholinesterase activity without interference by Koelle's copper thiocholine iodide precipitate. *Histochemistry* 78, 317–323.
- Tsuji, S., Nakatomi, R., Tsuchiya, H., Hirai, K., Katayama, Y., Motelica-Heino, I., Hashikawa, T., 2002. Perineuronal surface acetylcholinesterase activity of a fine neural network stained histochemically and observed with backscattered electron imaging and X-ray mapping methods. *Brain Res. Brain Res. Protoc.* 9, 16–22.
- Tucek, S., 1982. The synthesis of acetylcholine in skeletal muscles of the rat. *J. Physiol.* 322, 53–69.
- Turnbull, W.B., Daranas, A.H., 2003. On the value of c: can low affinity systems be studied by isothermal titration calorimetry? *J. Am. Chem. Soc.* 125, 14859–14866.

- Vaitkevicius, R., Saburkina, I., Rysevaite, K., Vaitkeviciene, I., Pauziene, N., Zaliunas, R., Schauerte, P., Jalife, J., Pauza, D.H., 2009. Nerve supply of the human pulmonary veins: an anatomical study. *Heart Rhythm Off. J. Heart Rhythm Soc.* 6, 221–228.
- Vallianou, N.G., Evangelopoulos, A.A., Bountziouka, V., Bonou, M.S., Katsagoni, C., Vogiatzakis, E.D., Avgerinos, P.C., Barbetseas, J., Panagiotakos, D.B., 2014. Association of butyrylcholinesterase with cardiometabolic risk factors among apparently healthy adults. *J. Cardiovasc. Med. Hagerstown Md* 15, 377–383.
- Van der Zee, E.A., Platt, B., Riedel, G., 2011. Acetylcholine: future research and perspectives. *Behav. Brain Res.* 221, 583–586.
- Van Liefferinge, J., Massie, A., Portelli, J., Di Giovanni, G., Smolders, I., 2013. Are vesicular neurotransmitter transporters potential treatment targets for temporal lobe epilepsy? *Front. Cell. Neurosci.* 7, 139.
- Velan, B., Kronman, C., Ordentlich, A., Flashner, Y., Leitner, M., Cohen, S., Shafferman, A., 1993. N-glycosylation of human acetylcholinesterase: effects on activity, stability and biosynthesis. *Biochem. J.* 296, 649–656.
- Vetter, F.J., Simons, S.B., Mironov, S., Hyatt, C.J., Pertsov, A.M., 2005. Epicardial Fiber Organization in Swine Right Ventricle and Its Impact on Propagation. *Circ. Res.* 96, 244–251.
- Wadhvani, K.C., Latker, C.H., Balbo, A., Rapoport, S.I., 1989. Perineurial permeability and endoneurial edema during Wallerian degeneration of the frog peripheral nerve. *Brain Res.* 493, 231–239.
- Walmsley, T.A., Abernethy, M.H., Fitzgerald, H.P., 1987. Effect of daylight on the reaction of thiols with Ellman's reagent, 5,5'-dithiobis(2-nitrobenzoic acid). *Clin. Chem.* 33, 1928–1931.
- Wang, H.-F., Yu, J.-T., Tang, S.-W., Jiang, T., Tan, C.-C., Meng, X.-F., Wang, C., Tan, M.-S., Tan, L., 2015. Efficacy and safety of cholinesterase inhibitors and memantine in cognitive impairment in Parkinson's disease, Parkinson's disease dementia, and dementia with Lewy bodies: systematic review with meta-analysis and trial sequential analysis. *J. Neurol. Neurosurg. Psychiatry* 86, 135–143.
- Wang, H., Lu, Y., Wang, Z., 2007. Function of cardiac M3 receptors. *Auton. Autacoid Pharmacol.* 27, 1–11.
- Wang, Y., Schopfer, L.M., Duysen, E.G., Nachon, F., Masson, P., Lockridge, O., 2004. Screening assays for cholinesterases resistant to inhibition by organophosphorus toxicants. *Anal. Biochem.* 329, 131–138.
- Wasserman, L., Doctor, B.P., Gentry, M.K., Taylor, P., 1993. Epitope mapping of form-specific and nonspecific antibodies to acetylcholinesterase. *J. Neurochem.* 61, 2124–2132.
- Wecker, L., Mrak, R.E., Dettbarn, W.D., 1986. Evidence of necrosis in human intercostal muscle following inhalation of an organophosphate insecticide. *Fundam. Appl. Toxicol. Off. J. Soc. Toxicol.* 6, 172–174.
- Weerasuriya, A., Hockman, C.H., 1992. Perineurial permeability to sodium during Wallerian degeneration in rat sciatic nerve. *Brain Res.* 581, 327–333.
- Wiesner, J., Kříž, Z., Kuča, K., Jun, D., Koča, J., 2010. Influence of the acetylcholinesterase active site protonation on omega loop and active site dynamics. *J. Biomol. Struct. Dyn.* 28, 393–403.
- Williams, L., Frenneaux, M., 2008. Assessment of right ventricular function. *Heart* 94, 404–405.
- Wilson, E.J., Massoulié, J., Bon, S., Rosenberry, T.L., 1996. The rate of thermal inactivation of Torpedo acetylcholinesterase is not reduced in the C231S mutant. *FEBS Lett.* 379, 161–164.

- Winteringham, F.P., Disney, R.W., 1962. Radiometric assay of acetylcholinesterase. *Nature* 195, 1303.
- Wolf, H.K., Buslei, R., Schmidt-Kastner, R., Schmidt-Kastner, P.K., Pietsch, T., Wiestler, O.D., Blümcke, I., 1996. NeuN: a useful neuronal marker for diagnostic histopathology. *J. Histochem. Cytochem. Off. J. Histochem. Soc.* 44, 1167–1171.
- Wu, J.-P., Huang, W.-B., Zhou, H., Xu, L.-W., Zhao, J.-H., Zhu, J.-G., Su, J.-H., Sun, H.-B., 2014. Intensity of stromal changes is associated with tumor relapse in clinically advanced prostate cancer after castration therapy. *Asian J. Androl.* 16, 710–714.
- Xie, W., Stribley, J.A., Chatonnet, A., Wilder, P.J., Rizzino, A., McComb, R.D., Taylor, P., Hinrichs, S.H., Lockridge, O., 2000. Postnatal developmental delay and supersensitivity to organophosphate in gene-targeted mice lacking acetylcholinesterase. *J. Pharmacol. Exp. Ther.* 293, 896–902.
- Xin, M., Olson, E.N., Bassel-Duby, R., 2013. Mending broken hearts: cardiac development as a basis for adult heart regeneration and repair. *Nat. Rev. Mol. Cell Biol.* 14, 529–541.
- Xu, Y., Colletier, J.-P., Weik, M., Qin, G., Jiang, H., Silman, I., Sussman, J.L., 2010. Long route or shortcut? A molecular dynamics study of traffic of thiocholine within the active-site gorge of acetylcholinesterase. *Biophys. J.* 99, 4003–4011.
- Yasuhara, O., Matsuo, A., Bellier, J.-P., Aimi, Y., 2007. Demonstration of choline acetyltransferase of a peripheral type in the rat heart. *J. Histochem. Cytochem. Off. J. Histochem. Soc.* 55, 287–299.
- Zhang, Y., Popovic, Z.B., Bibeovski, S., Fakhry, I., Sica, D.A., Van Wagoner, D.R., Mazgalev, T.N., 2009. Chronic vagus nerve stimulation improves autonomic control and attenuates systemic inflammation and heart failure progression in a canine high-rate pacing model. *Circ. Heart Fail.* 2, 692–699.
- Zhu, X., Cheng, Y.-Q., Du, L., Li, Y., Zhang, F., Guo, H., Liu, Y.-W., Yin, X.-X., 2015. Mangiferin attenuates renal fibrosis through down-regulation of osteopontin in diabetic rats. *Phyther. Res. PTR* 29, 295–302.